

2012

MRC Toxicology Unit

Alessio Mylonas

MAP4K3 AND THE POSTTRANSCRIPTIONAL CONTROL OF GENE EXPRESSION

A closer look at the MAP kinase control over the tumour promoting mTOR pathway

M.Phil thesis submitted to
The College of Medicine, Biological
Sciences and Psychology
University of Leicester

Abstract

A tight balance between growth and apoptosis is essential to a functional non-malignant cell. Cell growth is determined by one of its major regulators, mTOR, and is dependent on a number of nutrient- and energy-sensing input signals. These converge onto mTOR which controls protein synthesis and cell growth. Deregulation of this pathway is known to contribute to tumourigenesis and it is being investigated as a therapeutic target. Apoptosis, on the other hand, is an orderly choreography that comes together in causing the serene demise of a cell. Bcl-2 family members establish a tightly controlled balance over pro- and anti-apoptotic signals. Evasion from apoptosis is thought to be one of the hallmarks of cancer. MAP4K3 is a high order signal transducer that was recently found to both positively regulate mTOR through nutrient signalling and induce apoptosis through the intrinsic and extrinsic pathways.

Recently, MAP4K3 was shown to activate mTORC1 targets in an amino acid-dependent way and to cause cell growth. In another study, it was found to cause apoptosis through the JNK pathway and by upregulating pro-apoptotic Bcl-2 members through the mTORC1 pathway. These findings make it interesting to investigate its targeted translation changes. In addition to its role in apoptosis, MAP4K3 was found to be involved in a number of other pathways and diseases.

In the present study, I focus on the contribution of MAP4K3 to the translation initiation-inducing mTORC1 pathway and investigate the translational changes it causes. MAP4K3 induces cell growth and increases protein synthesis rates. It also causes an increase in the number of highly translated mRNAs in polysome profiling experiments. Put together, these observations led me to identify the genes modulated by MAP4K3 with the aim of establishing new leads in the paths paved by this high order signal transducer. I pinpoint the most interesting and most likely MAP4K3-modulated genes at the translational level, and propose new paths worth validating and pursuing.

Acknowledgments

First and foremost, I am very grateful to both my supervisors. A big thanks to Miguel Martins for showing a whole new side to science I wasn't even aware of and putting me head first in it, and a very warm one to Anne Willis for giving me a chance to finish and for continued interest and support.

I have also to thank all the brilliant members of the Tox unit:

Amandine Bastide and Lindsay Wilson, whose help has proven invaluable in making this work possible and steering me in the right direction. They have also inadvertently made me more critical of experiments and conclusions, and remodelled my way of designing them.

David Lam for long back and forth exchange of ideas and teaching me precision in experimental execution. Roberta Tufi for always having time to discuss about general science and being a good friend. Nicoleta Moiso for always having that right thing to suggest. Ana Costa for being such an adorable and good person, I hope to be there for her during her last months of her thesis as she has been there for mine. Sam Loh for making *Drosophila* interesting and helping to switch off every now and again. Mariana Santos for making the inducible cell line on her last breath in our lab and giving us soap opera-grade drama to keep things interesting.

Ewan Smith for long discussions about amino acid regulation of mTOR and invaluable input. Jashu for doing dialysis (and a great one at that) with me. Kate Dudek and Carolyn Jones for helping with the microarrays. Nick Burgoyne for analysing the data. Xavier Pichon for showing me Northern blotting and being quite the awesome guy.

The French quarter: Xavier Pichon, Amandine Bastide, Thomas Sbarrato and Emilie Horvilleur.

The Italian quarter: Franco Conforti, Francesca Grespi, Francesco Romeo, Alessandro Rufini, Max Agostini and Krupesh Mistri (yes, that's right he's in there)

The Spanish quarter: Maria Victoria (she can have her own section)

Contents

| | |
|--|-------------|
| Abstract | i |
| Acknowledgments | ii |
| List of Figures | viii |
| Abbreviations | x |
| | |
| Chapter 1 | 1 |
| 1. Introduction..... | 1 |
| 1.1 Biochemical mode of action | 2 |
| 1.1.1 Ste20p as an essential transducer of MAPK signalling first discovered in yeast | 2 |
| 1.1.2 Phylogenetic relationships hint to highly conserved mechanism across species and Ste20 members | 7 |
| 1.2 Apoptosis and cancer: kill and let live..... | 9 |
| 1.2.1 Intrinsic versus extrinsic induction | 10 |
| 1.2.2 Bcl-2 family proteins fighting over pro- vs anti-apoptotic balance..... | 12 |
| 1.2.3 Mitochondrial membrane permeabilization and executioner caspases..... | 17 |
| 1.3 Regulation of TORC1-dependent growth..... | 19 |
| 1.3.1 Growth factor regulation of growth | 23 |
| 1.3.2 Nutrient regulation of growth | 24 |
| 1.4 mTORC1 and posttranscriptional control of gene expression..... | 26 |
| 1.4.1 Regulatory steps of translation initiation..... | 26 |
| 1.5 Physiological effects conferred by an upstream activator of MAPK signalling and regulator of TOR pathway | 30 |
| 1.5.1 Ste20 kinase signalling in yeast and the mating process | 30 |

| | |
|--|-----------|
| 1.5.2 MAP4K3 signalling in mammalian cells, the JNK pathway and cell death | 31 |
| 1.5.2 MAP4K3-induced control of cell size, growth and protein translation via mTOR regulation | 35 |
| AIMS OF THE WORK..... | 44 |
| Chapter 2 | 45 |
| 2. MAP4K3 signalling activates JNK and causes chromatin condensation and morphological changes in 293s but not clear mTOR activation..... | 45 |
| 2.1 Introduction..... | 45 |
| 2.2 Materials and Methods..... | 47 |
| 2.2.1 Materials | 47 |
| 2.2.2 Plasmid preparations..... | 47 |
| 2.2.3 Tissue culture | 48 |
| 2.2.4 Western blots | 48 |
| 2.2.5 Nuclear stain | 48 |
| 2.2.6 Imaging fluorescence | 48 |
| 2.2.7 Western blot signal determination and statistics..... | 48 |
| 2.3 Results..... | 50 |
| 2.3.1 MAP4K3 phosphorylates JNK but not mTORC1 targets p70S6K1 or 4E-BP1 and does not upregulate Puma or Bad in transient overexpression | 50 |
| 2.3.2 MAP4K3 causes chromatin condensation and morphological changes in HEK293 cells in a kinase-dependent manner | 52 |
| 2.4 Discussion..... | 55 |

| | |
|--|---------------|
| Chapter 3 | 58 |
| 3. A more physiological MAP4K3 inducible system reveals control over size and protein synthesis | 58 |
| 3.1 Introduction..... | 58 |
| 3.2 Materials and Methods..... | 60 |
| 3.2.1 Materials | 60 |
| 3.2.2 Tissue culture | 60 |
| 3.2.3 MAP4K3-GFP Flp-In 293T-REx cell line generation under tetracycline control | 60 |
| 3.2.4 Western blots | 61 |
| 3.2.5 RNA extraction and qRT-PCR | 61 |
| 3.2.6 Quantification of relative MAP4K3 protein expression | 61 |
| 3.2.7 Imaging fluorescence | 61 |
| 3.2.8 Protein synthesis rate determination | 61 |
| 3.2.9 Flow cytometry | 62 |
| 3.2.10 Statistics | 62 |
| 3.3 Results..... | 63 |
| 3.3.1 Characterisation of MAP4K3-GFP 293T-REx system..... | 63 |
| 3.4 Discussion | 71 |
| Chapter 4 | 74 |
| 4. Amino acid restimulation MAP4K3 causes an increase in protein synthesis with no apparent activation of mTORC1 targets | 74 |
| 4.1 Introduction..... | 74 |
| 4.2 Materials and Methods..... | 75 |
| 4.2.1 Materials | 75 |
| 4.2.2 Tissue culture | 75 |
| 4.2.3 Western blots | 75 |

| | |
|--|------------|
| 4.2.4 Protein synthesis rate determination | 75 |
| 4.2.5 Statistics | 76 |
| 4.3 Results..... | 77 |
| 4.4 Discussion..... | 80 |
| Chapter 5 | 81 |
| 5. MAP4K3 causes up- down-regulation of various targets at the translational level with transcriptional control over some interesting targets..... | 81 |
| 5.1 Introduction..... | 81 |
| 5.2 Materials and Methods..... | 84 |
| 5.2.1 Materials | 84 |
| 5.2.2 Tissue culture | 84 |
| 5.2.3 Polysome fractionation and RNA collection | 84 |
| 5.2.4 Total RNA extraction..... | 85 |
| 5.2.5 RNA preparation and Microarrays | 85 |
| 5.2.6 Data analysis | 85 |
| 5.3 Results..... | 86 |
| 5.3.1 MAP4K3-GFP enhances high density polysome formation..... | 86 |
| 5.3.2 MAP4K3 and the modulation of gene expression..... | 90 |
| 5.4 Discussion..... | 92 |
| Chapter 6 | 95 |
| 6. Discussion – MAP4K3 and the proposed mechanism of control over translational regulation | 95 |
| Future directions..... | 99 |
| References..... | 104 |

List of Figures

| | |
|---|----|
| Figure 1: Structure of human Mitogen-activated protein kinase kinase kinase kinase 3 (MAP4K3)..... | 6 |
| Figure 2: MAPK pathway engagement causes morphological changes in a variety of different cells..... | 9 |
| Figure 3: Signalling network of the extrinsic apoptosis pathway..... | 11 |
| Figure 4: BH3-only protein modulation and intrinsic apoptosis pathway signalling network..... | 16 |
| Figure 5: mTOR pathway upstream regulation and downstream effects overview..... | 19 |
| Figure 6: TORC1-regulating pathways. TORC1 is negatively regulated by a multitude of different signals that result in TORC1 mislocalisation and Rheb inactivation..... | 21 |
| Figure 7: TORC1-regulating pathways. TORC1 is positively regulated by a multitude of different signals mainly converging on Rheb..... | 22 |
| Figure 8: Translation initiation mechanism and regulation. Translation initiation depends on the successful and timely formation of initiation complexes and their recruitment to ribosome (sub)units..... | 27 |
| Figure 9: MAP4K3 orthologues in yeast, fruit fly and humans: signalling pathways and their physiological effects..... | 30 |
| Figure 10: MAP4K3 induces chromatin condensation in U2OS cells in a kinase-dependent manner..... | 34 |
| Figure 11: MAP4K3 activates two branches of signalling pathways that lead to cell death..... | 42 |
| Figure 12: MAP4K3 activates JNK, but not mTORC1, signalling in transient overexpression models with no discernible change in BH3-only expression..... | 51 |
| Figure 13: MAP4K3 kinase activity causes chromatin condensation and marked morphological changes in HEK293 cells..... | 53 |
| Figure 14: Induction of M4K3-GFP is optimal at 0.1ug/mL in the 293T-REx line..... | 64 |
| Figure 15: GFP fluorescence intensity increases with doxycycline treatment..... | 65 |
| Figure 16: Induction is optimal at 0.1ug/mL in the 293T-REx line..... | 66 |

| | |
|--|----|
| Figure 17: M4K3 induction timecourse following doxycycline treatment on 293T-REx cell line..... | 67 |
| Figure 18: MAP4K3-GFP induction causes a progressive increase in cell size..... | 69 |
| Figure 19: M4K3 has an effect on protein synthesis in an amino acid-dependent way. | 78 |
| Figure 20: Experimental concept of sucrose gradient centrifugation, operational process of gradient fractionation and translation rate determination..... | 82 |
| Figure 21: MAP4K3 may be driving translation from monosomes to polysomes..... | 87 |
| Figure 22: Polysome profiles from doxycycline treated and untreated cells are similar..... | 88 |
| Figure 23: MAP4K3 induction increases polysome to sub-polysome ratio compared to doxycycline treatment..... | 89 |
| Figure 24: Proposed MAP4K3-mediated translational changes..... | 98 |

Abbreviations

| | |
|--------------------------------------|---------|
| Adenosine Diphosphate | ADP |
| Adenosine Triphosphate | ATP |
| Adult-onset Still's disease | AOSD |
| Alcohol Use Disorder | AUD |
| Apoptosis inducing factor | AIF |
| B-cell lymphoma 2 | Bcl-2 |
| Bcl-2 antagonist killer | BAK |
| Bcl-2 homology domain 3 | BH3 |
| Bcl-2-associated death promoter | BAD |
| Bcl-2-associated X protein | BAX |
| BH3 Interacting-domain Death agonist | BID |
| Cdc42/Rac Interactive Binding | CRIB |
| Cell division control 42 protein | Cdc42p |
| c-Jun N-terminal Kinase | JNK |
| Death-Inducing Signalling Complex | DISC |
| <i>Drosophila</i> MAP4K3 | dMAP4K3 |
| <i>Drosophila</i> S6K | dS6K |
| EGF receptor | EGFR |
| Endonuclease G | EndoG |
| Endothelial Growth Factor | EGF |
| Extracellular regulated kinase | Erk |
| Fas ligand | FasL |

| | |
|--|-----------------|
| Fas receptor | FasR |
| Fas-Associated Death Domain | FADD |
| Full-length | FL |
| Genome-Wide Association Study | GWAS |
| Germinal Centre Kinase | GCK |
| GLK | GCK-like Kinase |
| G-protein Coupled Receptor | GPCR |
| Green Fluorescent Protein | GFP |
| GTPase-Activating Protein | GAP |
| Guanine nucleotide Exchange Factor | GEF |
| Gene Ontology | GO |
| Guanosine Diphosphate | GDP |
| Guanosine Triphosphate | GTP |
| Haemagglutinin | HA |
| Happyhour | Hppy |
| Human Embryonic Kidney 293 | HEK293 |
| Inhibitor of Apoptosis Protein | IAP |
| JNK kinase | JNKK |
| Kinase-dead | KD |
| mammalian Target of Rapamycin | mTOR |
| MAP kinase kinase kinase kinase 3 | MAP4K3 |
| Mitogen-Activated Protein Kinase | MAPK |
| MAPK/ERK Kinase | MEK |
| Mitogen-activated protein kinase 4 | MKK4 |
| Myeloid Leukaemia cell differentiation protein 1 | MCL-1 |
| Macrophage stimulating 1 | Mst1 |
| p21 Activated Kinase | PAK |
| p53-Upregulated Modulator of Apoptosis | PUMA |
| PAK binding domain | PBD |
| Phosphoinositide 3-kinase | PI3K |
| Phosphoinositide-dependent kinase-1 | PDK1 |
| Pleckstrin homology | PH |
| Protein Phosphatase 2A | PP2A |
| Ribosomal p70 S6 Kinase | p70S6K |

| | |
|--|--------|
| Significance Analysis of Microarray | SAM |
| Second Mitochondria-Derived Activator of Caspase | Smac |
| Serine/Threonine Kinase | STK |
| SH2-containing tyrosine phosphatase 1 | SHP1 |
| Src-homology domain 2 | SH2 |
| Sterile 20 protein | Ste20p |
| Systemic Lupus Erythematosus | SLE |
| TNF Receptor | TNFR |
| TNFR-Associated Death Domain | TRADD |
| TNFR-Associated Factor 2 | TRAF2 |
| Tuberous Sclerosis Complex | TSC |
| Tumour Necrosis Factor | TNF |
| U-2 osteosarcoma | U2OS |
| Wild-type | WT |

Chapter 1

1. Introduction

The Mitogen-Activated Protein Kinase (MAPK) pathway is a complex hub of signalling that links outside stimuli to control and determine cellular fate. It links extracellular inducements to the three central MAP kinases p38, Erk and JNK which have a robust effect on gene expression changes, cell fate and apoptosis. The Target Of Rapamycin (TOR) pathway, on the other hand, has direct control over translation, metabolism and cellular growth. Deregulation of either of these signalling pathways has been directly linked to a number of diseases, in particular to cancer, and it is not uncommon for one pathway to deregulate the other during the development of cancers.

Mitogen-Activated Protein kinase kinase kinase 3 (MAP4K3), a *Sterile20*-family protein (Ste20p) that acts as a signal transducer of the MAPK pathway, a positive regulator of nutrient signalling to TOR and a strong inducer of apoptosis, has recently been linked to targeted mRNA stabilization and enhancement of pro-apoptotic protein expression. Clinical investigations into the state of MAP4K3 suggest that it is mutated in a considerable number of pancreatic and lung cancers from human patients. MAP4K3's direct pro-apoptotic activity, its involvement in the modulation of expression of downstream targets of the intrinsic cell death pathway, as well as the evidence of its aberrant nature in human cancers, make it a likely tumourigenesis hindering kinase whose loss of function may promote cancer progression. It is conceivable that this high hierarchy signal transducer may be a useful molecular target for disease treatment. The induction of specific genes by this potential tumour involved protein may also provide us with novel biomarkers that may be attributable to particular cancers. This should be of remarkable interest in the early diagnosis of pancreatic cancers, which have a very poor prognosis because, by the time symptoms arise, they are too advanced for effective treatment.

To understand how MAP4K3's dual role in both MAPK and TOR pathways may be cancer-linked, first I will describe its biochemical features and its physiological contributions observed *in vivo* and *in vitro*. I will then proceed to characterise the signalling pathways MAP4K3 has been involved in, with particular emphasis on two of its most important axes: 1) the MAPK pathways and the part MAP4K3 plays in cell death and the JNK pathway; and 2) its regulatory contribution and the downstream consequences related to TOR and its translational machinery partners. I will also briefly describe the pathways it has most recently been linked to: the EGFR and NF κ B axes. This should aid in understanding the MAP4K3-dependent contribution of TOR-mediated regulation of apoptosis and cancer progression.

1.1 Biochemical mode of action

Human MAP4K3, also called Germinal Centre Kinase (GCK)-Like Kinase (GLK) is a serine/threonine protein kinase belonging to the GCK-I family of the *Sterile20* (Ste20) superfamily. Also belonging to the same Ste20 superfamily are the p21 Activated Kinases (PAKs 1 and 2) which have considerable sequence homology to the GCKs and share many similarities in their regulatory mechanisms and biochemical function. The Ste20 family proteins were found to be early activators of the MAPK pathway, mediating extracellular signalling to transcriptional changes of gene expression. Ste20 family proteins were placed at the highest signal transducing hierarchy: as MAP kinase kinase kinase kinases (MAP4Ks). Human PAK (I and II) and GCKs (I through VIII) subfamily member genes are all phylogenetic relatives of a single gene first discovered in yeast – Ste20p. Genetic analyses of yeast mating in *Saccharomyces cerevisiae* led to the discovery of genes that, when mutated, induced sterility and they were termed *Sterile* (Ste) genes. Many of the Ste proteins are central players in the mating process in yeast. Mating in yeast initiates through pheromone responses between cells of opposite mating type, and is accomplished by the physical fusion of two haploid cells into a single diploid one. Ste20p was placed directly downstream of G protein-coupled pheromone receptors.

1.1.1 Ste20p as an essential transducer of MAPK signalling first discovered in yeast

Ste20p, MAP4K3's ortholog in yeast, acts high in the signal transducing hierarchy. In the budding yeast *S.cerevisiae*, following binding of the pheromone ligand to the pheromone receptor, Gpa1p (α -subunit of G-protein) displaces GDP for GTP in a reaction that releases its two binding partners Ste4p (β -subunit of G-protein) and Ste18p (γ -subunit

of G-protein) for uninhibited lipid binding. This promotes recruitment of the MAPK complex to the membrane through specific interaction sequences. The MAPK complex formed of the different MAP3Ks, MAP2Ks, and MAPKs (in *S.cerevisiae* Ste11p, Ste7p and Fus3p or Kss1p respectively) is held together and recruited to the membrane-bound Ste4p (G β) by the Ste5p. The scene is set for activation of the MAPK module and the engagement of the pathway. The different members of the MAPK pathway are then sequentially activated in a signalling cascade originating from Ste20p (Elion, 2000).

Ste20p recruitment to the membrane and activation through G-protein-binding. Ste20p is recruited to the membrane by the Ste4p (G β) much in the same way the MAPK scaffold complex is. Activation of the pathway was found to be dependent on specific sequences on the β -subunit of the G-protein, and that this was mediated by direct association of Ste20p with the subunit. Further stressing the importance of this recruitment mechanism is the need for pheromone binding where, under pheromone stimulation, Ste4p pulled-down Ste20p. Mutations abolishing interactions both on the Ste4p-binding sequence on Ste20p or *vice versa* significantly reduced activation of the pathway and greatly reduced mating efficacy (Leeuw *et al.*, 1998). Although this was not directly shown, this is the main model by which MAP4K3 is thought to be activated in the signalling cascade. As a MAP4K, it is thought to be recruited to the base of an activated receptor. Because it was shown to be activated by Tumour Necrosis Factor- α and to be upstream of the MAPK JNK (Diener *et al.*, 1997), MAP4K3 is thought to be recruited to the TNF receptor through TNFR-associated death domain (TRADD) and TNFR-associated factor 2 (TRAF2) for downstream events in the JNK pathway. Interestingly, because MAP4K3 was also linked to the Epidermal Growth Factor Receptor (EGFR) pathway through inhibition of the EGFR/extracellular-signal regulated kinase (ERK) pathway (Corl *et al.*, 2009), and through interactions with endophilin, a protein known to be recruited to the activated EGFR complex (Ramjaun *et al.*, 2001), it may also itself be recruited directly to the active EGFR complex.

Recruitment of MAP3K is important for downstream activation. Ste5p is also recruited to the plasma membrane through Ste4p-Ste18p in a molecular reaction that is purely dependent on the G $\beta\gamma$ -binding sequences of Ste5p and the Ste5p-binding sequences of the G $\beta\gamma$ subunits. It is an event that is independent of whether MAPK members Ste11p, Ste7p and Fus3p or even Ste20p are present in the cells and that only occurs in the

presence of pheromones. Interestingly, signal transduction in the pathway was purely dependent on G $\beta\gamma$ being localised to the plasma membrane and hence not in a freeform cytosolic state, suggesting that the pathway may get activated in the event of specific localisation of the MAPK module to the membrane independently of the G-protein. Indeed, targeting Ste5p (and thus the MAPK members it holds together) to the plasma membrane independently of G $\beta\gamma$ (through cloning of membrane targeting domains) was sufficient for reasonable activation of the downstream kinases as well as to maintain mating efficacy in Ste4p-Ste18p deletion strains. The molecular activity of the G-protein subunits on the MAPK pathway is purely centred on recruitment to the membrane of Ste20p and Ste5p-bound MAPK module. Binding of pheromones to their receptors engages the MAPK pathway at the cell's surface and creates a hub of signalling at the plasma membrane for downstream effects to take place. Integrating this signalling and mediating it to targets below it, is Ste20p (Wang and Dohlman, 2004).

Ste20p activation is dependent upon relief of autoinhibitory binding whilst MAP4K3 is activated by transautophosphorylation. The relocation of both Ste20p (enzyme) and Ste5p-MAPK complex (substrate) to the membrane gives way to a classical signal transduction mechanism in the form of phosphorylation events that initiate a cascade of reactions. These result in signal transduction to targeted cellular events. Regulation of the catalytic activity depends largely on autoinhibitory interactions from its own tertiary structure. This is relieved by Cell division control 42 protein (Cdc42p)-activated kinase of the p21 activated kinase 1 subfamily (PAK-I), formed of a serine/threonine kinase (STK) domain at the C-terminus and a regulatory domain at the N-terminus. Regulation of the kinase activity of Ste20p is achieved through the realization of three independent events that result in full activation of the enzyme. First, there is relief of the inhibitory effect on the kinase domain by the autoinhibitory domain lying alongside the Cdc42/Rac interactive binding (CRIB) motif. The intramolecular interaction is abolished by binding of Cdc42p to the CRIB (or PAK binding domain; PBD) of Ste20p. The CRIB motif is known to interact with Cdc42p in presence of Mg²⁺ and GTP through conserved sequences. Whilst inwardly-folded, the protein hides active sites, in particular substrate and ATP binding sites, and, more importantly, the activation loop. When activated, GTP-associated Cdc42p binds Ste20p. As a small Rho-family GTPase of the Ras superfamily, Cdc42p gets its guanine-nucleotide exchange factor (GEF) activity from Cdc24p. It was believed that Cdc42p was responsible for relief of the inhibitory effect on the catalytic

subunit of Ste20p, but *in vitro* results show that Cdc42p is not needed for phosphorylation of downstream targets of Ste20p. The interaction between Cdc42p and Ste20p gives way to a membrane targeting event that brings Ste20p at the membrane, where its substrate lies. This revolves around Cdc42p's role as a central contributor to cytoskeletal rearrangements for polarised cell growth. Following pheromone-triggered cellular events, Cdc42p localises to mating projections along with a number of binding partners, amongst which is also Ste20p. Fluorescence tracking of GFP-tagged Ste20p places it at bud and shmoo sites during mating in CRIB wild-type but not Cdc42p-Ste20p interaction abolishing mutants. The interaction itself exposes the activation loop to phosphorylation events that lead to full activation of the kinase activity (Dan *et al.*, 2001). MAP4K3 is thought to be activated in a similar manner. Although it contains several phosphorylation sites whose regulation and use are unknown, it is the ones on the activation loop that are important for its kinase function on the MAPK pathway. They are thought to be achieved through autophosphorylation like other GCK-I group members. It is thought that binding to the activated receptor causes autophosphorylation and conformational changes that allow for recruitment of downstream targets, but it is unclear how this happens. It has also been found to transautophosphorylate on Ser170 and this is known to be required for an entirely different function on regulation of mTORC1 (Yan *et al.*, 2010; Figure 1).

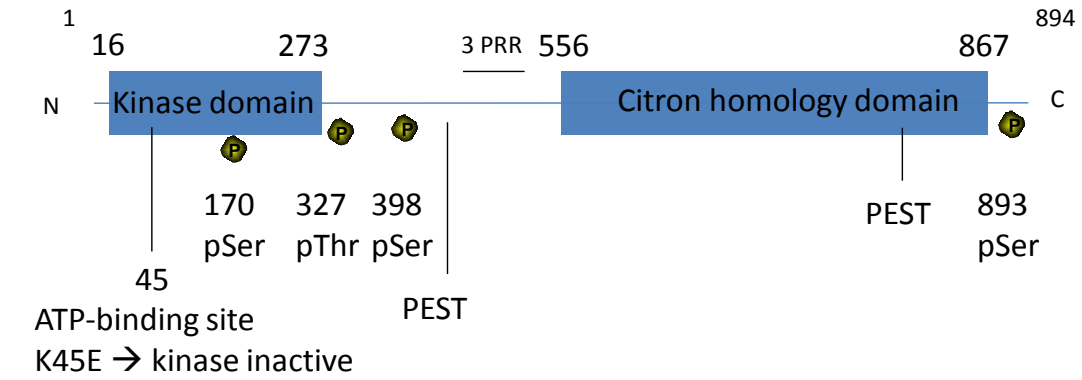


Figure 1: Structure of human Mitogen-activated protein kinase kinase kinase 3 (MAP4K3). The catalytic domain at the N-terminus (16-273) derives its activity from a serine phosphorylation site (170) and an ATP-binding domain in the activation loop. Three additional phosphorylation sites (Thr327, Ser398 and 893) have been found by Mass Spectrometry (MS) with unclear function. Two PEST (proline, glutamic acid, serine, threonine) domains may be linked to rapid degradation of MAP4K3 through ubiquitin-mediated targeting to the proteasome. Three proline-rich repeats (PRR) are responsible for protein-protein interactions, such as with endophilin and, likely, MAP4K3's mammalian target of rapamycin complex 1 (mTORC1) signalling-branch inhibitor Protein Phosphatase 2A (PP2A). Finally, the regulatory domain (556-867) lies at the C-terminus.

Downstream signal transduction. Ste20p binds Cdc42p and activation of its MAP3K target is merely facilitated by the co-localisation of MAP4K and the MAPK complex (of which MAP3K is part) to the membrane. It is therefore not considered as an integral part of the module but rather as a proper signal transducer. In fact, it behaves more like a central hub, integrating signals and activating the MAPK module through phosphorylation of Ste11p. It achieves this through direct phosphorylation of serine/threonine targets on the amino-terminal regulatory domain of Ste11p. This releases inhibition of the C-terminal catalytic domain allowing further signal transduction to the downstream MAP2K. Phosphorylation of serines 302 and 306 and threonine 307 on the N-terminus of Ste11p exposes the catalytic domain and this is thereby able to phosphorylate its downstream target and the signal is transduced directly to the MAPK Fus3p. In this sense, Ste20p is a MAP4K but it is independent of the MAPK module. Some mammalian MAP4Ks only need bind to the MAP3K for activation. Following autophosphorylation and self-activation at the base of an activated receptor (be it TNFR, EGFR), MAP4K3 is known to phosphorylate directly MAP3K1 (also known as MAPK/ERK kinase kinase 1; MEKK1), and this is known to transduce the signal downstream to MAP2Ks (Diener *et al.*, 1997).

1.1.2 Phylogenetic relationships hint to highly conserved mechanism across species and Ste20 members

Ste20p in yeast is the founding member of the mammalian Ste20 family of kinases. There are two p21 Activated Kinase (PAK) and 8 Germinal Centre Kinase (GCK) subfamilies in the Ste20 superfamily. These are so distributed mainly due to the location of their kinase domains. The main feature of this family of proteins is that the kinase domains are very highly conserved across the subfamilies, whilst the non-catalytic domains are rather diverse. They are grouped as either PAK members, which have their catalytic subunit on the C-termini, or GCK members, which have it on the N-termini. Phylogenetic relations between these Ste20 family members hint to a very well-preserved function between them and conserved regulation and mechanism of downstream activation (Dan *et al.*, 2001).

Conservation in the catalytic domain indicates similar kinase function. It is clear that Ste20p acts like a phosphorylating MAP4K, but some mammalian Ste20 family members do not necessarily phosphorylate downstream targets. Although all are MAP4Ks, in fact only three are known to bind and phosphorylate the MAP3Ks, where two of them are members of GCK-I (HPK1 and MAP4K3) and one is a PAK-I (PAK1). Most bind to their targets through their kinase domains and this is enough to produce downstream signal transduction. Importantly, all these MAP4Ks are known to be involved in either apoptosis or cytoskeletal rearrangements. Activation of the extrinsic pathway and caspase activation leads to an interplay between these kinases and the caspases. Many of them are known to on one side activate caspases which then further activate the kinases leading to apoptosis and on the other to cause cytoskeletal rearrangements. Macrophage stimulating 1 (Mst1) of the GCK-II group, for instance, causes activation of Caspase 3 which is itself shown to cleave Mst1 and other MAP4Ks such as Mst2, HPK1, SLK and PAK2 for increased activation of their catalytic domains by loss of their regulatory and self-inhibitory domains, and to mediate apoptosis (Kurokawa and Kornbluth, 2009).

From a biochemical perspective, MAP4K3 catalytic activity is attributed to the N-terminal kinase domain and has been shown to be dependent on multiple phosphorylation sites on the activation loop. The ATP-binding site was predicted to be significant for the activation of the MAPK pathway, as expected from comparisons with other GCK-I members HPK1 and GCK. It was shown to be important in the activation of the JNK pathway through a lysine to glutamic acid substitution at position 45 which abolishes the catalytic activity of MAP4K3 and leads to loss of the MAP4K3/MEKK1/MKK4/JNK

cascade (Diener *et al.*, 1997; Lam *et al.*, 2009). This was also found to eliminate the apoptotic potential of MAP4K3 (Lam *et al.*, 2009). Other phosphorylation sites have been identified by mass spectrometry, but it remains unclear what role they might play. MAP4K3 is also known to be more active in its (Δ C) regulatory domain truncated version (Lam *et al.*, 2009) like other MAP4Ks although it is not known whether this happens physiologically for MAP4K3 and what other, less apparent, effects this may have. It is fascinating that MAP4K3 is also phosphorylated on Ser170 in its catalytic domain leading to entirely different signalling events which involve regulation of growth through mTORC1 (Yan *et al.*, 2010). It is thought that what allows for this sort of diversity in function is attributed to the high level of dissimilarity between the regulatory domains of these kinases, making them powerful signal-integrating tools for diverse downstream effects such as apoptosis on one side and growth on the other.

Non-catalytic domain diversity allows for distinct types of regulation. Variation in the non-catalytic regions, both at the level of sequence as well as of structure, is the feature that permits the different roles each of the MAP4Ks play. Depending on the type of input signal they are known to lead to diverse downstream effects. These can be ultimately mediated by the catalytic domain, by a scaffolding effect or by oligomerisation. Some MAP4Ks have a double effect both on apoptosis and cytoskeletal rearrangements. One such MAP4K is SLK. This GCK-V member was found to be cleaved by active Caspase 3 and its N-terminal domain to promote apoptosis whilst its C-terminal domain was found to be involved in disassembly of the actin cytoskeleton. There are many other examples of this sort of regulation and each one of them may be specific to each of these Ste20 family members. Yet, there is some conservation in the overall function of these Ste20 kinases as the majority of PAK-I and PAK-II members are also involved in cytoskeletal rearrangements. Although there is no published data showing an involvement in cytoskeletal rearrangements for MAP4K3, it may be more closely related to SLK than previously thought. SLK has been shown to cause apoptosis and actin fibre dismantling causing clear morphological changes (Figure 2A). MAP4K3 is known to be an inducer of apoptosis through the JNK pathway (Lam *et al.*, 2009) and although this was previously undernoted in the last publication, it may well be causing morphological changes through cytoskeletal modifications. Interestingly, EGF treatment of pituitary cells elongates the otherwise round cells (Figure 2B) and that this is mediated by the MAPK pathway. A MAPKK was found to cause morphological changes attributed to S

phase entry (Figure 2C; Gotoh *et al.*, 1999). Overall, there are countless examples of MAP kinases that induce morphological changes in cells of almost all types.

Adapted from Lewis *et al.*, 2002; Sabourin *et al.*, 2000 and Gotoh *et al.*, 1999.

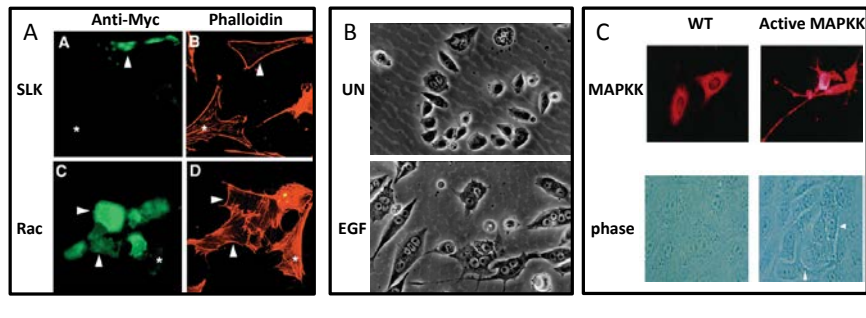


Figure 2: MAPK pathway engagement causes morphological changes in a variety of different cells. (A) Mouse myoblast lines transfected with SLK or Rac lose stress fibre integrity as shown the actin filaments (phalloidin staining) at 16h post transfection. (B) Pituitary cells treated with EGF gain an elongated morphology and this is reversible by treatment with a MAPK pathway inhibitor (not shown) following 4 day treatment as was appropriate. (C) Fibroblasts transfected with a constitutively active MAPKK change morphology to an elongated phenotype at 18h post transfection, but not wild-type MAPKK (WT) transfected cells.

Although it shares many functions with other Ste20 members, such as a role as a MAP4K and a hand in apoptosis, MAP4K3 is the only Ste20 kinase family member with so many roles in other pathways such as JNK, TOR, NFκB and EGFR. Regulatory mechanisms for its EGFR and NFκB pathway involvement are still to be elucidated. However, regulation of apoptosis and growth, have been linked to phosphorylation on the active loop of MAP4K3 and Ser170 respectively. Not everything is known about the biochemical function of MAP4K3, but much can be inferred from studies undertaken on other MAP4Ks in yeast. However, to understand its dual role in apoptosis and growth, and how that may be cancer linked, I first review the apoptotic process, and then the regulation of growth and mechanistic process of translation initiation. Understanding these will be key to placing all known evidence for MAP4K3 into the right context.

1.2 Apoptosis and cancer: kill and let live

Cellular destruction can be achieved either through autophagic cell death, a process that eats away at a cell's own organelles in sequence prior to terminal nuclear destruction; through necrosis which, in contrast to apoptosis, has an initiating cause external to the tissue or organ such as infection, exposure to toxins or trauma; or through apoptosis, a coordinated event that depends on a tightly controlled balance between pro- and anti-

apoptotic signals. Apoptosis is a natural event that determines the death of a cell but ultimately the life of a cellular microenvironment or a higher organism, and has evolved to occur through a variety of mechanisms under different circumstances.

The events that eventually lead to the “fall”, literally apoptosis (απο-πτώση), of a cell can either be initiated intrinsically or extrinsically. The extrinsic, purposefully also called death-receptor, pathways rely on membrane-bound receptors to convey signals directly to death effector molecules. Contrary to it, the intrinsic pathways depend on a finely tuned balance of signals between B-cell lymphoma-2 (Bcl-2) family members. The binary choice between life and death resides on something we have come to think as a threshold for apoptosis, whereby an excess in pro-apoptotic signals leads to death of the cell. A series of events that depend on mitochondrial integrity then mediate the needed events for a truly clean disposal and recycling of cellular components. Ultimately, apoptosis can be viewed as the effect of a binary choice between life and death under the microenvironmental circumstances of a cell. Cells that should be destined to die but that have acquired a resistance to apoptosis are liable to become cancerous. One of the hallmarks of cancer is evasion of this natural regulatory effect on death, and much effort is being invested in identifying ways of maximising death for cancerous cells (Green, 2005).

1.2.1 Intrinsic versus extrinsic induction

Induction of apoptosis is dependent on two types of signals: intrinsic and extrinsic. Intrinsic signals incorporate the overall state of the cell into a binary decision of whether or not to enter apoptotic cell death by initiating a Bcl-2 family-dependent tour de force. They then allow for permeation of the mitochondrial outer membrane for the release of death-mediating caspases. Extrinsic cell death, on the other hand, manages to bypass the Bcl-2 family members and directly recruit and activate caspases for effective cell suicide. The extrinsic pathway accomplishes this through certain ligand-receptor interactions, a number of extrinsic cell death-specific mediator proteins, and the caspase proteins (Figure 3).

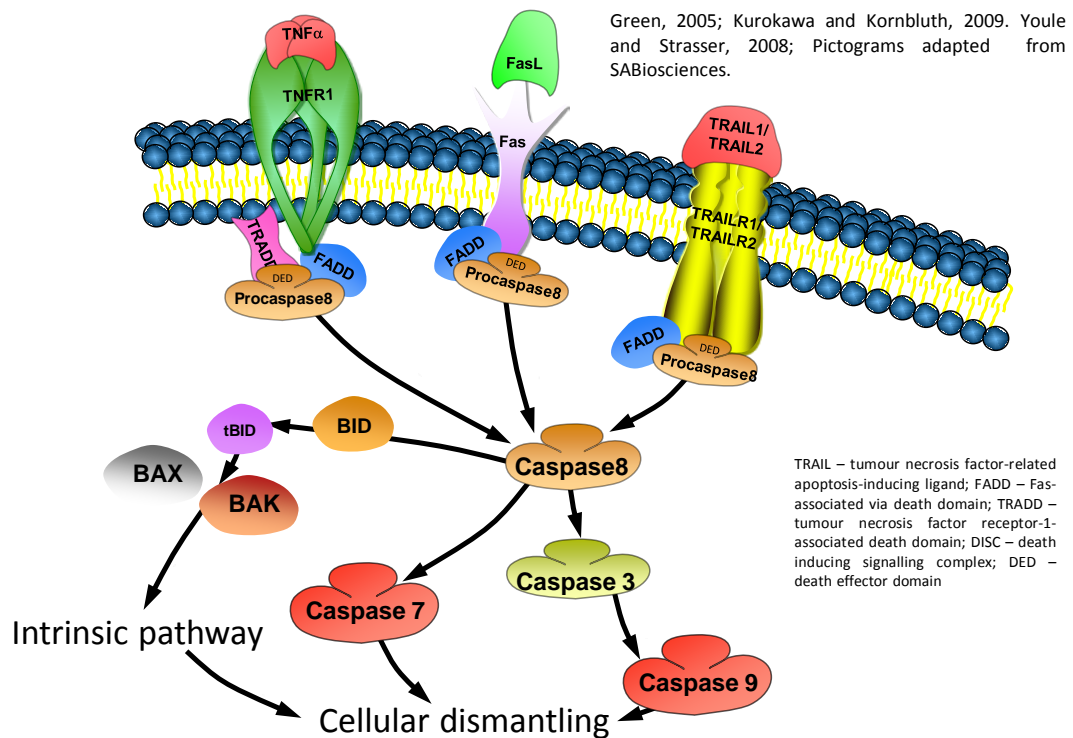


Figure3: Signalling network of the extrinsic apoptosis pathway. Extrinsic cell death is the result of a decision to enter apoptosis that originates from extracellular conditions. The pathway is initiated by specific extracellular signals onto target Death-receptors. Death ligands (TNF α , FasL, TRAIL, etc...) bind their specific receptor (TNFR1, Fas, TRAIL receptor, etc...) causing recruitment of proteins to their highly conserved intracellular Death domain. Other proteins that contain death domains (FADD, TRADD) are recruited to the trimerized (TRAILR, TNFR) or simply activated (Fas) receptors and they function as adaptor proteins for downstream signal propagation. Procaspase-8 is recruited to the receptor-adaptor complex through a DED, forming the DISC. This leads to oligomerisation, self-cleavage and activation of caspase-8. Caspase 8 activation can cause intersection with the intrinsic pathway through BID cleavage, and/or activation of caspases that, mostly directly, mediate cellular dismantling.

Ligands of the Tumour Necrosis Factor (TNF) family are known to bind so-called death receptors for trimerization. This leads to the formation of a death-domain-binding site for downstream-signal-conveying adaptor proteins. A higher order complex formed due to this receptor-initiated signalling then proceeds to recruiting initiator caspases and oligomerizing them for activation. These in turn activate effector caspases that have a direct hand in the death process. Whereas the intrinsic pathway mainly engages Bcl-2 family members for activation of effector caspases, the extrinsic pathway does not need to do so, altogether avoiding direct mitochondrial involvement. Interestingly however, it has been found that it can intersect the intrinsic pathway on BID. BID is a BH3-only protein of the Bcl-2 family that engages the pro-apoptotic intrinsic pathway as a result of extrinsically-induced death signals.

When the Fas ligand (FasL) binds its receptor Fas protein on the membrane of a cell targeted for apoptosis, it forms a trimeric complex termed the death-inducing

signalling complex (DISC). This is a docking site for the Fas-associated death domain (FADD) which actively recruits, oligomerizes and cleaves procaspases-8 and 10 for activation into their caspase 8 and 10 derivatives. Caspase-8 regulation has been found to be largely mediated by phosphorylation events that are function-suppressive in nature. Tyrosine phosphorylation on various residues by Src family kinases Fyn, Lyn and Src itself inhibits its apoptotic capabilities. In a yet unknown regulatory manner, caspase-8 is also phosphorylated onto a specific tyrosine for Src-homology domain 2-containing tyrosine phosphatase 1 (SHP1) for dephosphorylation of inhibitory posttranslational modifications by death-inhibiting kinases. When not phosphorylated on these key regulatory residues, caspase-8 is stimulated to activate the effector caspase-3 and/or BID through cleavage, thus directly engaging players of the intrinsic pathway. In the intrinsic pathway, death is reliant on interactions between Bcl-2 family members and mostly follows caspase-9 activation (Youle and Strasser, 2008).

1.2.2 Bcl-2 family proteins fighting over pro- vs anti-apoptotic balance

There are 12 core proteins of the Bcl-2 family and they are structurally related between themselves, but functionally have opposing roles. Of these Bcl-2 homologous proteins, it has been determined by *in vivo* studies in mice that 4 of them are pro-apoptotic in nature and the 8 remainder are anti-apoptotic. Studies of the signalling pathways have revealed that the pro-apoptotic proteins function by inhibiting those anti-apoptotic Bcl-2 family member proteins in tightly regulated signalling cascades and through physical interactions allowed by structural similarities. Additionally, one set of pro-apoptotic proteins that are not part of the 12 core Bcl-2 homologous proteins but contain related domains, the BH3-only proteins, have evolved to counteract the anti-apoptotic functions of some Bcl-2 family proteins, thus adding an extra level of complexity and regulation to the apoptosis pathway. Overall, there is a complex balancing interaction between these Bcl-2-related proteins that depends on upstream signalling events and that culminates in Bcl-2-associated X protein (BAX) and Bcl-2- antagonist killer (BAK)-mediated permeabilization of the outer mitochondrial membrane. To understand how this happens, it is important to review 1) the protein structures that allow for anti-apoptotic protein inhibition, 2) the resulting dynamic relocation of these Bcl-2 family members, 3) a series of BAX/BAK conformational changes, and 4) the signalling networks that input on these proteins (Youle and Strasser, 2008).

Protein structures and BH3-motifs are key for relief of anti-apoptotic grip. Bcl-2 family proteins are grouped into core Bcl-2 proteins and BH3-only proteins. The core Bcl-2 family proteins contain at least two Bcl-2 homology 1 through 4 (BH1-4) domains, whilst the BH3-only, as their name suggests, only have a BH3 domain as a common region with the rest of the Bcl-2 family. There is no common evolutionary link between the BH3-only proteins and the core Bcl2-members, except for BID which is a BH3-only protein with predicted tertiary structures highly related to the Bcl-2 core members. Most of the core Bcl-2 family members show great similarity between themselves and, from an evolutionary perspective, this is quite remarkable since they have opposing activities. In particular the multi BH-containing BAX-family proteins BAK and BAX are very similar to their inhibiting partners BCL-2 and BCL-XL. The three-dimensional structures of these main players in the Bcl-2 family protein balance are also conserved. On the other hand, all nine of the BH3-only proteins are pro-apoptotic in nature, yet they only share partial sequence similarity between themselves.

Importantly, Bcl-2 homologues possess membrane-anchoring domains on their C-termini, and the state they are in is particularly important to their localization. The membrane-anchoring domains of pro-apoptotic proteins BAX, BID and BIM are kept hidden when in their inactive form. They can either bind BH1, BH2 or BH3 motifs which form self-inhibiting hydrophobic pockets around them, or other BH3 domains from other anti-apoptotic Bcl-2 members. When being activated for downstream signalling, the membrane-anchoring domain from pro-apoptotic protein BAX is bound by BH3-motifs from BH3-only proteins. This leads to exposure of the membrane-anchoring domain and to its translocation to the mitochondria. Following translocation, these proteins change conformation to either destabilise the membrane, or to antagonise BCL-2 or BCL-XL via BH3-domains. All in all, structure and sequence similarities allow these proteins to interact and tip the balance in favour or against apoptosis. Additionally, one important step in their regulation is the cellular repositioning of these proteins. It is this relocation (described below) that leads to completion of two major needs for apoptosis: relief of the (self-) inhibitory grip on pro-apoptotic proteins and localisation to the mitochondria (Youle and Strasser, 2008).

Location, location, location – intracellular translocation events and precise repositioning of pro- and anti-apoptotic Bcl-2 members. Although many of the Bcl-2 family proteins have very different functions and some even have opposing effects, structure similarities

allow them to behave in similar manners. The relocation of both pro- and anti-apoptotic proteins is vital for successful regulation of the apoptotic balance that they hold. On one hand, anti-apoptotic members exhibit basal inhibition of the pro-apoptotic multi-BH domain Bax-family proteins. On the other hand, BH3-only proteins, that are pro-apoptotic in nature, bind the anti-apoptotic Bcl-2 members to relieve inhibition on the Bax-family proteins. This relief causes a mitochondrial-membrane destabilisation effect that results in cell death.

The major inhibitors of apoptosis, BCL-2 and BCL-XL, act by inhibiting the release of proteins that are sequestered within mitochondria. BCL-2 is known to be firmly anchored to mitochondria through a membrane-spanning domain on its C-terminus. It is known to reside there permanently, to basally inhibit apoptosis. It has also been found at the endoplasmic reticulum and nuclear envelope, but its function there is still not understood. BCL-XL, on the other hand, can be found in the cytosol or on mitochondrial surfaces under basal conditions. It is found to co-localise with BAX, which is mainly cytosolic, and BAK, which is found on the outer mitochondrial membrane. The precise biochemical mechanism for this is unknown. BAX is found to be monomeric, and not in direct interaction with BCL-XL but experiments using just the BH3 peptide liberate its anchoring domain from self-BH3-domain inhibition. Interestingly, tBID, the active form of BID, and BIM are found to bind to BAX and to directly activate it following apoptotic input. Overall, the relocation of the various Bcl-2 family members is directly responsible for the tight regulation over the apoptotic process. Pro-apoptotic BAX and BAK displace to the mitochondria upon apoptotic input, anti-apoptotic Bcl-2 and Bcl-XL follow and co-localise with them to hinder initiation of the apoptotic process, and BH3-containing proteins relocate and determine apoptotic initiation.

Following intrinsic stresses, the Bax-family proteins are activated. BAX is recruited to mitochondria but so is BCL-XL. BAX hides its membrane anchor in its own BH3 pocket and, as mentioned above, through still undefined mechanisms, is released from its self-inhibitory grip. More importantly, localisation of BCL-XL to mitochondria is known to inhibit oligomerization of BAK. This displacement is found to be dependent on a very similar mechanism as with BAX and is known to be mediated by BH3-only protein binding. The consensus is that binding of BH3-only proteins to BCL-XL relieves its inhibitory effect on BAK when localised to mitochondria. However, because this BH3-binding effect is the initiating force for BCL-XL recruitment to mitochondria, there may be other effects behind the BCL-XL relocation. Some reports suggest that BCL-XL may

be activated to become pro-apoptotic in nature because of its very similar way it inserts itself into the mitochondrial membrane, but it was not found to oligomerize nor form pores like BAX. Nonetheless, relocation of BAX and BCL-XL to mitochondria following the initiating input from small BH3-only proteins leads to a clear repositioning that sets the scene for the sequence of events that lead to apoptosis. The status quo is kept by the inhibition of BAX by BCL-2, which always localises to mitochondria, and inhibition of BAK, which also basally localises to mitochondria, by the newly recruited BCL-XL. Antagonising the binding of BCL-XL or BCL-2 to BAK and BAX is a balance shift brought about by BH3-only proteins. In the right conditions, pro-apoptotic signals overtake the anti-apoptotic ones and the balance shifts in favour of apoptosis (Youle and Strasser, 2008).

BH3-only protein mode of action and activation mechanism. BH3-only proteins are found to bind and inhibit the anti-apoptotic Bcl-2 members and cause apoptosis. Activation of BH3-only proteins has been found to be solely dependent on the detection of apoptosis-inducing signals and this makes them available for interaction with the anti-apoptotic Bcl-2 members. It is known that PUMA, BIM and active tBID can bind to all five anti-apoptotic members – BCL-2, BCL-XL, BCL-W, A1 and MCL-1 – and that this binding is sufficient to relieve inhibition of BAX and BAK and any of them can produce apoptosis. BAD and NOXA cannot interact with all of them, and it was found that they are needed in combination to produce apoptosis. BAD can interact with the main anti-apoptotic proteins BCL-2, BCL-XL and BCL-W, whilst NOXA is found to bind A1 and MCL1 (Youle and Strasser, 2008; Figure 4).

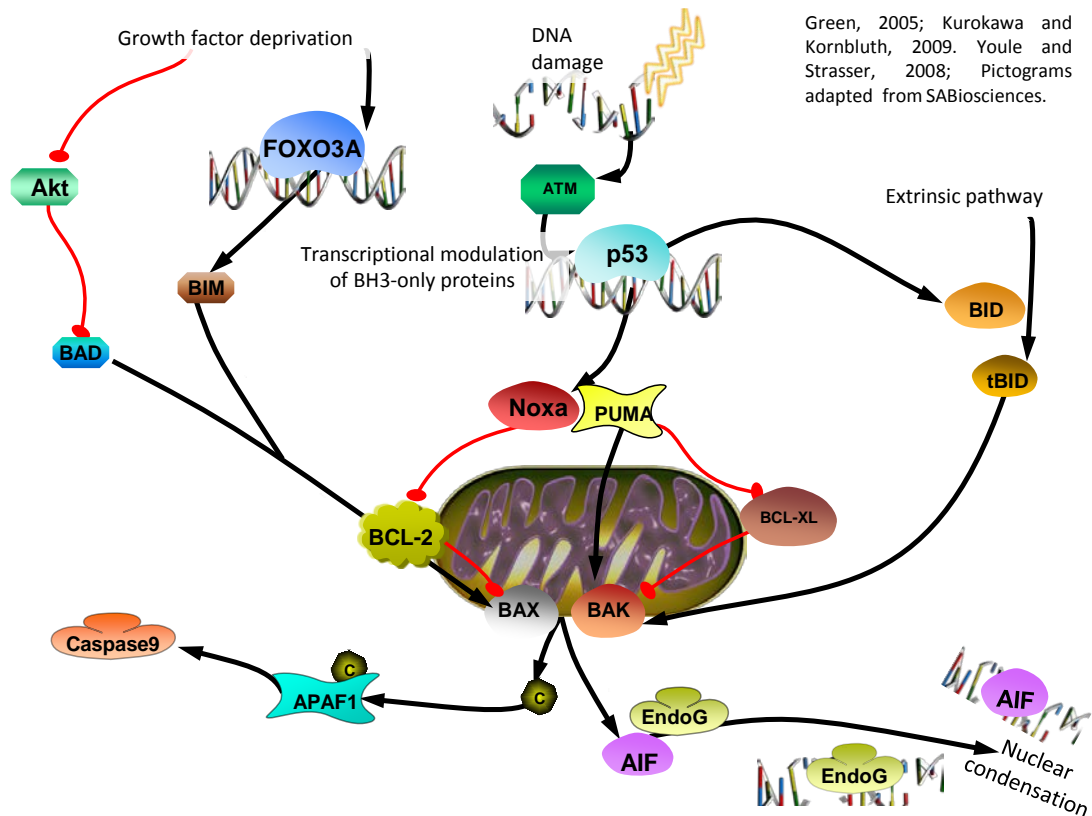


Figure 4: BH3-only protein modulation and intrinsic apoptosis pathway signalling network.

BH3-only proteins are sensitive to developmental death cues, such as growth-factor deprivation (BAD, BIM) or death-receptor signalling (BID), and intracellular damage, such as X-ray or UV-induced DNA damage (Noxa, PUMA, BID). Modulation of many of the BH3-only proteins leads to activation of BAX and BAK, either directly or indirectly, causing the release of cellular dismantling proteins, and cytochrome c, a major component of APAF-1, a caspase 9 activator. Nuclear fragmenting proteins EndoG and AIF are also released causing nuclear condensation.

BAX and BAK insert in the mitochondrial membrane and oligomerize. BAX and BAK are thought to operate in a similar manner. After translocation to mitochondria, they change conformation radically. BAX changes its N-terminal conformation so that three α -helices can insert into the outer mitochondrial membrane. This step, much like the translocation step, can still be reversed and the cell may at this step exit from apoptotic commitment. BAK has also been found to profoundly change conformation so as to accommodate membrane insertion mechanisms. Interestingly, BCL-XL and BCL-2, which are also known to translocate to the mitochondria like BAX in order to maintain its inhibition, are also found to insert into the mitochondrial membrane. Unlike BAX and BAK, however, these anti-apoptotic Bcl-2-family members do not oligomerize. Instead, the main model suggests that both BCL-XL and BCL-2 inhibit BAK and BAX chain elongation respectively by inserting into the mitochondrial membrane. Relief of this step of inhibition is found to engage the cell into entering apoptosis (Youle and Strasser,

2008). The Bcl-2-family interaction with mitochondria regulates apoptosis through changes in the integrity of the outer mitochondrial membrane. The release of various factors and proteins follows, and this leads to the activation of the executioner caspases: the last step in the initiation of the apoptotic process.

1.2.3 Mitochondrial membrane permeabilization and executioner caspases

All roads lead to caspases. The activation of caspases is the central event of apoptosis, whether intrinsic or extrinsic. These proteases coordinate disassembly of cells from the inside-out. In the intrinsic pathway, it is the release of a number of proteins from mitochondrial-sequestration that is the main cellular event leading to full caspase activation. Apoptosis through this pathway is dependent on the balance between pro- and anti-apoptotic members and conformational changes in some Bcl2-family proteins as discussed previously. This has an effect on mitochondrial integrity that allows for the release of cytochrome c and other caspase-regulatory proteins, subsequent resulting in the activation of caspases. The extrinsic-pathway, on the other hand, can either bypass Bcl2-family proteins and lead to direct activation of caspases, or it can intersect the intrinsic pathway through regulation of one Bcl2-family member, BID, and lead to caspase activation alongside it (Kurokawa and Kornbluth, 2009).

Release of proteins leads to effector caspase-3 activation and nuclear condensation. Following the intracellular stress-related decision to enter apoptosis, BH3-only protein recruitment, BAX/BAK insertion into the outer mitochondrial membrane, BCL-2/BCL-XL inhibition, oligomerization and pore formation on the organelle, the cell is committed to enter apoptosis and this is mostly irreversible. Release of some critical proteins leads to the inhibition of inhibitor of apoptosis proteins (IAPs) on one hand, and to nuclear condensation on the other.

IAPs have a hand in basally inhibiting caspase-3 activation, preventing it from cleaving downstream targets which include effector caspases such as caspase-9, or posttranslational modifiers such as phosphatases and kinases. XIAP binds and neutralises caspases 3 and 9, but is itself inhibited by the mitochondrially-released Second Mitochondria-Derived Activator of Caspase (Smac) following outer mitochondrial membrane permeabilization.

Amongst the proteins released from mitochondria are nuclear-bound proteins that mediate condensation followed by fragmentation of the nucleus, one major hallmark of apoptotic cells. Apoptosis inducing factor (AIF) is one such protein released from mitochondrion holding which is then targeted to the nucleus. It signals the cell to condense the nucleus and to fragment DNA. EndoG is a nuclease that is sequestered in mitochondria of healthy cells and at release it is known to actively translocate to the nucleus. It has been found to cleave chromatin DNA in large scale and to cause nuclear condensation during apoptosis. Nuclear condensation and fragmentation is a requisite for successful completion of the apoptotic process, and for effective disposal of the cell (Kurokawa and Kornbluth, 2009).

All in all, programmed cell death is reliant on intrinsic and extrinsic pathways that act in parallel to produce cell death through progressive dismantling of cellular components. This has the ultimate goal of recycling the cellular building blocks for an effective apoptosis. In broad terms, it is controlled by Bcl-2-family proteins, is regulated through a finely tuned balance on the mitochondrial outer membrane and mediated by the activation of caspases.

MAP4K3, as a well-established MAPK, was found to be an upstream mediator of the signalling pathway to mitochondrial apoptosis from UV-, and other, induced stresses. Interestingly, it is also thought to signal to mTOR. To understand this signalling branch, we will first explore the regulatory mechanisms that govern mTOR and then we will elucidate the downstream effects of this axis.

1.3 Regulation of TORC1-dependent growth

Target of Rapamycin Complexes 1 and 2 (TORC1 and TORC2) integrate a wide variety of signals and uses differential inputs to regulate growth (Figure 5). TOR, its main component, is a beast of a kinase that has evolved to receive vastly different intracellular sensing inputs and to relay them to effectors that lead to specific downstream consequences. Two of the major and best established consequences of TOR signalling are growth and protein synthesis. Cellular growth can be defined broadly as an increase in overall mass, size, anabolic energy potential and replicative likelihood of a cell. mTOR also has direct control over protein synthesis by determining the state of the translational machinery. Both seem to be largely related to each other, and one exists when the other has been engaged by the cell. Regulation of the pathway is very important in determining the right commitment from the cell, and mTORC1 acts in a different way to mTORC2.

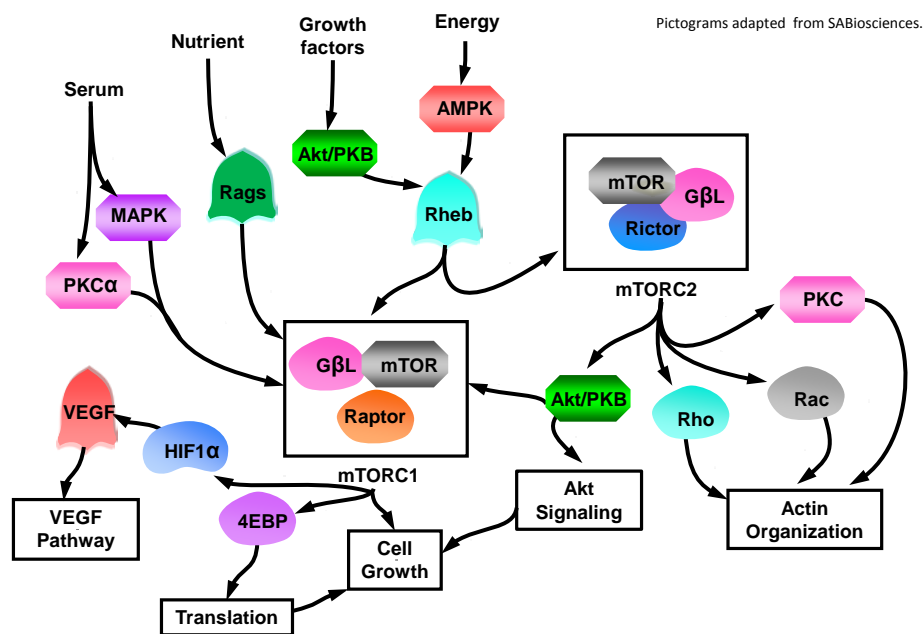
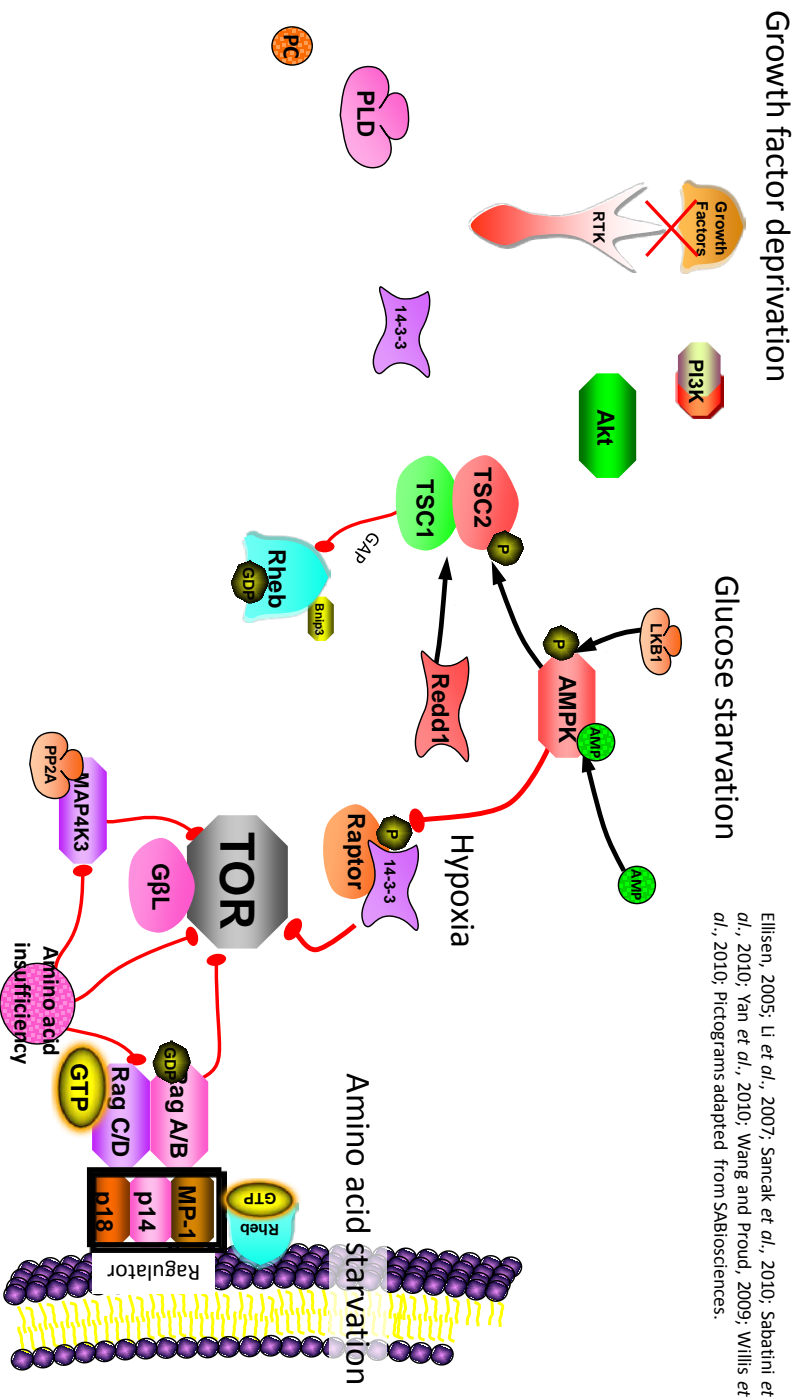


Figure 5: mTOR pathway upstream regulation and downstream effects overview. mTOR forms two distinct ternary complexes, mTORC1 and mTORC2. Depending on its binding partner, its regulation and effects are different. Generally, positive upstream regulatory signals (Energy, Growth factor, Nutrient and Serum signalling) activate mTORC1 and mTORC2 for induction of growth, translation cellular reorganisation and proliferation, whilst negative regulation shuts mTOR signalling off.

In regulating mTOR, there are growth-factor, hormonal, mitogenic and nutrient - sensing pathways and, through a number of binding partners that form the TOR complexes, it can incorporate various signalling pathways and coordinate responses

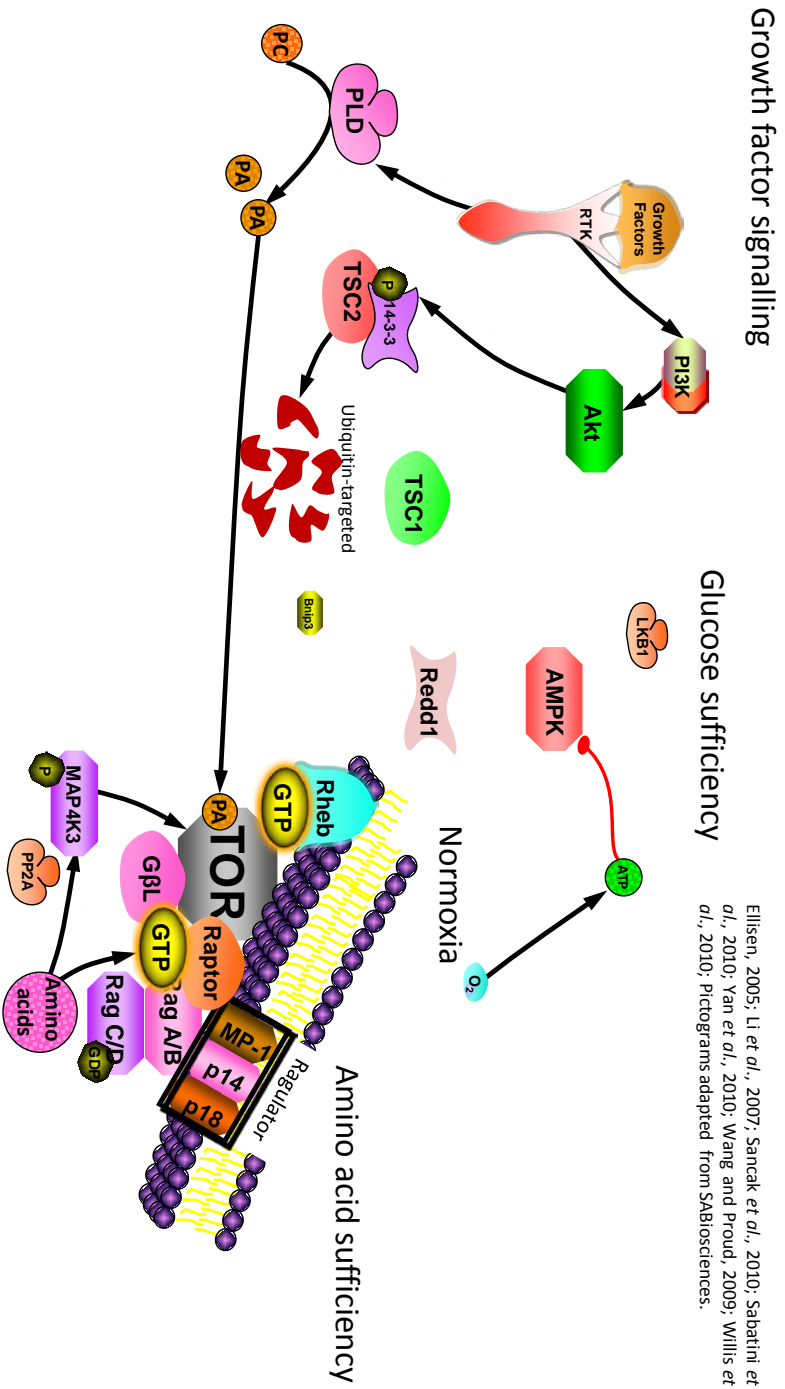
related to the growth of a cell in a number of different ways. These input signals are ultimately integrated into TORC1 through mediator proteins that are directly upstream of the complex and that ultimately control the growth of a cell. These signalling pathways are important in understanding TORC1-dependent growth responses in a cell. They converge onto small GTPases that act as molecular switches that relay a simple binary signal – ON or OFF (Sengupta *et al.*, 2010; Figures 6 and 7).

MAP4K3 has recently been found to participate in amino acid-dependent signalling to TORC1 and to have an influence on the growth of a cell (Findlay *et al.*, 2007; Yan *et al.*, 2010). It has also been involved in targeted, TORC1-dependent, gene expression changes linked to apoptosis (Lam *et al.*, 2009) which may well be tied to the translation machinery found downstream of TORC1. Understanding the TORC1 regulatory pathways is essential to pinpoint where MAP4K3 acts and its exact contribution.



Ellisen, 2005; Li *et al.*, 2007; Sancak *et al.*, 2010; Sabatini *et al.*, 2010; Yan *et al.*, 2010; Wang and Proud, 2009; Willis *et al.*, 2010; Pictograms adapted from SABiosciences.

Figure 6. TORC1-regulating pathways. TORC1 is negatively regulated by a multitude of different signals that result in TORC1 mislocalization and Rheb inactivation. Growth factor deprivation does not engage the RTK-PI3K-Akt axis nor the enzyme PLD. TSC2 is not targeted by Akt and thus is free to interact with its partner TSC1 forming the TSC complex. In glucose starved conditions, and also under hypoxic conditions, the AMP/ATP ratio is high and the AMP-sensitive AMPK changes conformation to accommodate AMP binding. This exposes the catalytic subunit to phosphorylation by LKB1 for activation of its kinase domain. It can then phosphorylate Raptor, leading to sequestration by 14-3-3 proteins and dissociation from TOR. Raptor is needed for amino acid-dependent recruitment of TORC1 to lysosomal membranes where active Rheb resides. Furthermore, in hypoxic conditions, Redd1 is upregulated by HIFs and promotes TSC2 stabilisation to TSC1 by being responsible for the dissociation from growth factor-induced binding to 14-3-3. Under the same glucose-starved and/or oxygen-deprived conditions AMPK activates TSC2 promoting TSC1-TSC2 GAP activity towards Rheb. Another way Rheb is inhibited is through binding of Bnip3, a BH3-only protein whose expression is induced by HIFs under hypoxic conditions. The Ragulator-bound Rag complex localises to lysosomal membranes, where active Rheb is also believed to reside. In amino acid starved conditions it is found in its inactive form (RagA or B are GDP-bound, and Rag C or D are GTP-bound) and does not act as a docking site for TORC1. Finally, a novel protein MAP4K3 is inhibited by amino acid insufficiency via dephosphorylation by PP2A which itself inhibits TORC1, possibly by acting through Rags.



Ellisen, 2005; Li *et al.*, 2007; Sancek *et al.*, 2010; Sabatini *et al.*, 2010; Yan *et al.*, 2010; Wang and Proud, 2009; Willis *et al.*, 2010; Pictograms adapted from SABiosciences.

Figure 7: TORC1-regulating pathways. TORC1 is positively regulated by a multitude of different signals mainly converging on Rheb. For downstream consequences to occur, TSC complex-mediated inhibition must be relieved. Rheb-facilitated activation must be present and amino acid sufficiency signals must recruit TORC1 to specific cellular locations for activation by Rheb and Rags. Under growth factor stimulating conditions, RTKs activate PI3K-Akt axis which results in a key phosphorylation on TSC2 that promotes 14-3-3 binding, relieving binding to TSC1 and TSC complex formation. Evidence suggests that TSC2 may also be targeted to the ubiquitin-proteasome. TSC complex does not form and it cannot inhibit TORC1 through its GAP activity on Rheb-GTP. RTKs also mediate activation of phospholipase-D and phosphatidic acid (PA), a product of PLD, binds directly to TOR on the FRB domain. Interestingly, PLD is itself needed for partial activation of TOR, and it is thought PA may have a role to play in this. Under normoxic conditions, Redd1 does not activate TSC1-TSC2, and its hypoxic-mediated transcription is stopped leading to reduced levels over time. Also, normal oxygen levels lead to relief of Bnip3-mediated inhibition of Rheb and also to consistent mediated inhibition of Rheb and glycolysis. Under glucose sufficiency, the low AMP/ATP ratio does not allow for AMPK activation by LKB1 and subsequent activation of the Rheb-inactivating complex TSC1-TSC2. Amino acid presence contributes to activation of TORC1 through a number of different ways. First and foremost, an unknown mechanism recruits TORC1 through Raptor to lysosomal membranes where it can interact with the Rag heterodimer and Rheb-GTP. Rags A or B and C or D are held together by the Ragulator scaffold which is membrane-bound and brings Raptor-bound TOR to the membrane for activation by Rheb. Finally, there is a considerable effect from MAP4K3 amino acid regulation of TORC1. It remains active in the presence of amino acids and activates TORC1 possibly through Rags.

1.3.1 Growth factor regulation of growth

Growth factor presence signals to TORC1 in a way that mirrors abundance. In multicellular organisms it allows for anabolic growth, protein synthesis and lipid and nutrient storage to occur at the level of the individual cell. The whole axis is mostly reliant on the GTPase Activating Protein (GAP) activity of the heterodimeric TSC1/TSC2 complex towards Rheb. Signals of growth factor sufficiency inhibit TSC1/TSC2 which cannot deactivate the Rheb-GTP switch. Other signalling networks exist, however, that are parallel to TSC in mediating growth factor signalling to TORC1.

TSC2 mediates basal inhibitory signalling to Rheb that is overcome through growth-factor derived Akt activation. Growth factor signalling to a cell is an external stimulus that needs a specific receptor-ligand interaction. This binding at the cell surface can then coordinate and initiate signalling responses downstream. These inputs eventually converge onto the tuberous sclerosis proteins 1 and 2. These form a complex that inhibits activation of the small GTPase Rheb. Rheb is bound to GTP when active and this has a direct activating effect on TORC1. TSC2, when bound to TSC1, promotes the exchange of GTP for GDP through its GAP, rendering Rheb unable to activate mTORC1. Activation of receptor tyrosine kinases by growth factors leads to the formation of membrane-anchored lipid by-products that contain Pleckstrin homology (PH) domains needed for the recruitment and activation of Akt, and of its activator Phosphoinositide-dependent kinase-1 (PDK1). Akt is then found to, not only activate TOR directly, but also to mediate inhibition of TSC2 via phosphorylation. Although it is still not entirely clear how TSC2 is inhibited, it was found that phosphorylation by Akt caused a decrease in the binding affinity between TSC1 and TSC2, and that this was responsible for ubiquitin-mediated targeting of TSC2 to the proteasome. Other mechanisms exist that are partly independent of TSC, but most growth factor-mediated regulation converges onto TSC (Sengupta *et al.*, 2010). mTORC1, however, is not only controlled at the level of systemic-wide regulation. Signalling networks exist that relay the cellular availability of nutrients. Many of these are still unclear, but the regulatory system around mTORC1 is becoming ever so clear and exciting with time.

1.3.2 Nutrient regulation of growth

Unlike growth factor signalling to TOR, amino acid signalling is less well understood. While growth factor signalling converges onto TSC1/TSC2, it is the Rag GTPases that integrate signals of nutrient availability and transmit them to TORC1. Nutrient sensing to TOR is a mechanism that is clearly needed for an appropriate metabolic and protein synthesis response. In oversimplified terms, without oxygen and glucose, energy cannot be produced to drive metabolic growth. Without amino acids, there cannot be any protein synthesis.

Amino acid-signalling to mTORC1 is dependent on Raptor/Rag interaction-mediated relocation to active Rheb pools. As for amino acid-signalling to TOR, it is the co-localisation of mTORC1 to sites where active Rheb is present that is of particular importance. The Ragulator, formed of a heterotrimeric complex, acts as a scaffold to a dimeric Rag complex that can be formed of four different Rag GTPases (Rag A, B, C and D). These, when together, can be complexed as Rag A or B interchangeably with Rag C or D and it can reside on lysosomal membranes through interactions with the Ragulator. It is their GTP/GDP state that is important for activating or inhibitory signalling to TORC1, and this is dictated by amino acid levels. During amino acid insufficiency, RagC/D is in its GTP-bound form whilst RagA/B is GDP bound. When in amino acid sufficiency, the GTP/GDP state is inverted but the exact mechanism that controls the switch from GTP to GDP for RagC/D and GDP to GTP for RagA/B is still unknown. Recently, new discoveries unveiled great insights into how these Rags control the activation state of TORC1, first through direct binding to Raptor (Sancak *et al.*, 2008), a defining component of TORC1, and secondly through the Ragulator scaffold complex that targets it to the lysosomal membranes (Sancak *et al.*, 2008; Sancak *et al.*, 2010) where active Rheb resides. The whole axis is also independent of TSC1/TSC2, as their loss does not make up for a loss of amino acids. Because the TSC is known to inhibit mTORC1, then its loss may lift amino acid signalling-driven inhibition during amino acid starvation. Interestingly, it was found that amino acid signalling is completely independent of the TSC axis to mTOR. What is particularly interesting is that amino acid-, Ragulator- and even Rag-independent targeting of mTORC1 to the lysosomes leads to activation of its downstream components. Yet, for amino acid signalling to activate TORC1 Ragulator and Rags are absolutely necessary, and constitutively active Rags activate it in amino acid insufficient conditions, making them directly upstream of TORC1. What lies upstream of

that and has the ability to sense amino acid level changes, however, is still unknown. A new protein, p62, acts as a scaffold and was recently found to mediate recruitment and binding of mTORC1 to the lysosomal membrane where active Rheb is found, besides the Ragulator (Duran *et al.*, 2011). How the two complexes, Ragulator and p62, can co-exist is not entirely understood. They are believed to mediate the same effect and can be engaged interchangeably.

MAP4K3, on the other hand, was involved in amino acid signalling to TORC1 but it does not seem to be found upstream of Rags. It is unknown what exact role it may play in the greater context of things, and there is still debate over its exact location and role on the pathway.

1.4 mTORC1 and posttranscriptional control of gene expression

Tight regulation of mTORC1 by various cellular inputs determines whether protein synthesis can occur and cell growth be achieved. Gene expression at the posttranscriptional level is mostly controlled by cap-dependent translation initiation. There are various factors that regulate and ultimately influence translational control of gene expression. More importantly mTORC1 has control over translation initiation, and coordinates a highly choreographed and precise mechanism to both maintain cellular stability and to respond to different conditions.

1.4.1 Regulatory steps of translation initiation

In relation to translation initiation, TORC1 is known to be responsible for formation of the eukaryotic initiation factor 4F complex (eIF4F), which is then assembled onto an mRNA. A 43S pre-initiation complex, formed of a ternary complex (TC) under the control of the eIF2 α kinase and of a multifactorial complex (MFC) that brings the initiator transfer RNA, is recruited and bound to eIF4F forming the 48S. This then recruits the 60S through eIF5B and translation can initiate (Figure 8; Sonenberg and Hinnenbusch, 2009).

eIF4F complex formation depends largely on mTORC1. mTORC1 has been found to control translation initiation mainly through relief of inhibition of mRNA cap-binding eIF4E, activation of the major eIF4G scaffolding frame and activation of the ribosome formation-promoting ribosomal S6 kinases (S6Ks). Indirect phosphorylation of the eIF4G scaffold protein creates a platform onto which other eIFs can bind and form the completed eIF4F complex. Direct phosphorylation of the 4E-binding proteins (4E-BPs) on Thr37 and Thr46 by TORC1 is the priming reaction that then leads to further phosphorylation events that result in dissociation from inhibitory-binding to eIF4E. This lifts translational repression by allowing the cap-binding eIF4F-associated eIF4E to bring the complex to the cap and to promote its stability by preventing exonuclease-mediated degradation of the mRNA. This, besides preventing mRNA degradation, also promotes recruitment of further eIFs to the target mRNAs (Sonenberg and Hinnenbusch, 2009).

Sonenberg and Hinnebusch, 2009;
Pictograms adapted from SABiosciences.

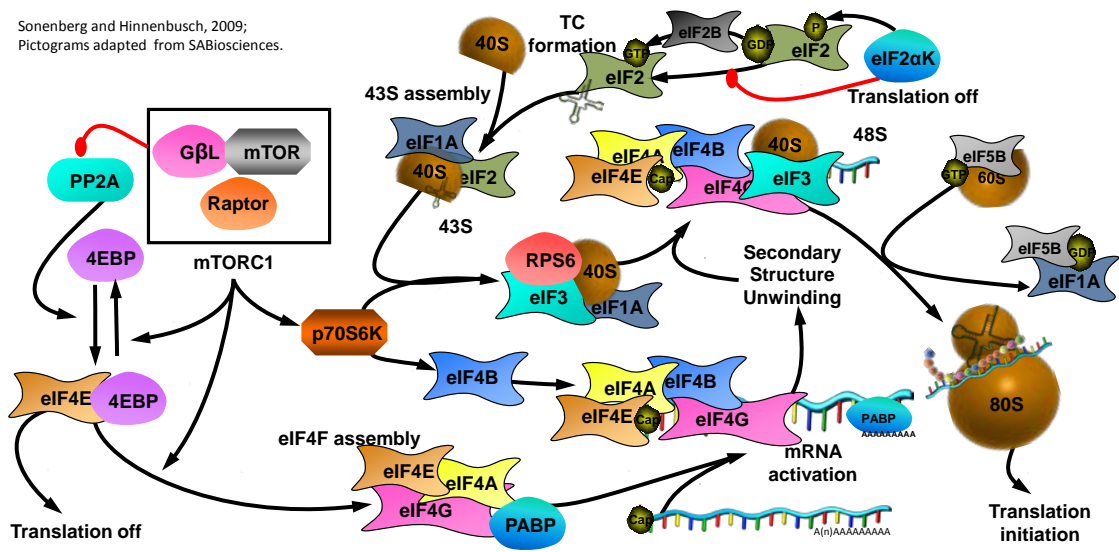


Figure 8: Translation initiation mechanism and regulation. Translation initiation depends on the successful and timely formation of initiation complexes and their recruitment to ribosome (sub)units. Eukaryotic initiation factors (eIFs) 4E and 4A are brought together by scaffolding protein eIF4G forming the eIF4F complex. Together with eIF4B, eIF4F binds to and activates mRNA containing a cap and a poly-A tail. eIF4G mediates the interaction between cap-binding eIF4E and poly-A tail-binding PABP, thus circularising the mRNA. The helicase eIF4A unwinds secondary structures making the mRNA able to bind the 43S complex. The 43S is formed of various eIFs (1, 1A, 3 and 5) as well as the ternary complex (TC). The TC is formed of the initiating methionine and eIF2 bound to GTP, and its assembly to the rest of the 43S is facilitated by eIF1A. Once the 43S comes together, rpS6 mediates the recruitment to the eIF4F bound mRNA, creating the 48S complex. eIF5B-GTP then permits 60S recruitment and joining to the 48S forming the final stage 80S and initiating translation. The whole process is regulated by factors controlling eIF4F assembly and TC formation. mTORC1 is the main architect behind formation of the eIF4F. When receiving positive regulatory signals mTORC1 directly mediates the formation of eIF4F by freeing eIF4E from binding to its inhibitory partners, the 4E-BPs. It does so by directly phosphorylating its target 4E-BPs, dissociating them from eIF4E and by inhibiting the phosphatase PP2A from dephosphorylating and reactivating 4E-BPs. mTORC1 also activates p70S6K which promotes eIF4F assembly through eIF4B and also activates rpS6 to form the 43S. TC formation is principally regulated by the eIF2α kinases which, when activated by stresses, inhibit the formation of the Met_i-eIF2-GTP complex by the eIF2B.

Regulation of 48S complex formation is achieved through formation, recruitment and binding of 43S to the eIF4F complex in an eIF2α-dependent manner. Another major step of regulation of translation initiation depends on formation of a 48S complex. This is highly conditional on the state of the small GTPase eIF2, whether it is in its active GTP state or inactive GDP-bound form. For the formation of a complete 80S complex, the 43S pre-initiation complex (PIC) must first be formed, recruited and then joined to the eIF4F cap-bound complex to form the 48S unit. These mainly sequential steps are achieved through eIF2 modifications by nutrient-sensing kinases, eIF3-initiated recruitment and eIF5 catalyzed joining to the fully formed eIF4F.

Formation of the 43S subunit depends on ternary complex (TC) formation, and this is a major regulatory step in translation initiation. The TC is formed of an active, GTP-bound form of eIF2, and the initiating methionine tRNA. Regulation of TC formation comes from eIF2B and its interactions with the guanosine-bound eIF2 and from upstream kinases that control whether eIF2B and eIF2 are bound (inactive) or unbound (active). It is clear that eIF2B catalyzes the displacement of GDP for GTP, and in doing so activates eIF2 for 43S PIC formation. Kinases that sense stress conditions such as those

arising from viral infections or amino acid and hemin deficiencies for instance, phosphorylate eIF2 α keeping the eIF2-GDP-eIF2B complex bound together. This inhibits eIF2B ability to activate eIF2 and is directly linked to overall inhibition of translation. Following its formation, various initiation factors are recruited onto the TC to form the multifactor complex (MFC). Keeping all members of the PIC bound together is likely achieved through eIF3 with its multiple sites of physical interactions for each of the members of the PIC. Additionally, it is thought that recruitment to the mRNA is dependent on interactions between eIF3 of the PIC and eIF4G of the cap-bound eIF4F complex. eIF3, a member of the 43S (composed of MFC and 40S), has been found to bind eIF4G directly making it a likely responsible for 43S recruitment to activated mRNA. Factors of the eIF4F are then known to mediate mRNA circularisation for their activation and subsequent 48S formation (Sonenberg and Hinnebusch, 2009).

Circularization of the mRNA is a critical step needed for assembly of the 48S complex. The PIC, formed of the ternary complex (TC) and eIFs 1, 1A, 3 and 5, is only recruited to active, circularised mRNAs. Activation of the mRNAs depends on the successful formation of the eIF4F complex (as described previously) and its simultaneous binding to the cap and polyA-tail. PolyA-binding protein (PABP) has been shown to be partly responsible for this regulatory step, both directly by promoting binding of eIF4E to the cap, and indirectly by stimulating the formation of 48S and subsequent 60S subunit joining. This is thought to be achieved by the interactions with eIF4G, stimulating recruitment of eIF4G to the target mRNA and more importantly increasing the affinity of the eIF4E to the cap. A mutation on PABP (M161A) has been shown to abolish interactions with eIF4G and cause reduced interactions with the cap, likely through ineffective conformational states that inhibit strong binding by its eIF4E binding-partner. Furthermore, PABP seems to be needed for ribosome recycling on the same active mRNAs, and there is noticeable reduction in sustained translation initiation in uncircularized mRNAs from PABP-depleted extracts (Kahvejian et al., 2005). Following PABP-enhanced mRNA activation and 43S recruitment, initiation factors of the MFC consolidate interactions between the eIF4F-bound mRNA and the 43S.

Joining of the 43S to the eIF4F has been shown to be dependent on interactions between the different initiation factors of the two distinct complexes. In particular eIF3-bound eIF5 is shown to be recruited to eIF4B as well as to the eIF4G scaffold protein and to directly mediate finalized subunit assembly. S6K1 has a distinct role in this. It activates eIF4B on Ser422 by enhancing its interactions with eIF3 as shown by mutational studies

on S6K1. Thr389 is known to be an activating phosphorylation site that is mediated by mTOR. By inducing a mutation that causes a permanently phosphorylated-like conformational change and a separate one that impedes its phosphorylation, it was shown that activity of S6K1 is dependent on being unbound from the PIC. When phosphorylated, it dissociates from the 12-protein eIF3 complex and can phosphorylate downstream targets. Amongst these, interestingly, is eIF4B. eIF4B then proceeds to interact with eIF3 and to maintain it associated to the eIF4F. This gives rise to a stable 48S complex that is ready for scanning of the mRNA and AUG recognition. Interestingly, eIF4B activation also regulates helicase activity arising from eIF4A, linking this nicely to subsequent steps of initiation. eIF4A is in fact required for correct unfolding of secondary structures along the mRNAs as the tRNA-containing 43S complex scans the transcript for the initiation site. Once this is achieved, and the AUG codon has been identified, the 60S is recruited in an eIF5B-dependent manner and the ribosome can enter final stages of formation (Sonenberg and Hinnebusch, 2009).

80S complex formation is dependent on eIF5B and A-site opening for tRNA recruitment. Final stages of complete ribosome formation include displacement and recruitment of further initiation factors for ultimate 80S complex formation. Following successful AUG recognition, eIF2 is hydrolysed to its GDP-bound form and released through eIF1 dissociation from the complex. eIF2 then cycles back to control ternary complex formation and 43S unit joining in another round of translation initiation, as described above. Meanwhile, it is GTP-bound eIF5B that brings the 60S to the 48S PIC through interactions with eIF1A, and this leads to release of eIF1A from the A-site and complete formation of the 80S (Sonenberg and Hinnebusch, 2009).

Having described the MAPK functions and phylogenetic relationships of this Ste20 family protein with other members of this kinase family, the role of Bcl-2-family proteins in intrinsic and extrinsic apoptosis pathways, the regulation of mTORC1 and its downstream effects on translation initiation, it is now time to look at how it all fits together. Understanding the published data and what their implications are is crucial to making suitable hypotheses. Here's a review of the published physiological functions of MAP4K3. They are put into context with the biochemical properties of MAP kinases, the pathways to mitochondrial apoptosis, and the regulation and downstream effects of mTORC1 previously described.

1.5 Physiological effects conferred by an upstream activator of MAPK signalling and regulator of TOR pathway

Physiologically, MAP4K3's role is very complex. While intricately linked to both growth and overall size of the organism, it is also responsible for regulating and transducing signals that promote cell cycle arrest and cell death. It has also been linked to immune regulatory mechanisms and to an EGFR-ERK inhibitory role. As mentioned earlier, it also has a part to play in the yeast mating process. Overall, it seems to play a role of signal transducer and to be at the crossroads of various signalling pathways. A picture of the signalling network is starting to unveil itself from its orthologues across different species (Figure 9).

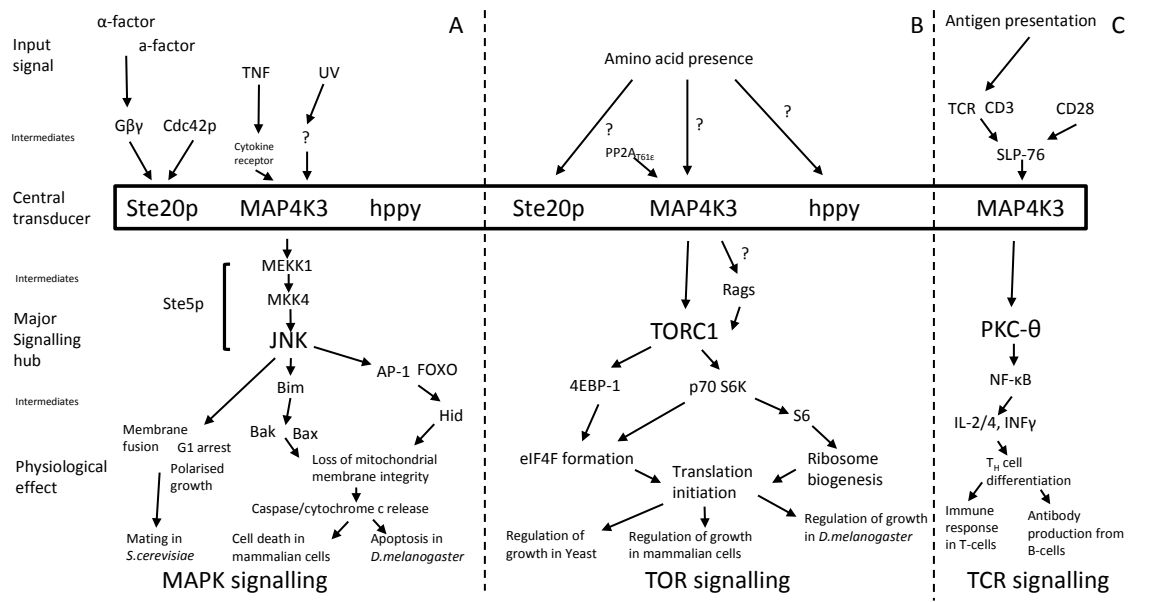


Figure 9: MAP4K3 orthologues in yeast, fruit fly and humans: signalling pathways and their physiological effects.

A) MAP kinase signalling and physiological effects in budding yeast, humans and flies. MAP4K3 has been linked to apoptosis in humans and flies. In yeast it has been linked to mating responses. In all three organisms, the JNK (Bsk in drosophila, Fus3p in *S.cerevisiae*) is activated via MEKK1 (Ste11p in *S.cerevisiae*) and MKK4 (dMKK4 in drosophila, Ste7p in *S.cerevisiae*) by MAP4K3/Ste20p/hppy. In humans this leads to phosphorylation of Bim, whilst in drosophila apoptosis is thought to be achieved through AP-1 and FOXO-dependent transcription of Hid. A cascade of events leads to OMM rupture, release of caspases and cell death. In yeast, Fus3p activation leads to G1 arrest, polarised growth and membrane fusion.

B) MAP4K3/Ste20p/hppy mediates amino acid presence to TORC1 (mTORC1 in mammals, dTORC1 in *D.melanogaster*) and activates it (possibly through Rags). In conditions of nutrient sufficiency, TORC1 mediates the signal to downstream 4E-BP1 and S6K for eIF4F formation on one side, and ribosome biogenesis on the other resulting in translation initiation and overall cellular growth.

C) Antigen presentation to T cells leads to TCR signalling and activation of PKC- θ through MAP4K3. NF- κ B-dependent transcription of key cytokines leads to T_H cell differentiation and appropriate T and B cell function.

1.5.1 Ste20 kinase signalling in yeast and the mating process

Saccharomyces cerevisiae is a single celled eukaryote that depends on haploid cells producing peptide pheromones to signal neighbouring haploid cells for mating. Two types

of pheromones exist: the a-factor and the α -factor. These exist as 12 and 13 amino acid long peptides called α and a-factors respectively and are secreted to attract cells of the opposite mating type. After expression of the pheromone encoding genes they are actively transported by Ste4, an ATP-dependent pump, and these can bind freely to the receptors of neighbouring yeasts of the appropriate mating type. It is this binding to the G-protein-coupled Ste2 receptor that initiates a cascade of events that activates the Fus3 MAPK pathway (Figure 9A). This controls expression changes that then allow mating of *S.cerevisiae*, formation of a diploid cell, chromosome reshuffling and the eventual birth of two daughter cells.

The Fus3 pathway is engaged following pheromone-pheromone receptor interactions which create dissociation of G β and G γ from the G α , promoting recruitment of the Cdc42-bound Ste20p and of the MAPK module as mentioned earlier. Following activation of Ste20p, this can then sequentially phosphorylate downstream targets of the Ste5p module that results in Fus3p activation. This is then followed by targeted changes in gene expression that cause G1 arrest and promote membrane fusion resulting in yeast mating (Wang and Henrik, 2004).

Ste20p has a dual role in mating – both initiating the cellular responses that lead to up to mating such as G1 arrest and transcriptional activation of target genes, as well as inducing polarized cell growth and the facilitation of membrane fusion. All of these pathways mediated by Ste20p converge onto the yeast JNKs.

In mammals and fruit flies JNKs have profoundly different roles, and they are varied. They have been involved in inflammation, neurological disorders, tumourigenesis and cell migration to name a few. One very powerful involvement was found in cell death, and there is mounting evidence to MAP4K3's contribution to this.

1.5.2 MAP4K3 signalling in mammalian cells, the JNK pathway and cell death

The c-Jun N-terminal Kinase (JNK) pathway, also known as stress-activated protein kinase (SAPK) pathway, is one of three mitogen-activated protein kinase (MAPK) cascades (Erk and p38 being the other two) and they are highly conserved across eukaryotic species. JNKs are known to mediate signals for a number of different cellular outcomes. They are known to activate a number of transcription factors and to have

immediate control over transcription and gene expression. They can also interact with a number of Bcl-2-family members for control over cell survival and apoptosis.

JNK is known to be activated by a direct JNKK, which is in turn activated by a JNKKK and itself in turn by a JNKKKK in a classical MAPK cascade of phosphorylation events. Mitogen-activated protein kinase 4 (MKK4), among a number of other JNKKs (or MAPKKs also MAP2Ks), is known to be directly upstream of JNK and to activate it by phosphorylation. Upstream of that is mitogen-activated protein kinase kinase kinase 1 (MEKK1) and that directly phosphorylates MKK4 (Davis, 2000).

MAP4K3 is first identified as a MAP4K, as a signal transducer in the JNK pathway that directly phosphorylates MEKK1 and whose kinase activity is induced by UV radiation and TNF α (Diener *et al.*, 1997). It also binds endophilin I through a proline rich sequence and this is needed for activation of the JNK pathway by MAP4K3 (Ramjaun *et al.*, 2001). More recently, it was identified as an inducer of mitochondrial cell death that can also inhibit proliferation and is likely to be tightly regulated by being targeted to the ubiquitin-proteasome (Lam *et al.*, 2009; Figure 9A).

MAP4K3 is a potent inducer of apoptosis with an anti-proliferative effect. To identify novel kinase mediators of cell death, Martins and colleagues (2009) infected U2OS cells with shRNA-carrying viruses targeting human kinases, selected the cell lines effectively expressing the shRNAs and then further selected for cells resistant to DNA damage-induced cell death. By sequencing the shRNAs that are expressed in the UV damage-resistant cells they identify MAP4K3-targeting shRNAs to be enriched in UV-resistant cells. Downregulating MAP4K3 also revealed increased resistance to apoptosis, further supporting their findings from the phenotypic screen. They exposed MAP4K3-silenced cells to UV or cisplatin, a DNA crosslinking and apoptosis-inducing chemical agent, at intensities and concentrations that would kill most of the control cells. The MAP4K3 cells showed a 3 to 3.5-fold (UV) and 2.5 to 3-fold (cisplatin) increase in survival. Furthermore, they also noted overall high abundance of shRNAs targeting MAP4K3 in cells even before exposure to UV and they argue that this may be indicative of a proliferative advantage in MAP4K3-silenced cells. *MAP4K3* could be a proliferation inhibiting gene and they decided to assess proliferation using bromodeoxyuridine (BrdU) incorporation. They find that there is an almost two-fold increase in DNA synthesis in MAP4K3-suppressed cells, indicating that it may be responsible for some anti-proliferative effects in cells.

Through this RNAi screen, they find that MAP4K3 mediates apoptosis induced by DNA damage, and that it has an antiproliferative effect. Through a series of overexpression experiments, they then try to understand how MAP4K3 induces cell death.

MAP4K3 induces apoptosis through the intrinsic cell-death pathway, mostly via its kinase activity. After identifying MAP4K3 loss as a selective proliferation and survival mechanism following DNA damage induction, they decided to investigate how it promoted cell death. To assess apoptosis they concentrated on the morphological changes in nuclei and used these as apoptosis detection markers. Pyknosis, literally condensation, of nuclei was detected (using Hoechst, a fluorescence DNA-binding compound) in full-length wild-type transfections, accounting for 65% of condensation, and C-terminal truncated (but kinase intact; 70%) versions of MAP4K3-GFP-transfected U2OS cells (Figure 10). These were very similar to caspase-8 transfected cells (75%), but significantly less in kinase inactive (30%), N-terminal truncated (8%) and controls (GFP; 8%). Furthermore, this condensation effect was also reversed by treatment with zVAD-fmk, a caspase inhibitor that leaves mitochondrial modifications intact, in full-length MAP4K3-GFP-expressing cells in a similar way to caspase-8 transfected and zVAD-fmk treated cells.

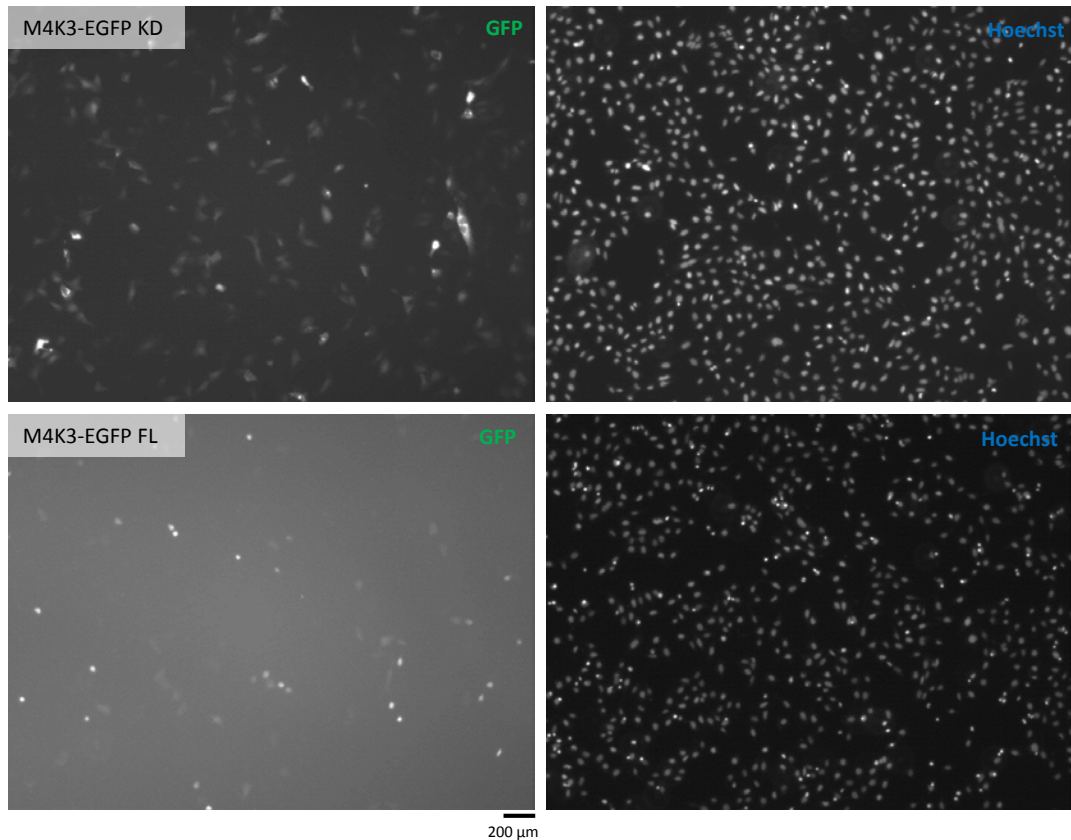


Figure 10: MAP4K3 induces chromatin condensation in U2OS cells in a kinase-dependent manner. Cells positive for transfection correlate highly (60-70%) with condensed chromatin in kinase-active, but not inactive (25-30%), transfections. Cells were seeded onto 6-well plates to obtain 70% confluence 24h later, and were then transfected using 1ug DNA and 1uL Lipofectamine 2000. 24h post-transfection they were fixed in 10% formalin for 20min and Hoechst 33342 stained in 10ug/mL for 10min.

They then expressed the kinase active and kinase inactive forms of MAP4K3-GFP and looked at BAX activation by immunostaining using an antibody that can only detect active BAX. They found that considerable BAX activation was detected in about 70% of MAP4K3-GFP expressing cells, about 60% more than their GFP transfection controls. They also compared the kinase-inactive version of MAP4K3 and found they were very similar (10%) to the GFP control, hinting to a purely kinase-dependent mode of action on activation of the mitochondrial intrinsic cell death-death pathway. To further support their previous findings that MAP4K3 mediates DNA-damage induced cell death through the mitochondrial pathway, they silenced MAP4K3, subjected the cells to UV as previously, looked at BAX activation and found a statistically significant reduction in BAX activation in MAP4K3-suppressed cells.

Finally, they coexpressed MAP4K3-GFP with an RFP-tagged BCL-XL, the inhibiting partner of BAX, and looked at chromatin condensation in green and red

fluorescent cells. BCL-XL was able to rescue (30% cell death) MAP4K3-driven apoptosis in a similar way as in the BCL-XL-RFP and BAX-GFP cotransfections (20% cell death) compared to BAX-GFP and MAP4K3-GFP transfections (70% death). By looking at activation of BAX, Lam *et al.* manage to show that apoptosis due to MAP4K3 is achieved through the mitochondrial pathway (2009). They then investigated whether there was a link with MAP4K3's recently described regulation of mTORC1 (Findlay *et al.*, 2007) and found that it induced posttranscriptional modulation of a number of BH3-only proteins reviewed in the section below, some via mTORC1 (Lam *et al.*, 2009) and one via the extrinsic apoptosis pathway (Lam and Martins, 2009).

1.5.2 MAP4K3-induced control of cell size, growth and protein translation via mTOR regulation

MAP4K3 regulates cell size and growth through a nutrient sensing mechanism that it relays to mTORC1. More recently, it has also been linked to the induction of translation initiation of a group of specific genes. As explained previously, the TOR pathway regulates growth by maintaining a balance between anabolic and catabolic processes and cell size majorly through promotion of translation initiation. MAP4K3 is known to relay signals of amino acid sufficiency and control cell size through mTORC1 in similar manner to mTORC1-specific inhibition, and to activate the mTOR pathway through a number of targets needed for eIF4F translation complex formation (Figure 9B).

MAP4K3 was linked to nutrient-signalling to mTORC1 pathway one decade after its discovery and attribution to the JNK pathway in mammalian cells. mTOR, as discussed earlier, controls cell growth, cell size and translation. It integrates signals from growth factor presence, energy states, oxygen levels, DNA damage-response proteins and amino acid sufficiency to control metabolic responses of cells and either support growth or pause it. Amino acid presence is key to protein translation for obvious reasons, and it makes sense that the mTOR pathway should be regulated according to amino acid availability.

Much is known about the pathway that directly regulates growth-factor sensing to mTOR, since mTOR is important for cellular growth. Amino acid-sensing signalling to mTOR is just as important for cell size and translation initiation, but there are few clues as to how this is regulated. Findlay *et al.* (2007) first identified MAP4K3 as an important player in this and, in conjunction with additional studies performed to elucidate

MAP4K3's role in the regulation of the mTOR pathway, we will attempt to put this serine/threonine kinase in perspective with other known players in the amino acid-sensing pathway to try and understand how it all falls together.

MAP4K3 was first identified as a participant in the mTOR pathway in drosophila cells by screening for regulators of S6K phosphorylation in a growth-factor independent manner. Depletion of *Drosophila* Tsc1 (dTsc1), which is known to be part of a higher order complex with dTsc2 inhibiting Rheb, leads to constitutively active *Drosophila* S6K (dS6K). This is true in mammalian cells as well, where TSC1-2 complex is known to regulate Rheb, a small GTPase, according to the energy state of the cell. As described in the previous sections, the TSC complex has GAP activity that stimulates hydrolysis of the GTP in the active (GTP-bound) form of Rheb to inhibit its ability to activate mTOR. By silencing dTsc1 in the S2 cells, the dTsc complex does not form and it cannot inhibit the mTOR pathway. This is an elegant way to create a system where S6K is active, making it feasible to find new players that have an effect on activation of TOR, and that this putative player in the growth pathway is independent of TSC and hence the growth-factor sensing pathway. By then co-suppressing 200 kinases they identified CG7097, a protein that caused a reduction on the phosphorylation state of S6K in a TSC-independent manner. The closest sequence ortholog in humans was MAP4K3, and they then proceeded to validating these results using human cells. Many experiments were undertaken to understand the extent of MAP4K3 involvement in the mTOR pathway using various human cell lines (293, HeLa and U2OS; Findlay *et al.*, 2007).

MAP4K3 has a distinct mTORC1-dependent role in both activating the translation pathway and regulating cell size under amino acid sufficiency conditions. Lamb and colleagues show that taking MAP4K3 away leads to loss of a key S6K phosphorylation on Thr389 and phosphorylation of S6 by S6K in HeLa (2007). Overexpression experiments show that S6 phosphorylation at key residues Ser235/236 is undertaken in a kinase-dependent manner, alongside S6K activation. In parallel, MAP4K3 overexpression also causes 4E-BP1 phosphorylation and these effects are lost through rapamycin treatments, making them clearly downstream of the TORC1 complex. Inhibitors of the PI3K-PKB pathway (wortmannin) and ERK pathway (PD184352) do not affect MAP4K3 activity on S6K phosphorylation revealing a growth factor-

independent mode of action, further re-enforcing the postulation that this kinase acts through amino acid signalling.

Amino acid presence itself was found to be needed for MAP4K3 activity but not insulin, which is known to inactivate TSC1-2 and stimulate TORC1 signalling. MAP4K3 kinase activity was found to be inhibited in amino acid deprivation conditions but stimulated after re-addition. This effect was registered for both general phosphorylation by MAP4K3 (on myelin basic protein; MBP), as well as specifically for S6K. As expected MAP4K3-dependent phosphorylation onto S6K was rapamycin-sensitive (hence mTORC1 mediated), but MAP4K3 kinase activity was not. This places it upstream of TORC1 but downstream of amino acid signalling.

Finally, silencing of MAP4K3 leads to a decrease in cell size comparable to rapamycin treatment or Rheb silencing, giving further proof that MAP4K3 is an mTORC1 regulator. By affecting cell growth, both through phosphorylation of targets downstream of TORC1 as well as having an effect on cell size, it is clear that MAP4K3 has a major role to play in the regulation of growth. Because this is clearly independent of the TSC complex and PI3K/PKB signalling but highly stimulated by amino acid presence and inhibited by amino acid deprivation, it is apparent that regulation of growth by MAP4K3 is through the amino acid pathway of TORC1 regulation. This, however, raises more questions about amino acid signalling to TOR, and it is still unknown how intracellular amino acid levels are detected.

The next logical step undertaken was to understand how MAP4K3 is regulated in amino acid signalling to TORC1 in order to clarify this level control over translation initiation and cellular growth. To further understand the mechanisms of regulation of amino acid signalling to MAP4K3, Yan *et al.* (2010) turned to identifying (the) key amino acid signalling-dependent phosphorylation event(s) on MAP4K3, finding how this/these are mediated and what regulates it/them.

MAP4K3 transautophosphorylates on Ser170 in an amino acid sufficiency-dependent manner that is specifically sensitive to PP2A PR61ε subunit dephosphorylation and solely reliant on amino acid signals to MAP4K3, not PP2A. Lamb and colleagues identify Ser170, by phosphopeptide analysis on mass spectrometry data of purified MAP4K3, as a critical phosphorylation site for kinase activity. The phosphorylation of this residue was found to be amino acid-dependent. Using an antibody specific to this phosphorylation site that does not detect overexpressed S170A mutant MAP4K3, it was found that amino acid

deprivation caused loss of the phosphorylation whilst re-addition of amino acids for as few as 15min partially restored phosphorylation at this site. This phosphorylation event was independent of Wortmannin, Rapamycin and importantly insulin. This supports the idea that the phosphorylation of Ser170 on MAP4K3 is independent of the PI3K kinases, is undertaken upstream of mTORC1 and, importantly, is growth factor-independent. These results are conformant to the hypothesis of a member of a novel amino acid-dependent regulatory pathway to mTOR that is not on the TSC-Rheb axis.

The phosphorylation itself was determined to be a transautophosphorylation event. Because overexpression of catalytically inactive forms of MAP4K3 are not detected by the phospho-specific antibody, it was tested whether the phosphorylation was self-directed or arising from an upstream Ser170 kinase. By co-expressing a catalytically active and an inactive form of MAP4K3 (GFP and myc tagged for both active and inactive) in 293s they found that in the presence of the catalytically active form the site was phosphorylated whilst not in the catalytically inactive form. Hence, the *trans* Ser170 phosphorylation was an autophosphorylation event. To understand what regulated the amino acid-dependent dephosphorylation of Ser170, which occurred quite rapidly from as little as 5min of amino acid deprivation, they tested Ser170 dephosphorylation, MAP4K3 kinase activity and phosphorylation status of downstream targets S6K and S6 in the presence of okadaic acid. This is a known protein phosphatase 1 and 2A (PP1 and PP2A) inhibitor that selectively inhibits PP2A at specific concentrations. They found that this inhibited Ser170 dephosphorylation and MAP4K3 inactivation, and that S6K and S6 are being kept phosphorylated at residues Thr389 and Ser240/244. Conversely, treatment of purified MAP4K3 with PP2A *in vitro* leads to dephosphorylation of the residue.

Mass spectrometry analysis of myc immunoprecipitated samples that overexpressed myc-tagged MAP4K3 revealed direct binding of both catalytically active and inactive forms of MAP4K3 with PR61ε, a PP2A subunit needed for its targeting to specific substrates. It was also found that this PP2A dephosphorylation effect was specific to the PR61ε subunit and that it was dependent on amino acid levels. In PR61ε co-overexpression experiments, MAP4K3 was more prone to dephosphorylation in amino acid-sufficient conditions than in MAP4K3-only overexpression, and that co-overexpression of another regulatory subunit (PR72) of PP2A had no effect on the Ser170 phosphorylation levels, demonstrating specificity. This effect was also found to be relatively consistent with downstream targets S6K and S6, where their dephosphorylation

by amino acid deprivation was abolished in PR61 ϵ -silencing and exacerbated in PR61 ϵ overexpression.

In conjunction with previous studies on cell size (Lamb *et al.*, 2007), it was found that PR61 ϵ silencing resulted in a moderate increase in cell size in 293s, a result that is consistent with the hypothesis of a PP2A-dependent regulation of MAP4K3. It was then determined that binding with PP2A is needed for amino acid control over MAP4K3 activity. In pull-down experiments, an increasing amount of PP2A was found bound to MAP4K3 with decreasing amino acid presence. Additionally, abolishing binding of PP2A with MAP4K3 by deletion of a C-terminal segment maintained MAP4K3 kinase activity following amino acid withdrawal.

All in all, these studies on MAP4K3 reveal an involvement in the amino acid signalling pathway to mTORC1 that is more complex than initially thought. MAP4K3 activates mTORC1 and regulates growth in an amino acid-dependent manner, and is itself regulated by amino acid sufficiency in a protein phosphatase-dependent manner. Unfortunately, this latest study on amino acid regulation of MAP4K3 is only part of the story. It does not identify the amino acid mediating input signal to MAP4K3 for downstream regulation of growth and translation, which would likely be a major scientific breakthrough in the understanding of a new mechanism for a protein to sense amino acid availability. It rather provides us with an extra regulatory step on MAP4K3 amino acid signal transduction to the TORC1 pathway. Fortunately, this latest study on amino acid regulation of MAP4K3 is only part of the story, and there still are exciting (new) questions to address on the subject matter.

To further understand the biological significance, and possibly the medical applications, of such involvement of PP2A in the regulation of MAP4K3 signalling to TORC1, it would be interesting to understand what regulatory mechanisms lie between amino acids and PP2A-MAP4K3. The next logical steps are to comprehend what controls the PP2A-MAP4K3 association, an effect which may be a novel mechanism of intracellular amino acid level detection in cells, and how MAP4K3 relays the signal to TORC1, which is likely to involve new intermediate phosphorylation targets between them.

MAP4K3 was found to mediate an interesting effect downstream of mTORC1. It was found to dictate selective translation of targets.

MAP4K3 induces cell death through mTORC1-mediated targeted translation of specific genes. In the previous section, we've seen how MAP4K3 participates in apoptosis through the JNK pathway, and how it engages the intrinsic cell-death pathway. We're also starting to comprehend how it regulates growth through TORC1. Yet, in all of these studies, MAP4K3 was looked at as either an inducer of cell death or as a regulator of growth – roles which can be contradictory at times – but never in conjunction to facilitate a physiological role. Its dual role in growth regulation and apoptosis are fundamentally puzzling until we look at the mechanisms regulating MAP4K3 itself. Understanding these regulatory mechanisms may be key to harmonising MAP4K3's pro-growth and apoptotic effects.

Now, one new and particularly interesting link was recently established that encompasses the translation initiation-related effect of MAP4K3 to further explain its mechanism for the induction of apoptosis. Lam *et al.* (2009) conduct an RNAi screen and identify a potent inducer of apoptosis – MAP4K3 – that, as it turns out, utilises two very distinct branches of signalling – JNK and TOR – to mediate intrinsic cell death. They further reinforce the importance of MAP4K3 for cancer progression by showing significant underexpression in human pancreatic cancers.

MAP4K3 modulates Puma and BAD mostly via regulation of mTORC1. Following evidence gathered on MAP4K3's induction of cell death through the mitochondrial pathway by Lam *et al.* (see previous section) on one side (2009), in particular BAX activation by MAP4K3 and BCL-XL rescue, and the known role of MAP4K3 in activating translation components downstream of mTORC1 on the other (Findlay *et al.*, 2007), Lam *et al.* next looked at expression levels of some BH3-only proteins known to mediate mitochondrial cell death. The rationale was that if MAP4K3 had a role in translation and one in apoptosis, it may be mediating apoptosis through targeted translation of pro-apoptotic mitochondrial-pathway proteins. To test this, they conducted western-blotting analyses on Puma, BAD, BIM and BAX. They found that BAD and, particularly, Puma levels were increased in MAP4K3 kinase active, but not kinase dead, prompting them to deduce that MAP4K3 kinase activity was somehow linked to targeted expression of these BH3-only proteins. Interestingly, BAX levels remained similar to GFP transfection controls, hinting that that the Puma and BAD upregulation is unlikely to be a p53-mediated transcriptional change. To assess whether this change was due to involvement in the JNK or mTOR pathways, they treated cells with mTORC1

(rapamycin) or JNK inhibitors and found that expression levels of Puma and BAD were reduced in rapamycin but not JNK inhibitor treated cells. Because MAP4K3 targets downstream of mTORC1 include 4EBP1 and p70S6K (Findlay *et al.*, 2007), and because mTORC1 has an effect on translation initiation through promotion of eIF4F cap-binding complex formation, they decided to look at whether these mRNAs were bound by eIF4F. One way they decided to test this indirectly was to block transcription and look at whether or not overexpression of MAP4K3 had an effect on maintaining the availability of these mRNAs. This could shed light on whether or not MAP4K3 was having an effect on the stability of these mRNAs. Thrillingly, they found that Puma and BAD mRNAs were kept from being degraded in a rapamycin-sensitive manner. They argue that this may be due to stability conferred by the formation of an eIF4F complex onto the cap of these mRNAs (Ramirez *et al.*, 2002). In this way, MAP4K3 seems to modulate the expression of the pro-apoptotic Puma and BAD through the mTORC1 pathway. Taken together with its proliferative effect and participation in the JNK pathway, MAP4K3 seems to be a likely contributor to tumorigenesis.

MAP4K3 promotes upregulation at the posttranscriptional level of BID in an mTORC1-independent manner. As a follow up to work from Lam *et al.* (2009), Lam and Martins (2009) looked at expression of BID. Following the logic that TNF α activates MAP4K3 leading to engagement of the JNK pathway and that the extrinsic apoptotic pathway is also downstream of TNF α signalling, they wanted to investigate if MAP4K3 had a hand in this. As seen earlier, the extrinsic pathway leads to caspase activation independently of mitochondria, but can intersect the intrinsic pathway through BIM, a small BH3-only protein of the Bcl2 family known to bind and inhibit anti-apoptotic BCL-XL. Additionally, taken in conjunction with the recent finding that MAP4K3 can modulate BH3-only proteins Puma and BAD at the posttranscriptional level in the context of apoptosis, this supported the idea for a regulatory role on the extrinsic pathway. In a comment on their previous work, Lam and Martins also report upregulation of BID at the protein level, by western blot. BID levels are up in kinase active and C-terminal truncations of MAP4K3-GFP overexpressing cells compared to kinase inactive and GFP controls. They maintain that they could not see increased mRNA levels of BID by qRT-PCR and that this protein upregulation was insensitive to rapamycin treatments suggesting a kinase-dependent posttranscriptional upregulation independent of mTORC1. Given the (minute) increase in the kinase-intact C-terminal deletion

overexpressing cells compared to the full-length wild-type, these BH3-only protein modulations may be regulated by its C-terminal domain.

Nonetheless, MAP4K3's role in the induction of aimed translation is still being pursued for a deeper understanding of the general process of regulation of apoptosis on the one hand, and for its close connection with cancer (Figure 11).

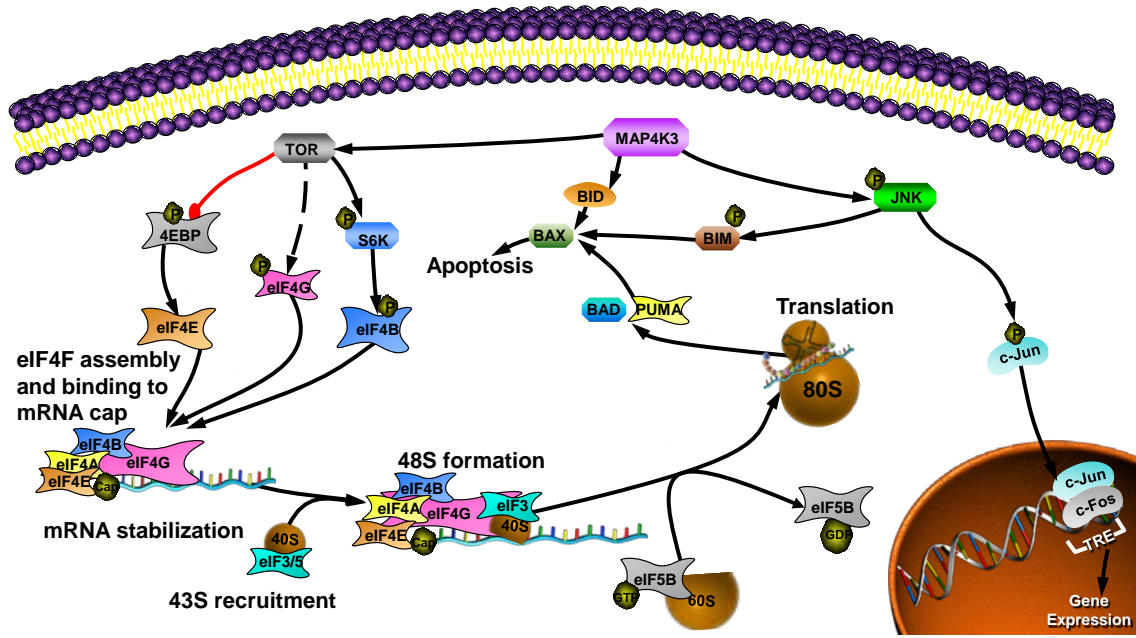


Figure 11: MAP4K3 activates two branches of signalling pathways that lead to cell death. On one side, MAP4K3 activates the c-Jun N-terminal Kinase (JNK) pathway via the MAP3K MEK1 and the MAP2K MKK4. This leads to the activation of the MAPK JNK which results in the regulation of biological effects such as the determination of cell fate through posttranslational modifications of BIM, and transcriptional changes in gene expression through activation of its downstream target Jun. On the other side, MAP4K3 is a regulator of nutrient signalling to TOR. It is responsible for hyperphosphorylation of downstream targets of TOR 4EBP and S6K. Subsequently, there is a cap-dependent eIF4F stabilisation of specific mRNAs that may lead to the expression of the BH3-only proteins Puma and BAD. MAP4K3-induced death is an elegant bipartite mechanism that functions through the modulation of small pro-apoptotic BH3-only proteins BIM, BAD and Puma, that may also engage expression of extrinsic BID. Diener *et al.*,1997; Holcik and Sonenberg, 2005; Sonenberg and Hinnenbusch, 2009; Findley *et al.*, 2007; Lam *et al.*, 2009; Lam and Martins, 2009. Pictograms adapted from SABiosciences.

MAP4K3 contribution to regulation of the TOR pathway is of a diverse nature. It is a clear mediator of amino acid sufficiency signals to mTORC1 and itself regulates purposeful activating signals for targeted translation of pro-apoptotic proteins. Regulation of MAP4K3 itself, however, is a different matter altogether. We're starting to discover the different mechanisms by which MAP4K3 activity is regulated, but putting them together in a biological context is a fascinating signal-integration mechanism that still needs more research. However, understanding MAP4K3-mediated regulation on translational control of gene expression may well be key to preventing progression of certain cancers. This prevention may be related to the early diagnosis of cancers through the identification of new tumour biomarkers in cancers that are difficult to diagnose early, or new cancer targets for treatment. For its application in humans, an *in vivo* model is

essential, and some work has been carried out with MAP4K3's ortholog in *D.melanogaster* – happyhour.

MAP4K3 has also been found to be part of a variety of other pathways and physiological processes, such as the Endothelial Growth Factor Receptor (EGFR) pathway and ethanol sedation (Corl *et al.*, 2010), and the NF- κ B pathway and T-cell Regulation (TCR; Chuang *et al.*, 2011).

AIMS OF THE WORK

MAP4K3 was demonstrated to have a positive regulatory effect on the mTOR pathway and to control growth, but it has not been investigated whether it controls posttranscriptional gene expression. MAP4K3 has also been found to be important in different physiological processes, and mainly attributed to its MAPK characteristics.

With the aim of investigating MAP4K3's contribution to posttranscriptional gene expression and to identify novel downstream pathways and physiological contributions, I set out to explore its control over mTOR and the resulting extent of gene expression changes. To better understand its regulation of the mTOR pathway, I set out to clarify 1) the type of control that MAP4K3 has over its downstream targets 4E-BP and S6K, 2) whether this control affects posttranscriptional gene expression, and 3) the targets under MAP4K3 affecting general gene expression and specific processes.

Chapter 2

2. MAP4K3 signalling activates JNK and causes chromatin condensation and morphological changes in 293s but not clear mTOR activation

2.1 Introduction

Proteins are the workhorses of a cell, performing actions needed for a cell to function properly. Post-transcriptional modulation allows for quick gene expression changes that are crucial to sustaining various cellular needs, such as development, cell fate, and to react to a variety of extracellular conditions. Apoptosis is just such a cellular event that needs to be tightly controlled in order to avoid uncontrolled death on one side, and malignant transformation on the other. It is not uncommon for cancerous cells to downregulate pro-apoptotic proteins in an attempt to evade cell death (Hanahan and Weinberg, 2011) or for normal cells to induce the expression of pro-apoptotic proteins when they are engaged on the death pathway (Spriggs *et al.*, 2010).

Previously, Martins and colleagues reported that MAP4K3 was modulating the expression of pro-apoptotic BH3-only proteins (2009). They also demonstrated the mTORC1 contribution to MAP4K3 kinase activity-induced cell death by using a gain-of-function approach on a HEK293 cell line. They use transient transfections of MAP4K3 in kinase-active and kinase-inactive conditions to show various effects. One is phosphorylation of JNK and it has a dual purpose. Firstly, they use it to establish the link with previous work on MAP4K3 that showed activation of the JNK pathway in a kinase-dependent manner (Diener *et al.*, 1997) and secondly to demonstrate MAP4K3-induced and JNK-mediated cell death.

They also find that its kinase activity has a hand in activating the mTORC1 substrate p70S6K. It is well established that p70S6K is phosphorylated in response to increased activity by the mTORC1 complex, and that this has direct consequences on regulation of both targeted and global gene expression through control of assembly of the translational machinery (Spriggs *et al.*, 2010; Sengupta *et al.*, 2010; Sonenberg and

Hinnenbusch, 2009). They show an increase in protein levels of Puma and Bad, and argue that this is due to an enhancement of mRNA-binding factors to their respective mRNAs causing an increase in stability. To support this, they show that there is no upregulation of these mRNAs at the transcriptional level, and that their half-lives are increased thanks to MAP4K3. They shut down transcription and look at half-lives of these mRNAs in time and report that MAP4K3 is increasing the half-life of *PUMA* mRNA by 12h. *BAD* mRNA half-life is hard to assess, however.

Finally, they use chromatin condensation to assess cell death and to support MAP4K3 kinase-induced cell death. They then use this to discriminate between the contribution of JNK and mTORC1 pathways to MAP4K3-induced cell death. They silence pro-apoptotic BH3-only proteins and report a reduction in MAP4K3-induced cell death. Also, an unreported feature of MAP4K3 overexpressing cells was a morphological change giving them a rounded phenotype. In a personal communication, one of the conductors of the research remarked that a few of the kinase-active MAP4K3 transfected HEK293 cells would exhibit a round morphology compared to their kinase-inactive counterparts.

To attempt and reproduce these results I used the same system that was used to produce them and subjected it to the same conditions in order to investigate the extent of mTORC1 control by MAP4K3. From the results obtained, we can then build on the system.

2.2 Materials and Methods

2.2.1 Materials

Materials were obtained from the following suppliers: Bovine Serum Albumin (BSA), Tween, 4x NuPAGE LDS, Hoechst 33342 from Invitrogen; Lipofectamine 2000, Opti-MEM I, DMEM 61965, Foetal Calf Serum, Penicillin Streptomycin from Life Technologies; ECL enhanced chemoluminescence reagent (Amersham).

XL-10 gold ultracompetent E.coli (#200314) obtained from Stratagene. QIAGEN Plasmid Maxi (#12163) obtained from QIAGEN. Antibodies were obtained from the following suppliers: phospho-S6 Ser240/244 (#2215), phospho-p70S6K (#9206), Puma (#4976), phospho-JNK Thr183/Tyr185 (#9255), phospho-4E-BP1 Thr37/46 (#2855), α -Tubulin (#2144) from Cell Signaling; HA (3F10) and GFP (c13.1) from Roche; Puma (ProSci) from ProSci Incorporated (#3043); Puma (LMM) and Bad antibodies were supplied by Dr. Miguel Martins (#4976 Cell Sign and #610391 BD); anti-Rabbit (#RPN4301) and anti-Mouse (#NA931) from Amersham. Total S6 and phospho-S6 antibodies were a kind gift from Dr. Ewan Smith.

Vectors were obtained from the following suppliers: Puma from Bert Vogelstein through Addgene; pMAX-GFP and M4K3-GFP pcDNA3.1 CT-GFP-TOPO FL wt and KD from Invitrogen (made by Dr. David Dickens); MAP4K3-HA pcDNA3.3-TOPO was cloned from the M4K3 sequence of M4K3-GFP pcDNA3.1 CT-GFP-TOPO into the HA-containing pcDNA3.3-TOPO vector from Invitrogen and then mutated lysine 45 to glutamic acid using Stratagene QuickChange site-directed mutagenesis.

2.2.2 Plasmid preparations

50ng of M4K3-GFP pcDNA3.1 CT-GFP-TOPO FL WT/KD and M4K3-HA pcDNA3.3-TOPO WT/KD were transformed into bacteria using heat shock at 42C for 30 seconds and selected on LB agar plates containing either kanamycin or ampicillin respectively for 18h. Colonies were regularly picked from fresh plates and put into a moving incubator at 37°C and 175rpm for 18h and then used QIAGEN Maxiprep kit to extract DNA as per the manufacturer's instructions. Plasmids were sequenced after every maxiprep to confirm K45E mutation in KD plasmids and that no new mutations were present.

2.2.3 Tissue culture

HEK293 cells (donated by Dr. Amandine Bastide) were cultured in DMEM 61965 supplemented with 10% heat-inactivated foetal calf serum (FCS) and 1% penicillin and streptomycin at 37°C in 5% CO₂ atmosphere. Following transfections cells were kept in antibiotic-free DMEM supplemented with FCS.

2.2.4 Western blots

HEK293s were seeded to 4x10⁵ cells/well on a 6-well plate 18h prior to transfection to get 70% confluence. Cells were then transfected according to Lipofectamine 2000™ transfection protocols. Optimised protocols were, in brief, using 1.2µg of total DNA in 50µL of Opti-MEM I (31985) with 1µL Lipofectamine reagent mixed in a total 100µL volume, and then added directly to the cultured cells in the absence of antibiotics. 24h post-transfection, cells were handled at 4°C, washed once in PBS and harvested directly in 1x NuPAGE LDS sample Buffer containing β-mercaptoethanol. Samples were run on 12% or 16% polyacrylamide gels, transferred onto Hybond PVDF membranes and blotted with the according antibodies for the recommended times in either 5% BSA in TBS-Tween or 5% milk in TBS-Tween and then incubated with the appropriate secondary HRP-conjugated antibody and visualized by ECL.

2.2.5 Nuclear stain

Cells were treated as for western blots and 24 hours post-transfection cells were washed once in PBS and fixed for 20min with 10% formalin at room temperature, and then incubated in 10µg/mL Hoechst 33342 for 10min. They were then washed twice in PBS and visualised using a Zeiss Axiophot microscope equipped with a Zeiss AxioCam colour CDD camera.

2.2.6 Imaging fluorescence

Cells were treated as for western blots but co-transfected using 0.2µg of pMAX-GFP and 0.8µg of either MAP4K3-HA FL or KD. 24h post-transfection cells were visualised under the microscope and fluorescence and bright field images were acquired.

2.2.7 Western blot signal determination and statistics

Quantification of the western blot signals was done using ImageJ 1.46r of duplicate biological repeats. Statistics and graphs were subsequently obtained using Prism 5.03 by

applying a one-way Analysis of Variance (ANOVA) with Bonferroni's multiple comparison test.

2.3 Results

2.3.1 MAP4K3 phosphorylates JNK but not mTORC1 targets p70S6K1 or 4E-BP1 and does not upregulate Puma or Bad in transient overexpression

In order to visualise activation of the two signalling branches that lead to cell death in the model from Martins and colleagues, HEK293 cells were transfected using MAP4K3-GFP expressing constructs. Transfections were then optimised to consistently obtain 90-95% of MAP4K3 overexpressing cells using flow cytometry to detect green fluorescence (not shown). A MAP4K3-HA tagged construct was also made and optimised using western blot and flow cytometry techniques in co-transfections with pMAX-GFP and achieving consistent and high levels of expression (not shown).

Kinase activity from MAP4K3 was found to reliably activate JNK (Figure 12 A and B) only when overexpressed in its kinase-active, but not inactive, forms. This is true across the board, with the tag making no difference in the phosphorylation of JNK at Thr183/Tyr185. Various transfections controls were used, including pcDNA3, the backbone to the MAP4K3-expressing vectors, Puma expressing vectors and pMAX-GFP expressing vectors.

Puma and Bad were not detected at different levels of expression between KD and FL forms of MAP4K3, and neither between either of them and transfection, or even untreated controls. Puma was transfected into HEK293s and expressed at high levels as a positive control. Different antibodies from different companies were used for this (Cell Signaling, ProSci Incorporated), including the antibody that was initially used and successfully showed an increase in its expression (from Lam *et al.*, 2009) but no differences were detected. Bad expression was also invariable.

Phosphorylation of mTORC1 targets 4E-BP1 and p70S6K was not apparent in the present work as in the previous works conducted, either. There was no detectable change in phosphorylation of p70S6K or its downstream target rpS6 in MAP4K3 transfected cells. Rapamycin treatment abolished phosphorylation of p70S6K and rpS6 as expected. eIF4E-BP1 phosphorylation was also found unchanged between kinase active and kinase inactive overexpressing cells. Isoforms γ , β and α were detected at similar levels for all

except rapamycin controls that lost their heavier, hyperphosphorylated γ and most of the β isoforms.

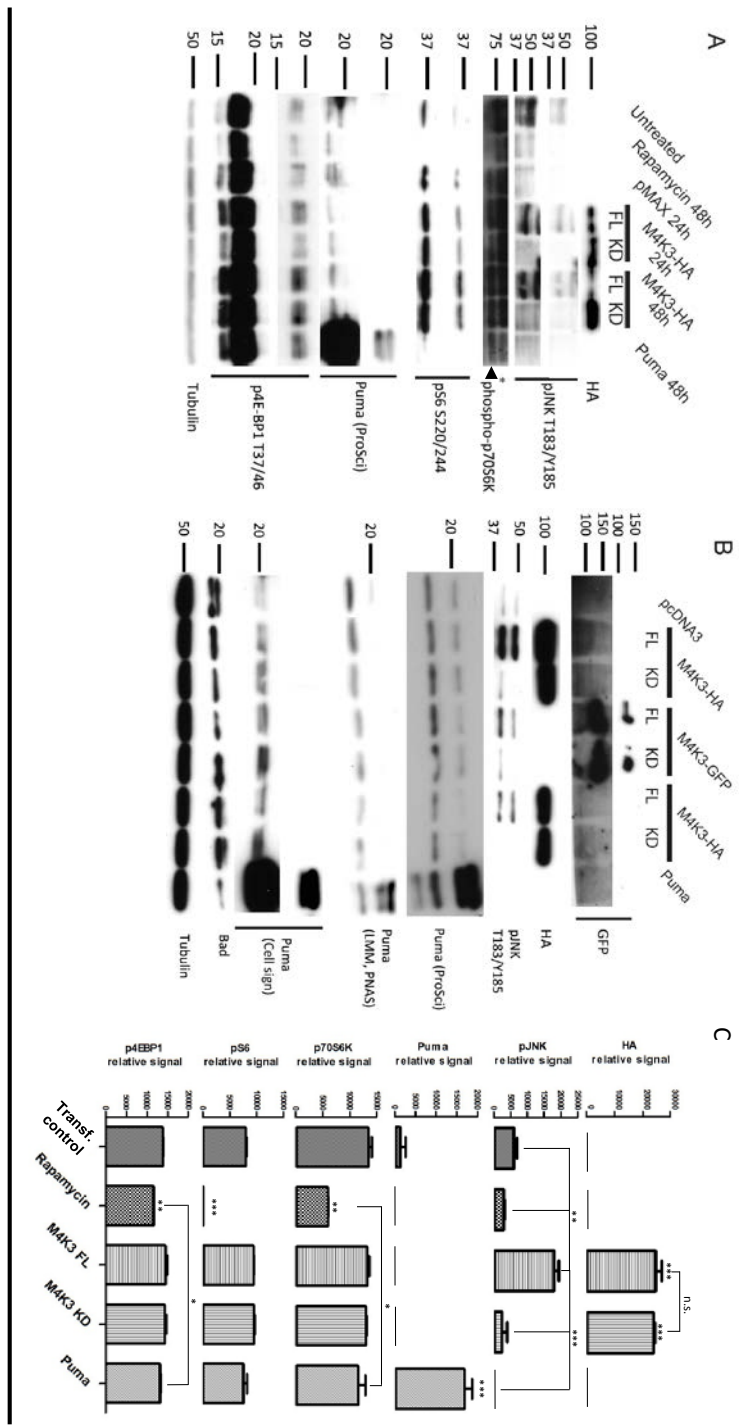


Figure 12: MAP4K3 activates JNK, but not mTORC1, signalling in transient overexpression models with no discernible change in BH3-only expression. (A) Transient expression of M4K3 activates JNK in a kinase-dependent manner but has no effect on mTORC1 targets 4E-BP1, p70S6K or S6. M4K3 transient expression does not induce Puma expression. Cells were either transfected with the indicated plasmid or treated with 100nM rapamycin 18h post seeding for the times indicated and then harvested into 1x NuPAGE LDS Sample Buffer containing β -mercaptoethanol. (Asterisk: p85S6K, Arrow: p70S6K). (B) Transient expression of M4K3 does not induce expression of BH3-only proteins Puma and Bad in a kinase-dependent manner. Cells were treated and harvested 24h post transfection as in A. Blots shown are representative of results obtained. (C) One-way ANOVA with bonferroni's multiple comparison tests of western blot signals. Western blot signal quantification was performed using ImageJ and normalised against the background of the blot and error bars represent standard errors. Results show duplicate biological repeats, and asterisks denote statistical significance (n.s.: not significant $p > 0.05$, * significant $0.01 < p < 0.05$, ** very significant $0.001 < p < 0.01$, *** extremely significant $p < 0.001$). Where there are no annotations, there is no significance.

2.3.2 MAP4K3 causes chromatin condensation and morphological changes in HEK293 cells in a kinase-dependent manner

Taken together, the previous results show that the system was working at its full potential and to the maximum of its capacity but there was no apparent activation of mTORC1 components, nor upregulation of BH3-only proteins Puma and Bad under these conditions.

Something that is particularly apparent, however, is a change in the morphology of the cells following MAP4K3 overexpression (Figure 13B). Overexpressing MAP4K3 with a kinase-inactivating mutation on the ATP-binding site of the catalytic domain on lysine 45 does not cause any type of morphological change. Cells were co-transfected with pMAX-GFP to further pronounce this striking effect.

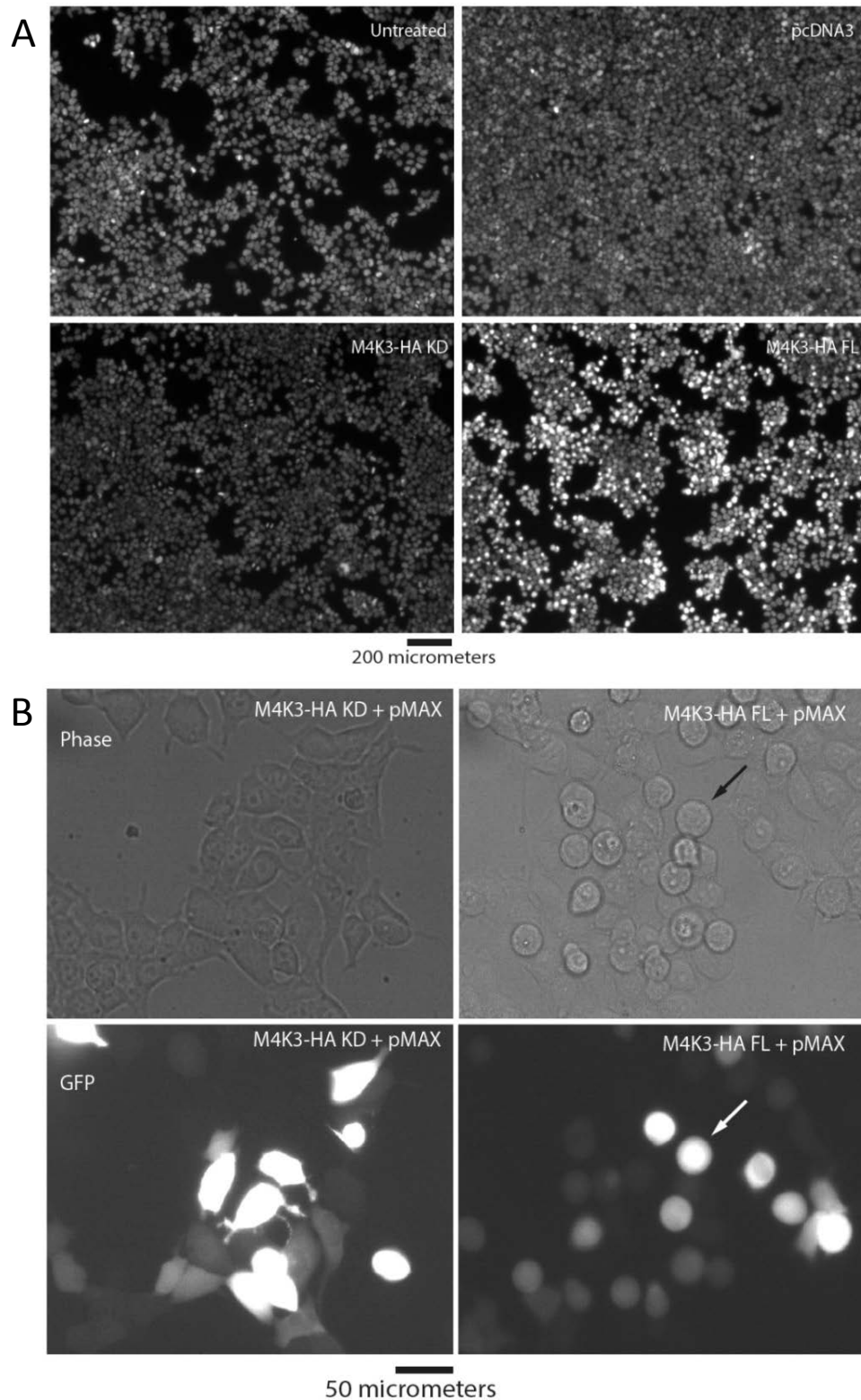


Figure 13: MAP4K3 kinase activity causes chromatin condensation and marked morphological changes in HEK293 cells. (A) Kinase-dependent chromatin condensation of M4K3-transfected 293 cells. Cells were treated as above and then fixed and Hoechst stained 24h post-transfection. (B) Kinase-dependent morphological changes of 293 cells transfected with M4K3. Cells were co-transfected with M4K3 and transfection reporter pMAX. Kinase-active (M4K3-HA FL + pMAX) transfected cells change morphology to a round phenotype whilst kinase-inactive (M4K3-HA KD + pMAX) transfected cells maintain normal morphology.

MAP4K3 kinase activity causes chromatin condensation on HEK293 cells as expected from previous work performed on U2OS (see Figure 10 and Lam *et al.*, 2009). There is clear chromatin condensation in kinase-active MAP4K3 transfections but not in kinase-inactive MAP4K3. The nuclear stain for the K45E mutant transfections is very similar to transfection controls pcDNA3 and untreated cells, pointing to a purely kinase-driven and easily discernible effect.

2.4 Discussion

Previous results show a direct activation of mTORC1 target S6K by MAP4K3 kinase activity and a direct modulatory effect on the expression of some target proteins of the same family, making it highly attractive to identify genes post-transcriptionally modulated by MAP4K3. However, these effects were difficult to observe despite: 1) using the same system used to initially identify these effects, 2) confirming that the system was working properly and 3) optimising it beyond the quality of its initial use.

The system that was used to investigate this branch of MAP4K3 influence was HEK293 transient overexpression which is ideal for studying signalling pathways due to its versatility and robustness. The initial MAP4K3 study was performed on an identical system to identify it as a mediator of JNK signalling (Diener *et al.*, 1997). This was not, however, the system of choice used to identify its regulatory role over mTOR. Lamb and colleagues first use a loss-of-function approach (2007) and then an inducible system (2010) to establish the link with mTOR and to investigate its mechanism of action. Furthermore, to be able to discern the effect, they used phosphorylation reporters for both S6K and 4E-BP1, a testament to the limited extent of control over this pathway.

Nonetheless, the system used initially was working well, and phosphorylation of JNK was easily detected. The system was then further enhanced by putting to the test different transfection reagents and optimising the transfection conditions. Initially, Effectene (QIAGEN) was being used for transfections, as per the previous work, but then was replaced for the more effective Lipofectamine (Invitrogen). Other transfection reagents were also tested, such as FuGENE (Promega), GeneJuice (Millipore) and Effectene Reverse Transfection (QIAGEN). Following optimisation, effects like JNK activation remained, but morphological changes and chromatin condensation became more readily discernible.

JNKs are known to have a number of substrates. These include transcription factors such as the AP-1 members c-Jun and ATF2 (Shaulian and Karin, 2001) to name a few. It is this particular axis that has been studied the most and gene expression is found to be stimulated under activation of AP-1 transcription family members. Overexpression of MAP4K3 is very likely to lead to stimulation of transcription, and it could be of interest to understand what targets are being modulated transcriptionally. This is especially

exciting in the context of cancer progression as JNK signalling was found to be genetically altered in the vast majority of lung cancers with members such as *MAP4K3* along with *ATF2* and *TNF* directly identified as mutated (Jones *et al.*, 2008). In that screen for somatic mutations it was found that the *MAP4K3* sequence was mutated causing an E351K missense mutation. Because Lam *et al.* (2009) find *MAP4K3* expression deregulated in lung adenocarcinomas, it may be interesting to investigate whether this loss has a direct influence over cancer progression in the context of the transcription-controlling JNK pathway.

Other JNK substrates include microtubules. It has been linked to epithelial sheet movement (Riesgo-Escovar *et al.*, 1996), phosphorylation of Paxillin and regulation of migration (Huang *et al.*, 2003), and phosphorylation of α - and β -catenin and regulation of adherens junctions (Lee *et al.*, 2009; Lee *et al.*, 2011). Given the clear morphological changes identified in the present study, it would have been more complete to pinpoint whether JNK was mediating this effect using a JNK inhibitor. Because most pathways that lead to cytoskeletal rearrangements are being investigated for tumour invasiveness, this result may not support an anti-tumorigenic model for *MAP4K3*. Nonetheless, the result stands, and although they are beyond the scope of the present work, they may be of interest in *in vivo* wound healing (Ramet *et al.*, 2002).

Importantly, it was not possible reproduce results by Martins and colleagues on the apparent posttranscriptional upregulation of pro-apoptotic Puma and Bad. Although it is clear that the protein levels are up, and that there is no detectable upregulation of their transcription by qPCR, the stability of *PUMA* and *BAD* mRNAs should be looked at more carefully.

The mRNA decay method to investigate induced stability of mRNAs is widely used (Jacobson and Peltz, 1996), even in genome-wide studies (Grigull *et al.*, 2004), but with a sizeable limitation that is the treatment itself. With no way to control for the effect of silencing genome-wide transcription, this always has the possibility to be a response to the treatment itself. It is, however, mediated by mTORC1, as shown by the rapamycin treatment that cuts half-life even further, provided that the cells are not under massive stress from 24h transfection, 16h rapamycin and 12h α -amanitin treatments prior to harvest up to 60h post final treatment. The whole experiment also hinges on the effectiveness of the α -amanitin treatment, and the reliability across different cells under

different treatment conditions. If α -amanitin is not inhibiting transcription to the same extents everywhere, it becomes harder to compare between conditions, and with no reliable way to assess effectiveness of the treatment other than looking at the steady decay of transcripts.

One simpler way of determining whether MAP4K3 is enhancing protection *PUMA* and *BAD* mRNA, may be to look at their decapping rates in MAP4K3 overexpressing cells during amino acid starvation. MAP4K3 is known to regulate mTOR in an amino acid-dependent way, and amino acid starvation-mediated shutdown of mTORC1 was found to be slowed by MAP4K3 (Findlay *et al.*, 2007). Because amino acid starvation is known to inhibit global translation, if MAP4K3 were to have an effect on these specific transcripts then it would slow their rate of decapping by enhancing cap-binding to them. This may have been a more direct way to assess whether these mRNAs are stabilised by MAP4K3 without the use of long timepoints and precise treatments as amino acid starvation is invariably easy to achieve.

MAP4K3 kinase involvement in the mTOR pathway is hard to reconcile with the results from Lam *et al.*, but by using more physiological systems we may be able to understand the extent of amino acid regulation of the mTOR pathway by following work from Lamb and colleagues.

Chapter 3

3. A more physiological MAP4K3 inducible system reveals control over size and protein synthesis

3.1 Introduction

To investigate the MAP4K3 regulation of mTORC1, we generated an inducible cell line with a stable genomic one-site insertion of an additional copy of the MAP4K3 sequence. This system was also used by Lamb and colleagues (2010) to investigate regulation of MAP4K3 during amino acid signalling. The reasoning was that using an amino acid-regulation approach, MAP4K3 contribution to mTOR signalling would be more apparent. Furthermore, a controlled induction of expression from the 293T-REx system would provide a more physiological overexpression model than the transient overexpression system.

Lamb colleagues use cell size variation to involve MAP4K3 in the regulation of the overall size of the cell and support a contribution to mTOR regulation. A number of studies use cell size variation to demonstrate an involvement in the mTOR pathway (Fingar *et al.*, 2002; Zhang *et al.*, 2010). Importantly, mTOR is known to be a determinant of cell size and its negative regulation is known to cause a decrease whilst its overactivation causes an increase in cell size (Kim *et al.*, 2006). Lamb and colleagues exploit this effect twice to support an involvement of MAP4K3 in the pathway of mTOR regulation.

First, they show a reduction in overall cell size following silencing of MAP4K3, in HeLa cells. They found that to be very similar to silencing Rheb, which is known to act as a switch for mTOR, and to inhibiting mTORC1 itself using Rapamycin (Findlay *et al.*, 2007).

On their follow up study, they demonstrate that MAP4K3 is inhibited by Protein Phosphatase 2A (PP2A) during amino acid signalling, and they pinpoint it to one of its regulatory subunits – PR61ε. When they then proceed to silence this PP2A subunit, they find that this has an effect on cell size. In what they hint is a MAP4K3-dependent cell

size gain, they support the model that postulates that PP2A-PR61 ϵ has a regulatory role on cell size. In the present study, I report direct evidence of an effect on cell size by MAP4K3 by exploiting GFP fluorescence from the tag in flow cytometry analyses.

Besides cell size and growth, the mTORC1 complex is also known to directly control protein synthesis (Ma and Blenis, 2009), and is found to do so directly and through its downstream targets 4E-BP1 and p70S6K1 in response to nutrient availability (Holz *et al.*, 2005; Sonenberg and Hinnebusch, 2009). Since MAP4K3 was demonstrated to increase activation of these targets in amino acid signalling to mTOR, I decided to investigate the effect it has on global translation. In my first approach, I find translation to be enhanced by MAP4K3-induction. Further investigations (in the next chapter) show us that this is further increased by amino acid restimulation, and this further supports a role for MAP4K3 in signalling to mTOR.

Additionally, tetracycline drugs were found to inhibit radioactive methionine incorporation rates. This is widely reported in the literature and it was found by others to do so by inhibiting mitochondrial protein synthesis (McKee *et al.*, 2006). Interestingly, this effect was found to be present even at concentrations normally used for induction.

With the aim of understanding the extent of MAP4K3 control over mTOR, I characterise this inducible cell line and find that MAP4K3-GFP directly contributes to cell size increase and that it enhances protein synthesis rates.

3.2 Materials and Methods

3.2.1 Materials

Materials were obtained from the following suppliers: Flp-In 293T-REx cells (R780-07), pOG44, pcDNA5/FRT/TO, Zeocin (R250-05), Blasticidin (R210-01), Hygromycin (R220-05), Doxycycline from Invitrogen; MAP4K3 and GAPDH qPCR primers (designed by Dr. David Lam), QIAshredder, RNeasy Mini System, QuantiTect SYBR Green RT-PCR system from QIAGEN; TET-free Foetal Bovine Serum from Biosera; radioactively labelled ³⁵S methionine from Hartmann Analytic; 5x Passive Lysis Buffer from Promega; Glass fibre filters from Whatmann; Bradford reagent from Biorad. MAP4K3 antibody was provided by Dr. Miguel Martins as a kind donation from external sources. Doxycycline was prepared in aliquots by Dr. Nicoleta Moiso and used for a few experiments. It was then reordered from the same supplier, resuspended and prepared into aliquots afresh to rule out incorrect preparation.

3.2.2 Tissue culture

Flp-In 293T-REx cells were kept in DMEM 61965 supplemented with 10% certified TET-free (< 19.7ng/mL) FBS and 1% penicillin and streptomycin. MAP4K3-GFP inserted cells were additionally kept in 15µg/mL Blasticidin and 100µg/mL Hygromycin B selection until 24h prior to seeding for experiments. Empty Flp-In 293T-REx cells were kept instead in 15µg/mL Blasticidin and 100µg/mL Zeocin selection until 24h prior to seeding for experiments.

3.2.3 MAP4K3-GFP Flp-In 293T-REx cell line generation under tetracycline control

The MAP4K3-GFP sequence of M4K3-GFP pcDNA3.1 CT-GFP-TOPO FL was cloned into the Blasticidin resistance gene-containing pcDNA5/FRT/TO (performed by Mariana Santos) and co-transfected with pOG44 for FRT recombination of a single copy of the MAP4K3-GFP sequence into the FRT site. Cells were then selected for correct insertion using Blasticidin and Hygromycin B and foci of isogenic cells resistant to both selection drugs were then frozen as stocks and used for subsequent experiments. This procedure was performed following the manufacturer's instructions for handling and production of the Flp-InTM T-RExTM Cell Line (Invitrogen R780-07).

3.2.4 Western blots

MAP4K3-GFP Flp-In 293T-REx cells were seeded at 4×10^5 cells per well on a 6-well plate kept in media supplemented with serum and penicillin and streptomycin but no selection antibiotics. Cells were then treated with 0.01, 0.1 or $1 \mu\text{g}/\text{mL}$ of doxycycline for 24h or $0.1 \mu\text{g}/\text{mL}$ for 6h, 12h, 24h, 48h or 72h or left untreated for either 24h or 72h prior to harvest. They were then harvested in 1x LDS and samples treated as per all western procedures.

3.2.5 RNA extraction and qRT-PCR

Total RNA was isolated from cells treated as above with all doxycycline treatments as above using the QIAshredder and RNeasy Mini System. Quantitative real-time RT-PCR was performed using the Mx4000 real-time cycler and the QuantiTect SYBR Green RT-PCR system. MAP4K3 mRNA levels were determined using the comparative Ct method and normalised to GAPDH levels.

3.2.6 Quantification of relative MAP4K3 protein expression

Following harvest of samples treated with $0.1 \mu\text{g}/\text{mL}$ doxycycline for 24h, western blot was performed using the MAP4K3 antibody and quantifying the signal of the 130kDa band (MAP4K3-GFP) of treated cells and comparing it to the 100kDa band (MAP4K3) of untreated cells using ImageJ.

3.2.7 Imaging fluorescence

Cells were seeded and treated with 0.01, 0.1 or $1 \mu\text{g}/\text{mL}$ doxycycline or left untreated for 24h as above and Hoechst stained as previously described. Images were taken as described in the previous chapter and analysed using Adobe Photoshop CS3 for production of overlays. Overlays were skilfully produced alongside Dr. Miguel Martins for demonstration purposes. Fluorescence intensity was captured on processed images using Adobe Photoshop CS5 intensity tool and normalised to background fluorescence of each individual image analysed.

3.2.8 Protein synthesis rate determination

Cells were seeded and doxycycline treated at 0.01, 0.1 and $1 \mu\text{g}/\text{mL}$ doxycycline or left untreated for 24h as above and spiked with $3 \mu\text{L}$ of $37\text{TBq}/\text{mmol}$ radioactively labelled ^{35}S methionine for 30min in their usual incubation conditions (37°C and $5\% \text{CO}_2$). Cells were then washed twice in PBS, harvested in 1x PLB, TCA precipitated and passed

through the Whatmann filters using a vacuum manifold. The Whatmann filters were then washed in IMS and acetone and transferred into scintillation vials with scintillation fluid. Counts per min (CPM/min) were then normalised to protein (by Bradford protein quantification). Experiments performed independently of one another are depicted as separated bar charts and have their appropriate controls as normalised relative radioactivity. HEK293 1µg/mL doxycycline treatment was performed alongside Dr. Amandine Bastide who did most of the procedure as demonstration.

3.2.9 Flow cytometry

Cells were seeded and doxycycline treated at 0.1µg/mL for 6h, 12h, 24h, 48h and 72h as described above. They were then handled at 4°C, washed with PBS, trypsinised, collected into flow cytometry tubes, centrifuged at 200g for 5min at 4°C and resuspended for flow analysis using the BD FACScan and cells were analysed for green fluorescence (488nm argon laser on FL1) and on forward scatter for size (FSC-H). For analysis, cells were first gated to the events that were not debris on the FSC vs SSC scatter plots. GFP fluorescence for each treatment was then overlaid. Size analysis was performed on the GFP positive cells for doxycycline treated cells and the geometric mean values of the population of cells were compared to the general population of untreated cells.

3.2.10 Statistics

RNA quantification was obtained from triplicate biological repeats. Quantification of the western blot signals was done using ImageJ 1.46r of duplicate biological repeats as previously. Radioactive incorporation values were obtained using triplicate biological repeats for each set of conditions. Cell size variation data were obtained in triplicate biological repeats. Statistics and graphs were subsequently obtained using Prism 5.03 by applying a one-way Analysis of Variance (ANOVA) with Bonferroni's multiple comparison test.

3.3 Results

3.3.1 Characterisation of MAP4K3-GFP 293T-REx system

We generated an inducible 293T cell line that expresses a GFP tagged form of MAP4K3 under the control of tetracycline drugs. The MAP4K3-GFP sequence was inserted into a single, transcriptionally active, locus of the genome using FRT sites and expression of a Flp recombinase. The sequence inserted carries an upstream cytomegalovirus (CMV) promoter that has two Tet-operator (TetO) sequences. These sequences bind 2 homodimers produced by the Tet repressor gene (TetR). TetR is itself expressed by a stably integrated plasmid in the cell line, basally expressing TetR and thus basally repressing the transcription of the MAP4K3-GFP sequence. When tetracycline drugs are present, they bind the TetR homodimers and render it unable to bind the TetO sequences and thus relieving inhibition of transcription of the extra MAP4K3 copy inserted.

Doxycycline dosecourse determines best concentration of induction for experimental procedures. Successful induction was achieved at different concentrations with best mRNA and protein expression at 0.1 µg/mL of doxycycline on 70% confluent HEK-type cells, 24h post-treatment (Figure 14 A and B). The MAP4K3 specific antibody reveals an increase of 6-fold in expression 24h post induction compared to endogenous levels of the protein (100kDa band) in untreated conditions (Figure 14 C and D).

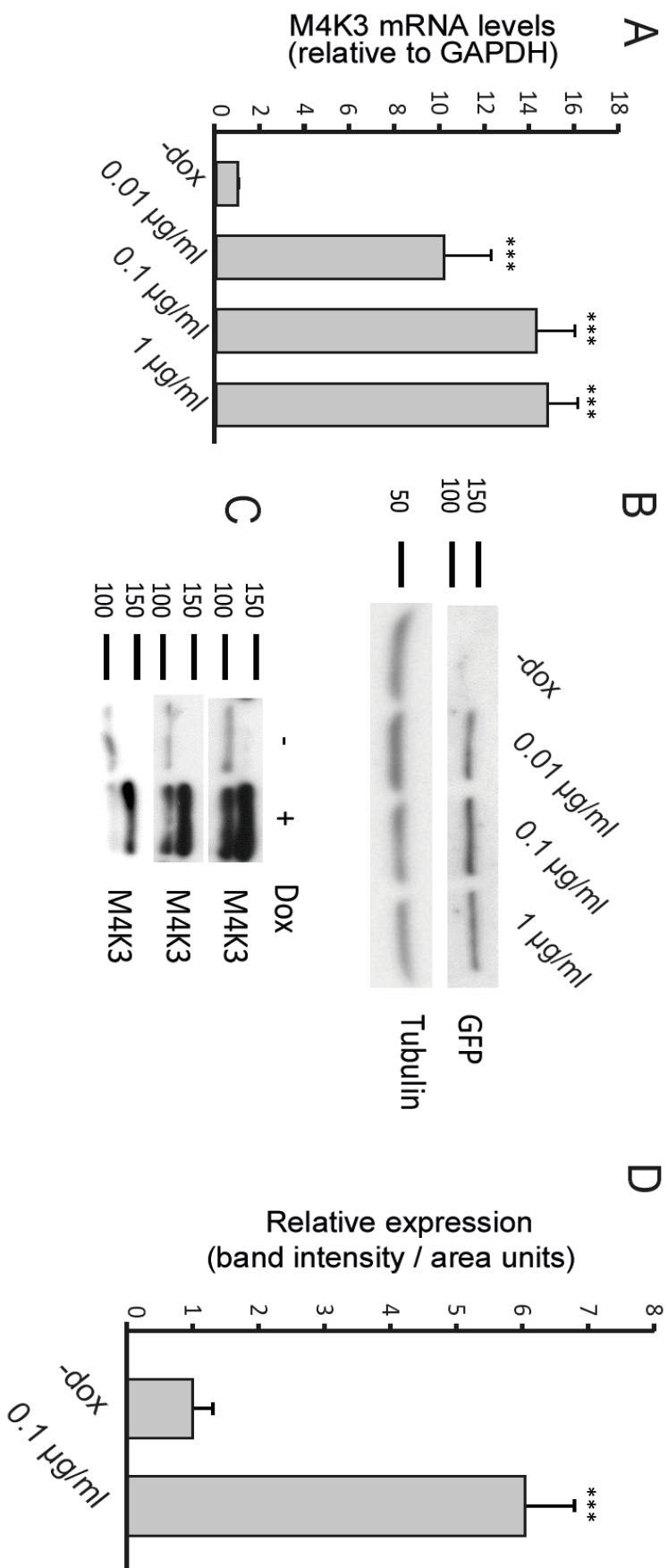


Figure 14: Induction of M4K3-GFP is optimal at 0.1µg/ml in the 293T-REx line. M4K3-GFP was induced using 0.01, 0.1 and 1 µg/ml of doxycycline for 24 hours prior to (A) RNA extraction for qPCR, (B) harvest for western blotting, (C and D) protein level quantification. (A) M4K3 mRNA levels increase 14-fold with 0.1µg/ml dox treatment for 24 hours. Results are triplicate technical replicates. (B) M4K3 protein levels are highest following 0.1µg/ml doxycycline treatments. Blots from B and C are representative of three biological replicates. (C and D) Induced protein levels are 6-fold higher than endogenous M4K3 in untreated cells. Statistics performed on triplicate biological repeats (n.s. not significant $p > 0.05$, * significant $0.01 < p < 0.05$, ** very significant $0.001 < p < 0.01$, *** extremely significant $p < 0.001$). Where there are no annotations, there is no significance.

Green fluorescence is also detectable from as little as 0.01 $\mu\text{g}/\text{mL}$ concentrations of doxycycline, and progressively increases with higher concentrations (Figure 15).

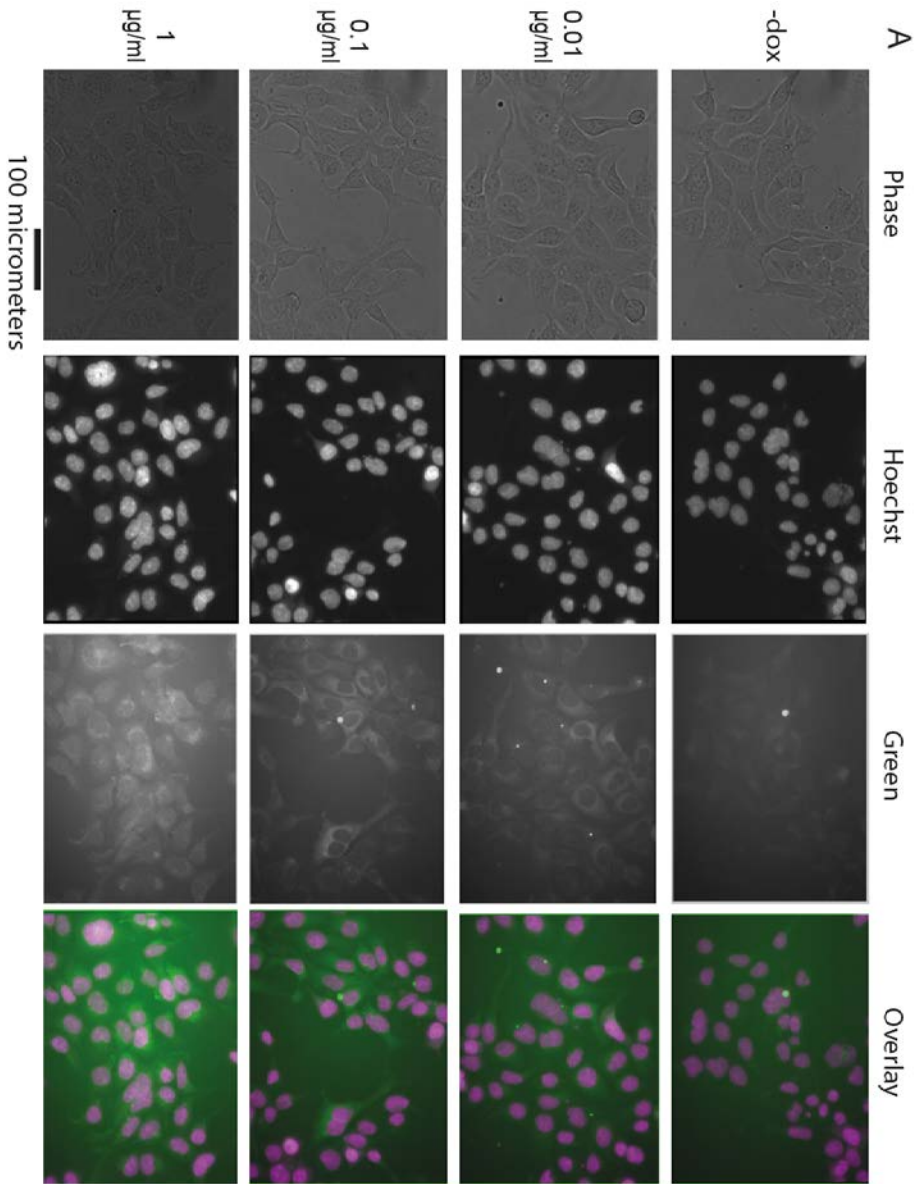


Figure 15: GFP fluorescence intensity increases with doxycycline treatment. (A) and (B) Green fluorescence and hoechst stain reveal an increase in GFP fluorescence following doxycycline treatment. Relative intensity was determined using Photoshop CSS intensity tool to determine fluorescence intensity per area units and individual image backgrounds were subtracted from those values.

Interestingly, 1µg/mL concentrations of doxycycline reduced protein synthesis rates by up to 40% in the inducible cell line and 70% in the parent HEK line. Lower concentration treatments did not reduce protein synthesis rates in 70% confluent cells at 24h post-treatment (Figure 15).

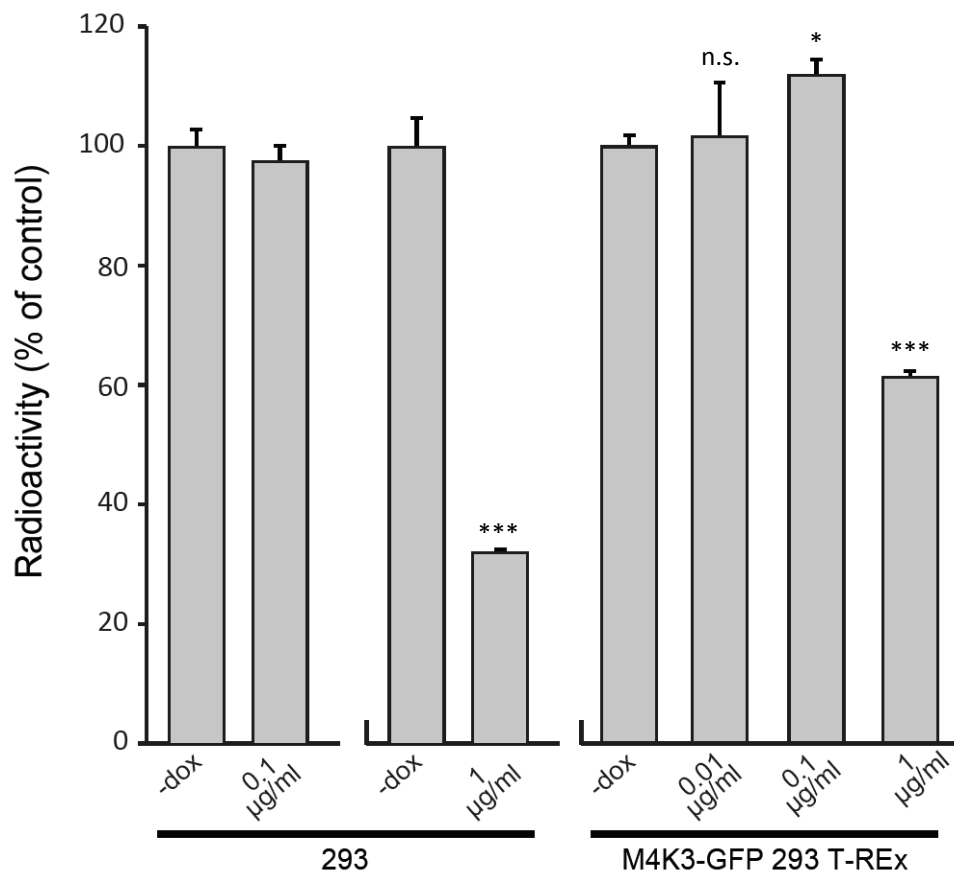


Figure 16: Induction is optimal at 0.1µg/mL in the 293T-REx line. ³⁵S-methionine incorporation rates for MAP4K3-GFP 293T-REx and for HEK293 cells under different doxycycline treatment conditions. Doxycycline inhibits methionine incorporation considerably at 1µg/mL concentrations in both HEK293 and the 293T-REx cell line. Cells were treated with 0.01, 0.1 and 1 µg/mL of doxycycline or left untreated for 24 hours prior to methionine labelling for determination of protein synthesis rates. Radioactivity is expressed as counts per minute (CPM) per µg of protein (CPM/µg) and then normalised to control (untreated cells). Results are representative of duplicate biological repeats with triplicate technical repeats (n.s. not significant $p > 0.05$, * significant $0.01 < p < 0.05$, ** very significant $0.001 < p < 0.01$, *** extremely significant $p < 0.001$). Where there are no annotations, there is no significance.

Overall, the doxycycline dosecourse treatment has revealed that 1) there is expression of MAP4K3-GFP, that 2) 1 μ g/mL concentration in our experimental conditions inhibits protein synthesis and that 3) 0.1 μ g/mL doxycycline is sufficient and the best in balancing effectiveness and side-effects.

Doxycycline timecourse determines best timings for experimental settings. Following determination of appropriate doxycycline doses for successful protein expression, I undertake a timecourse study to further characterise the cell line. The aim is to identify minimal timing for successful induction and, more importantly, for effects to start being detected. MAP4K3 mRNA levels start rising prior to 6h post-induction and achieve plateau levels from 24h (Figure 17A). The same applies for protein levels, as detected by western blotting against the GFP tag (Figure 17B), and green fluorescence detected by flow cytometry (Figure 17C).

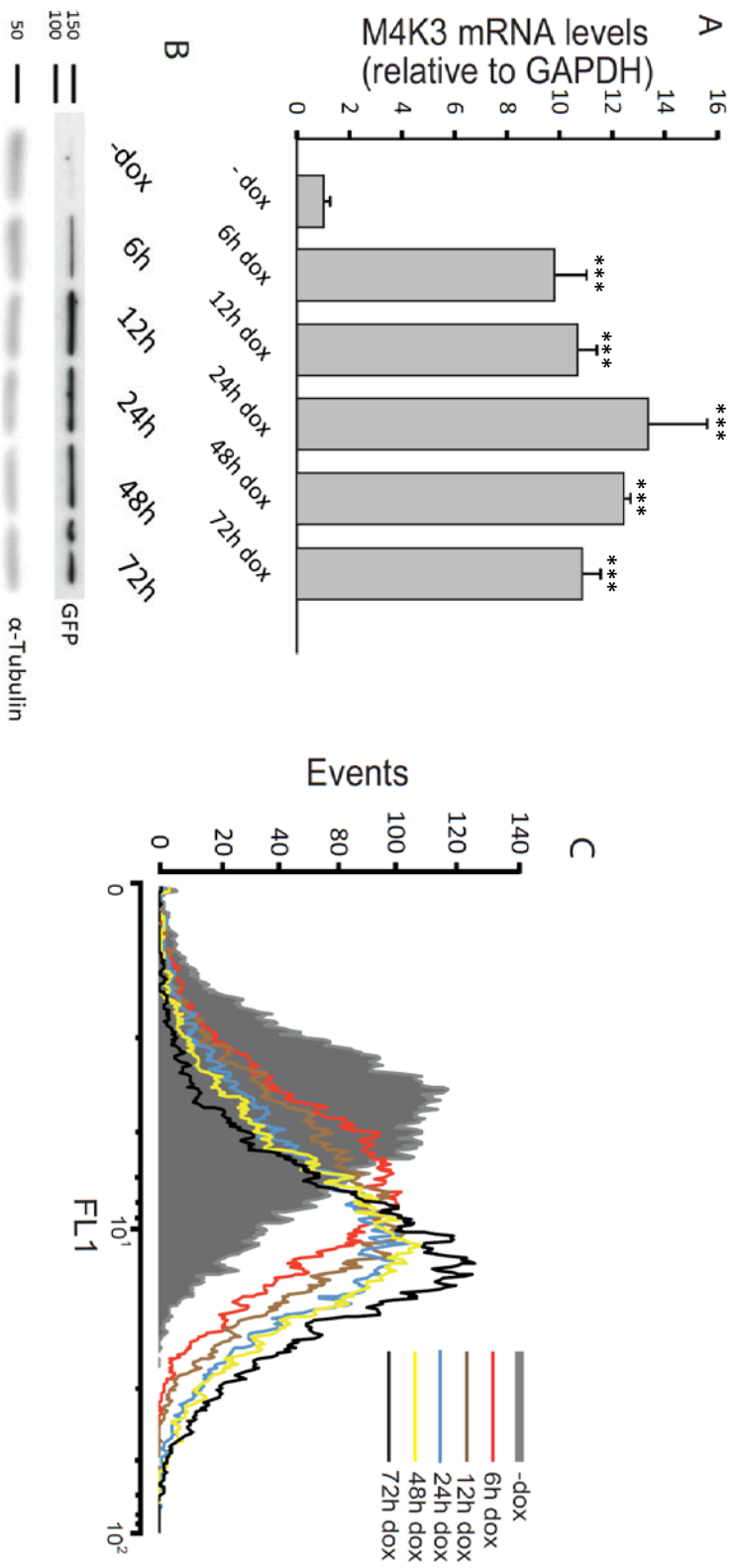


Figure 17: M4K3 induction timecourse following doxycycline treatment on 293T-REx cell line. M4K3 induction is optimal from 24h post-treatment. (A) M4K3 mRNA levels increase to 13-fold at 24h treatment with 0.1 μ g/ml doxycycline. Results are representative of triplicate technical repeats. (B) M4K3 protein levels increase up to 12h following treatment with 0.1 μ g/ml doxycycline and plateau at about 24h post-treatment. Results are representative of duplicate technical repeats. (C) Fluorescence on FL1 of M4K3-GFP 293T-REx cells treated with 0.1 μ g/ml doxycycline for the indicated times show highest fluorescence from 12h post treatment. Results are representative of triplicate biological repeats. (n.s. not significant $p > 0.05$, * significant $0.01 < p < 0.05$, ** very significant $0.001 < p < 0.01$, *** extremely significant $p < 0.001$). Where there are no annotations, there is no significance.

Interestingly, MAP4K3-GFP induction was found to cause a progressive cell size increase at different times post-induction with the effect plateauing following 24h treatment (Figure 18A). This was found to be independent of the doxycycline treatment as a parental HEK cell line did not vary following prolonged 0.1 μ g/mL doxycycline treatment, and to be maintained at similar levels after 24h treatment for the positive green population (Figure 18B).

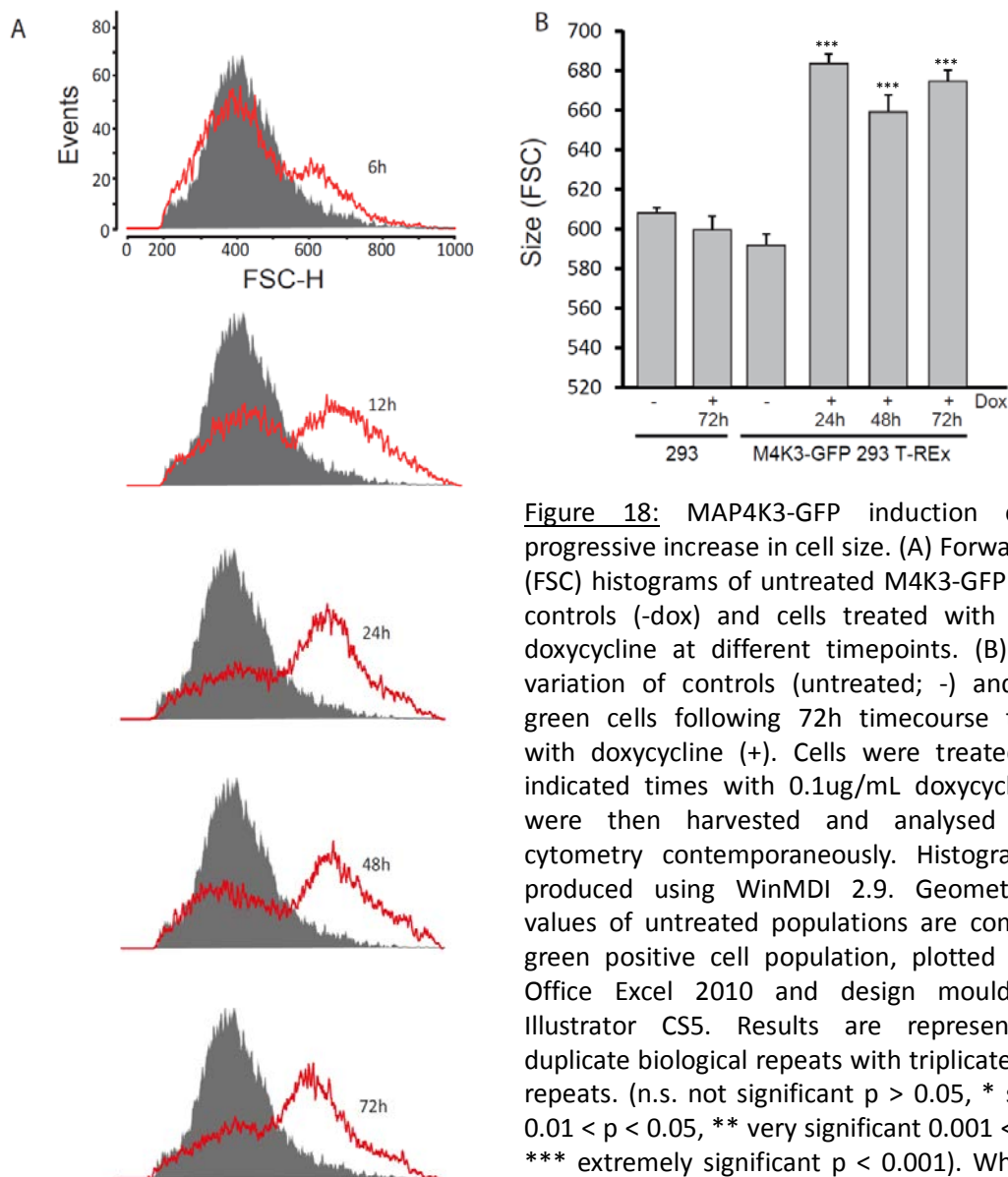


Figure 18: MAP4K3-GFP induction causes a progressive increase in cell size. (A) Forward Scatter (FSC) histograms of untreated M4K3-GFP 293T-REx controls (-dox) and cells treated with 0.1 μ g/mL doxycycline at different timepoints. (B) Cell size variation of controls (untreated; -) and positive green cells following 72h timecourse treatment with doxycycline (+). Cells were treated for the indicated times with 0.1 μ g/mL doxycycline. Cells were then harvested and analysed by flow cytometry contemporaneously. Histograms were produced using WinMDI 2.9. Geometric mean values of untreated populations are compared to green positive cell population, plotted using MS Office Excel 2010 and design moulded using Illustrator CS5. Results are representative of duplicate biological repeats with triplicate technical repeats. (n.s. not significant $p > 0.05$, * significant $0.01 < p < 0.05$, ** very significant $0.001 < p < 0.01$, *** extremely significant $p < 0.001$). Where there are no annotations, there is no significance.

Overall, results from this inducible HEK line reveal steady and consistent induction of MAP4K3 expression. Minimal side effects with maximal effectiveness from the drug were achieved at 0.1µg/mL concentrations and the MAP4K3 influence on the cell line were started to be noticed within 24h post-treatment, including changes in cell size and an increase in protein synthesis rates.

To further investigate the effect MAP4K3 is having on cell signalling pathways around mTORC1 and on protein synthesis, we decided to investigate the extent of regulation by MAP4K3 on the amino acid pathway to mTOR.

3.4 Discussion

By characterisation of the cell line reveals the importance of dose and timing in achieving the desired expression and downstream effects. We have determined doxycycline doses to be important in reducing undesired artefactual events.

Doxycycline is a known inhibitor of mitochondrial protein synthesis. The endosymbiotic (literally living within each other) theory suggests that these organelles are of an ancestral, microbial origin. Mitochondria have their own DNA, transcriptional and translational machinery. Mitochondrial protein synthesis functions using ribosomes that are more similar to the prokaryotic 70S ribosomes than human 80S ribosomes (Pel and Grivel, 1994), making them a target of a number of antibiotics that inhibit microbial protein synthesis (McKee *et al.*, 2006).

Tetracycline drugs such as doxycycline, are toxic to prokaryotes because they bind to their 30S ribosomal subunit impeding the introduction of a charged tRNA to the A site of the 70S ribosome. Many antibiotics, including tetracycline, potently inhibit mitochondrial protein synthesis. By using radioactive methionine incorporation rates to assess protein synthesis, McKee *et al.* submit isolated human mitochondria were found to be inhibited by tetracycline to $IC_{50} = 2.1\mu\text{M} \pm 0.5\mu\text{M}$ which corresponds to about $4.725\mu\text{g/mL} \pm 1.125\mu\text{g/mL}$ concentrations being enough to inhibit protein synthesis by half (2006). These results by themselves are enough to indicate the need for caution in the use of tetracycline drugs in the study of active translation. Our results show a clear decline in the rates of protein synthesis in both parental HEK as well as our inducible cell lines prompting us to use more appropriate concentrations that do not inhibit protein synthesis, but still allow for MAP4K3 expression and its downstream effects.

MAP4K3-GFP expression causes increase in protein synthesis rates. mTOR integrates signals from nutrient, growth factor and energy availability, and controls cell size and protein synthesis. It is well established that nutrient deprivation inhibits protein synthesis through mTOR.

To determine appropriate doxycycline concentrations for use in assessing global protein synthesis, I submitted the cell line to various doses of doxycycline and measured radioactive methionine incorporation following 24h incubation. Given the nature of what

was being investigated, the experimental setting was kept so that doxycycline was present in the culture during the methionine incorporation experiment and so to fully assess the secondary effects of the drug. This meant that the cells' media were not replenished prior to submitting the cells to experimental procedures. In the next section, media were replenished prior to undertaking the experiment making for a fundamentally different experiment, with more pronounced difference with controls. The possible reasons for this are discussed in the next section.

I have ruled out that the increase in synthesis seen under 0.1µg/mL is an effect brought about by doxycycline itself. I used a parental, non-inducible, cell line and treated it with doxycycline. There are only reports of doxycycline inhibiting protein synthesis rates, not enhancing it. However, it's not possible to rule out an effect by the GFP itself. Ideally, one GFP inducible 293T-REx cell line could rule out any artefactual effects by GFP. There are no reports, as yet, of protein synthesis enhancement caused by GFP. Furthermore, the increase seen supports Lamb and colleagues' and Miguel and colleagues' models, whereby MAP4K3 activates mTORC1 and mediates translation of target genes, making it most likely a MAP4K3 effect rather than a GFP one.

MAP4K3-GFP expression causes an increase in cell size. As discussed in earlier sections, the mTOR pathway is regulated from multiple angles and this determines activation of its downstream targets, cell size and growth. HEK cells grown to confluence lose in cell size compared to actively growing cells (Kim *et al.*, 2006). To fully exploit the activation status of a pathway that is constraint by contact inhibition, I have kept the cell line and treated it with doxycycline so that 24h post-treatment the cells were about 70% confluent.

In an attempt to characterise the green fluorescence from MAP4K3-GFP induction, I found that green cells showed an increase in cell size compared to the general population of untreated cells. Like previously, I cannot rule out that this effect may be due to GFP, and an inducible cell line expressing GFP alone would have been an excellent control to have. In experiments performed previously, however, I find that transient expression of GFP does not cause increase in cell size (data not shown) and although these are fundamentally different experiments, it makes it unlikely to be the reason behind the increase in cell size. Furthermore, there are no reports of GFP affecting cell size. If GFP does not affect cell size under transfection conditions, whose expression vastly exceeds the one in our inducible line, then it is improbable to be a conventional artefact.

Furthermore, it would be interesting to investigate the cell cycle progression of these cells following MAP4K3 induction. Of course, cells are still proliferating following prolonged induction, which is indicative that they are not arresting in some particular phase of the cell cycle and that progression is achieved. Nonetheless MAP4K3 may well be affecting progression and it is interesting to understand how.

After having 1) optimised the cell line's induction conditions to match the most appropriate for our experimental settings and 2) pinpointed an effect on cell size and protein synthesis, I decided to investigate MAP4K3 amino acid-regulation of the mTOR pathway. I use amino acid restimulation, as used by Lamb and colleagues, to assess changes in translation rates and polysome shifts.

Chapter 4

4. Amino acid restimulation MAP4K3 causes an increase in protein synthesis with no apparent activation of mTORC1 targets

4.1 Introduction

As described in the previous section, while characterising the inducible cell line, I found a progressive increase in cell size following induction. I also noticed a consistent increase in protein synthesis rates. Previously, Lamb and colleagues had established an amino acid-dependent role for MAP4K3 on the mTOR pathway (2007). I decided to investigate the effect MAP4K3 would have, upon amino acid restimulation, on protein synthesis rates.

Amino acid starvation, as discussed previously, is known to inhibit activation of mTORC1 targets p70S6K and S6 through phosphorylation, and to activate 4E-BP1 by dephosphorylation (Hara *et al.*, 1998). Activated p70S6K and S6 are known to facilitate ribosome biogenesis through phosphorylation and activation of eIF4B, which then facilitates interaction with eIF3, and through phosphorylation and activation of S6, which then enables 40S complex formation. 4E-BP1, on the other hand, when dephosphorylated will bind to eIF4E, and render it unable to form the cap-binding eIF4F complex of translation initiation.

MAP4K3 was shown to have a positive regulatory effect on the amino acid pathway to mTOR. Briefly, it was found that amino acid restimulation lead to 1) an inability to re-phosphorylate p70S6K in silencing of MAP4K3 and 2) increased phosphorylation of p70S6K in overexpression. Following the same procedures for amino acid starvation and restimulation described in Findlay *et al.* (2007), I investigate the effect of this signalling pathway on downstream targets of mTORC1 p70S6K and eIF4E-BP1, and explore its contribution to protein synthesis.

4.2 Materials and Methods

4.2.1 Materials

Amino acid-free media was made using DPBS 14040 (Invitrogen) supplemented with 10% dialysed tetracycline-free FBS, 1x MEM Vitamins 11120 (Invitrogen), 1% penicillin and streptomycin, and brought to final 4.5g/L D-Glucose. Amino acid containing media was made using DMEM 61965 (4.5g/L D-Glucose and same salt composition as DPBS 14040) supplemented with 10% dialysed tetracycline-free FBS and 1% penicillin and streptomycin. Non-phospho-4E-BP1 Thr46 (#4923) from Cell Signaling. All other materials used for western blots and ³⁵S methionine labelling have been previously described.

4.2.2 Tissue culture

Cells were kept under selection under normal maintenance conditions and taken away from selection 24h prior to seeding for experiments as described in previous sections.

4.2.3 Western blots

Cells were seeded, and treated with 0.1µg/mL doxycycline or left untreated as described in previous sections and then were either amino acid starved for 30min (-AA), amino acid starved and re-stimulated for 30min (-AA+AA) or left under normal culture conditions and then harvested as described previously. Samples were ran for western blot analyses using the specified antibodies.

4.2.4 Protein synthesis rate determination

Cells were seeded and treated with 0.1µg/mL doxycycline or left untreated as described in previous sections and then were either amino acid starved and re-stimulated for 30min (-AA+AA) or left under normal culture conditions. Media from cells left in normal culture conditions were also changed for control purposes, at the same time as amino acid starvation was performed on the -AA+AA cells (1h prior to harvest). During this media replenishment, doxycycline was not added to the cultures. Cells were then spiked for 30min then radioactivity counts per minute per µg of protein were determined as described in the previous section and normalised to control.

4.2.5 Statistics

Quantification of the western blot signals was done using ImageJ 1.46r of duplicate biological repeats as previously. Radioactive incorporation values were obtained using triplicate biological repeats for each set of conditions. Statistics and graphs were subsequently produced using Prism 5.03 by applying a one-way Analysis of Variance (ANOVA) with Bonferroni's multiple comparison test.

4.3 Results

To assess MAP4K3's contribution to the phosphorylation state of p70S6K, S6 and eIF4E-BP1 in the amino acid pathway to mTORC1, I used amino acid starvation and restimulation protocols used by Lamb and colleagues and our MAP4K3 inducible cell line.

Briefly, for amino acid starvation I incubated the cells in DPBS containing salts and supplemented with glucose, vitamins, Tet-free serum and antibiotics, following 24h induction of MAP4K3-GFP expression. For amino acid restimulation, cells were then placed back in DMEM containing amino acids, salts and vitamins and supplemented with serum and antibiotics. Cells kept under normal culture conditions were put in fresh media to control for the change in media from amino acid starvation and amino acid restimulation conditions.

Amino acid regulation of mTORC1 targets. Amino acid starvation for 30min caused clear dephosphorylation of the p70S6 kinase, and of S6 itself. 4E-BP1 was highly dephosphorylated as shown by phospho and total antibodies, with almost complete loss of γ and β subspecies. The non-phospho antibody increase in signal strength confirms dephosphorylation of 4E-BP1 (Figure 19A).

Amino acid restimulation, conversely caused an increase in phosphorylation of p70S6K compared to normal culture conditions and also translated to S6 and 4E-BP1. 4E-BP1 was found to be mostly in its γ , hyperphosphorylated, specie as shown in both its phospho and total antibody stains. The non-phospho signal is the faintest, confirming that there is most rephosphorylation.

MAP4K3, although induced at desirable levels, did not reveal apparent amino acid starvation maintenance of phosphorylation of downstream targets of mTORC1. This was also observed under amino acid restimulation, where their activation levels were equal between induced and uninduced.

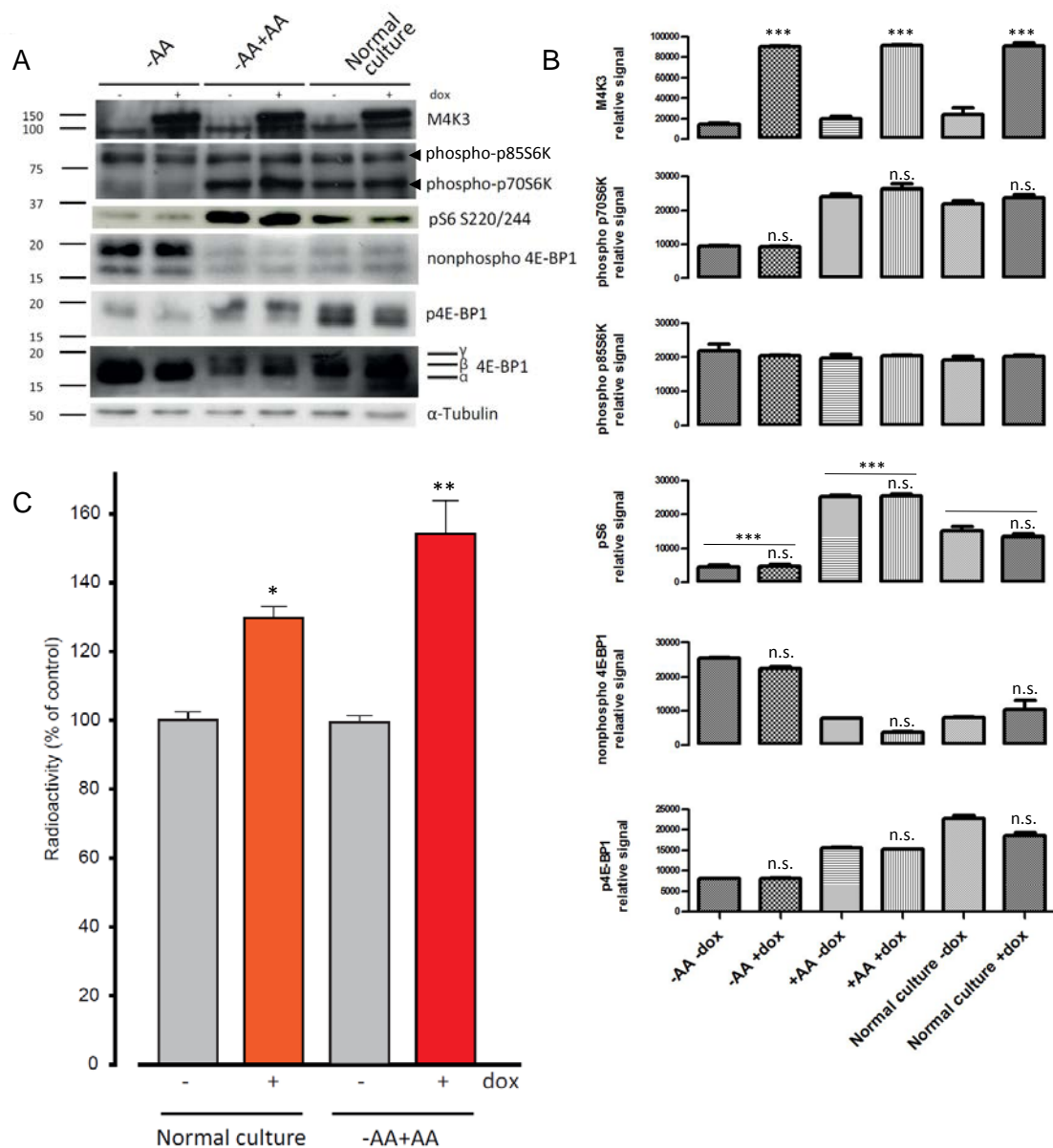


Figure 19: M4K3 has an effect on protein synthesis in an amino acid-dependent way. (A) M4K3-induction does not cause massive phosphorylation of mTORC1 targets 4E-BP1 and p70S6K even in amino acid restimulation conditions. M4K3-GFP 293T-REx cells were either treated with 0.1ug/mL doxycycline (+) or left untreated (-) and amino acid-starved for 30min (-AA), amino acid starved and restimulated for 30min (-AA+AA) or treated under normal culturing conditions (Normal). Results are representative of duplicate biological repeats. (B) Western signal quantification was performed using ImageJ and statistical analyses and graphical representations obtained using Prism. Results are from duplicate repeats. (C) Protein synthesis rates increase following doxycycline induction of M4K3 in amino acid restimulation conditions. Like in (A) cells were treated with 0.1ug/mL doxycycline (+dox) or left untreated (-dox) and amino acid starved and restimulated (-AA+AA) or left under normal culturing conditions. Incorporation of radioactive methionine was used to determine protein synthesis rates. Results are representative of triplicate biological repeats with triplicate technical repeats. (n.s. not significant $p > 0.05$, * significant $0.01 < p < 0.05$, ** very significant $0.001 < p < 0.01$, *** extremely significant $p < 0.001$).

MAP4K3 enhances protein synthesis rates following amino acid restimulation. Induction of MAP4K3 was found to cause a marked increase in radioactive methionine incorporation in replenished, normal culturing, media in induced compared to uninduced cells. Interestingly, amino acid restimulation further increased protein synthesis rates of MAP4K3 induced compared to uninduced cells during the recovery phase.

MAP4K3 did not activate mTORC1 targets in an obvious way, neither during amino acid starvation or restimulation, but interestingly had an effect on protein synthesis rates. This supports the model proposed by Martins and colleagues where MAP4K3 may be enhancing expression of target genes. Intrigued by this result, I decided to examine the polysome profiles under these conditions, and to identify target genes being up- and down-regulated, making a distinction between the translational and transcriptional contributions of MAP4K3.

4.4 Discussion

I investigated the signalling pathways activated by MAP4K3 in amino acid signalling to mTORC1 and the protein synthesis rates during amino acid restimulation. It is interesting that it is possible to both observe an amino acid restimulation-mediated enhancement of translation, and no significantly detectable phosphorylation of mTORC1 targets.

Findlay *et al.* investigated activation of mTORC1 targets by MAP4K3 by using phosphorylation reporters to accurately describe the phosphorylation changes due to MAP4K3 in amino acid signalling to mTORC1. This could be part of the reason why we are unable to distinguish between induced and uninduced in terms of phosphorylation statuses of p70S6K and 4E-BP1. Amino acid starvation and amino acid restimulation yield clear loss and gain of mTORC1 target phosphorylation respectively, compared to normal culturing conditions. In fact, there are very strong statistically significant differences between amino acid deprived and This, however, was not enough to reveal distinct phosphorylation caused by MAP4K3 in either of them, and the use of phosphorylation reporters may have been more appropriate in reproducing data from Lamb and colleagues.

Nonetheless, it was possible to detect a difference in protein synthesis rates that increased when cells were amino acid stimulated. Interestingly, when controlling for the change in media, it is possible notice a further increase when media were replenished, even without amino acid starvation, and simulating a sort of amino acid stimulation. This supports the model supported by Lamb and colleagues as well as Martins and colleagues, where MAP4K3 is having a positive regulatory effect on protein synthesis.

To identify which targets MAP4K3 may be modulating at the translational level, I collect and discriminate between actively translated and lowly translated and untranslated mRNAs, and submit them to spotted DNA microarrays to identify up- and down-regulated genes as per the method described by Melamed and Arava (2007).

Chapter 5

5. MAP4K3 causes up- down-regulation of various targets at the translational level with transcriptional control over some interesting targets

5.1 Introduction

To further investigate the translational changes brought by MAP4K3, I collected fractions of mRNA under different ribosome-bound conditions by using a technique called polysome profiling (Figure 20).

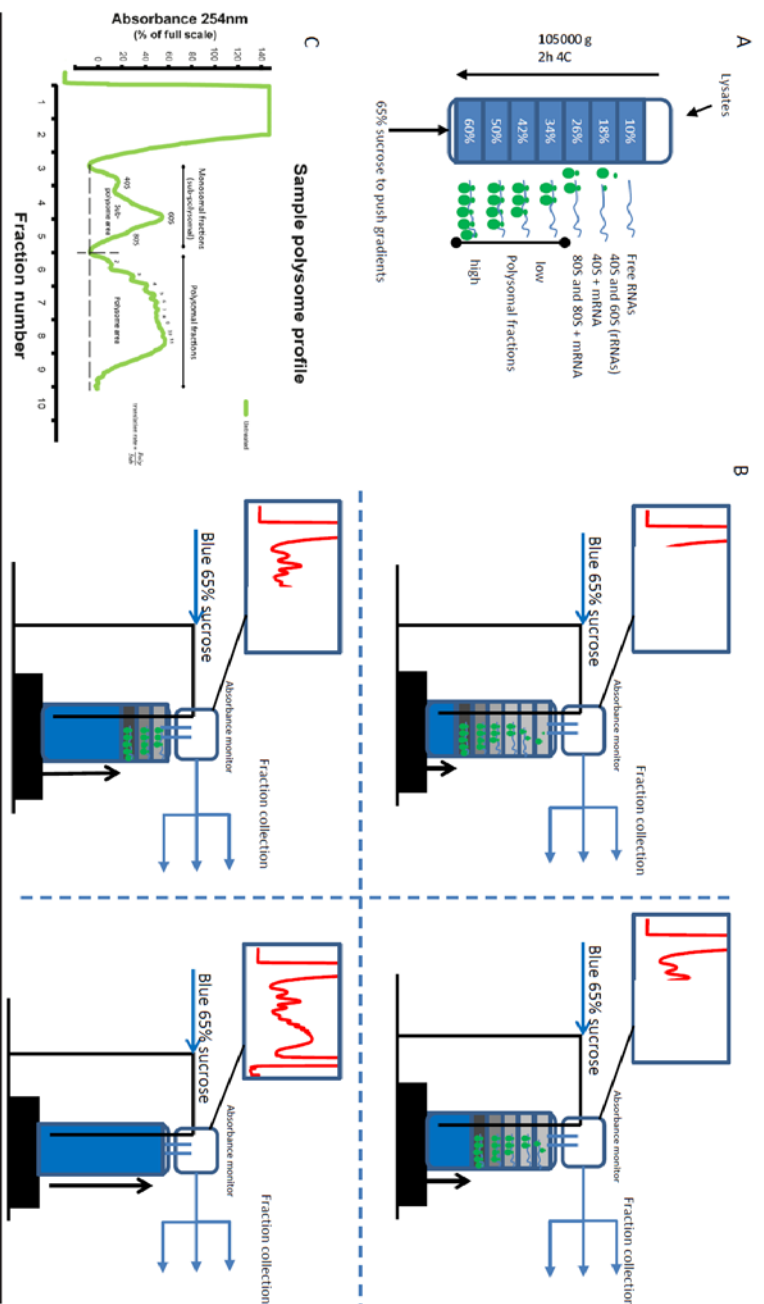


Figure 20: Experimental concept of sucrose gradient centrifugation, operational process of gradient fractionation and translation rate determination. (A) Samples are loaded onto a 10 to 60% sucrose gradient and tubes are centrifuged at high speeds both in the presence of cycloheximide at 4C to maintain mRNA-ribosome interactions. (B) Tubes are loaded onto the machine after centrifugation and 65% blue sucrose is used to push the different 10% to 60% fractions up through the absorbance reader of the gradient machine. The sucrose layers progressively pass through the machine at a set constant speed (usually 1mL/min) using a pump. The profile was traced as explained in (A) and (B) and the 40S, 60S, 80S and dimeric to entecameric (1:1 subunit) complexes are shown. 40S, 60S and 80S form the monosomal (also known as sub-polysomal and/or free) pool (fractions 1 to 5) and the dimeric and heavier complexes are considered the polysomal pool. To determine translation rates, the areas under the sub-polysomal and polysomal curves are determined using Adobe Illustrator CS5 Telegraphics filter for area calculation and the ratio Poly/Sub represents a relative value for translation rates. The effect on translation by the treatment can then be determined by calculating the ratio between Treated and Untreated (not shown).

Polysome profiling takes advantage of the density of ribosomes in differentiating between actively translated and translationally repressed and lowly translated mRNAs. Following collection of 'free' and 'ribosome bound' mRNA fractions, I submitted them to a type I, or direct comparison, by hybridising the 'free' and 'ribosome bound' genes onto the same arrays. This method is a powerful tool that links changes in the translation rates to a detection mechanism as described by Melamev and Arava (2007).

A normal step undertaken to pinpoint the pure translational variations in gene expression, is to deduct from the above method the transcriptional variations in gene expression. To this aim, microarray analysis on the steady-state mRNA levels, hence without the polysome fractionation step, was also performed. This ensures 1) that translational data is not confounded by transcriptional data giving a purely translational effect, and 2) a broader idea of the extent of gene regulation, thus providing genes that change at the transcriptional and translational levels, for a better understanding of the dynamics of gene expression in play.

We then submit the identified gene lists to high-throughput data mining techniques aimed at identifying statistical significant groups of genes in order to shed some light into the paths paved by MAP4K3.

5.2 Materials and Methods

5.2.1 Materials

Cycloheximide (C4859) from Sigma; Foxy Jr. (69-3873-169) from ISCO; RNA Nano kit and chips (5067-1511), Agilent 2100 Bioanalyzer, One- (4140-90040) and Two- (4140-90050) Color Microarray-Based Gene Expression Kit and Chips, Agilent Scanner from Agilent; Trizol/TriReagent (15596) from Invitrogen. All other materials used were described in previous sections.

5.2.2 Tissue culture

Cells were kept under selection as described previously up to 24h before plating.

5.2.3 Polysome fractionation and RNA collection

Cells were seeded to 4×10^6 and treated as previously described. Cells were then treated with 100 μ g/mL cycloheximide for 3min prior to harvest on ice. Cells were washed in PBS containing cycloheximide and then harvested using trypsin containing cycloheximide and with cold PBS/cycloheximide washes. Cells were kept on ice or at 4°C after this step. Cells were spun at 270g for 6min at 4°C on a benchtop centrifuge, the supernatant was discarded and cells were resuspended in PBS containing cycloheximide. Cells were then spun at 900g for 1min at 4°C in a microfuge, supernatant was discarded and cells were lysed in 1x sucrose buffer (300mM NaCl, 15mM MgCl₂, 15mM TrisHCl pH 7.5, 100 μ g/mL cycloheximide) containing 1% Triton-X 100. Cellular debris and intact nuclei were removed by centrifugation at 15700g for 1min at 4°C, and the supernatant was loaded onto 10%-60% sucrose gradients. Gradients were then spun at 15700g for 2h at 4°C, passed through the Foxy Jr. fractionator and fractions were collected in 0.1% SDS. Fractions were then mixed to 2.5 volumes of ethanol and incubated at -20°C for 18h. RNA was pelleted by centrifugation at 1650g for 1h at 4°C and they were resuspended in Trizol/TriReagent and the RNA supernatant (clear) was kept according to the manufacturer's protocol. RNA was then ethanol precipitated, cleaned through an RNeasy column and checked for RNA integrity on Agilent's 2100 Bioanalyzer.

5.2.4 Total RNA extraction

Cells were seeded to 4×10^6 and 18h-post seeding were either doxycycline treated or left untreated. RNA was then extracted using the QIAshredder and RNeasy Mini System and RNA integrity was checked on Agilent's 2100 Bioanalyzer.

5.2.5 RNA preparation and Microarrays

Pooled monosomal and polysomal fractions were made first into cDNA and then into Cy3 or Cy3 and Cy5 dye-incorporated cRNA according to Agilent Microarray Chips manufacturer's instructions and using their reagents and materials. Volumes, rather than concentrations, were taken into account for cRNA synthesis to maintain the differences observed between sub-polysomal and polysomal fractions, unlike transcriptional microarrays which compared total RNA differences. cRNAs were then loaded in a randomised configuration onto the arrays and the resulting fluorescence was visualised. Dye-swap was performed for two-colour arrays as per the manufacturer's instructions. The microarray slides were then scanned using lasers for excitation of the fluorochromes and photomultiplier tubes to image fluorescence.

5.2.6 Data analysis

Data analysis up to the generation of gene set was performed by the Genomics group (Dr. Nick Burgoyne), including signal determination, background compensation, and application of statistical methods (Significance Analysis for Microarrays: SAM; and RankProd). Gene list enrichment and statistical network interpretation analyses were performed alongside Dr. Martins using the web interface BioProfiling.de.

5.3 Results

To complement our protein synthesis data, I decided to assess the translational profile changes brought by MAP4K3 in an attempt to verify whether there was an apparent enhancement of translation.

5.3.1 MAP4K3-GFP enhances high density polysome formation

Polysome profiles for MAP4K3-GFP 293T-REx, as well as without the MAP4K3-GFP insertion, were acquired using sucrose density centrifugation to separate mRNAs at different densities.

Briefly, progressively heavier ribosomes would migrate to denser sucrose fractions carrying with them any mRNAs attached to them. The fractions containing the different ribonucleoproteins are then individually quantified in signal intensity and collected by the fractionator. Each peak defines a detected ribonucleoprotein complex and describes its quantity on the absorbance scale.

I performed polysome profiling analyses on both MAP4K3-GFP 293T-REx, along with their doxycycline untreated controls (Figure 21), and on the parental 'Empty' 293T-REx cell lines, along with its doxycycline untreated controls (Figure 22), to rule out any translational changes by doxycycline itself.

MAP4K3-GFP was expressed using doxycycline as previously, and endogenous MAP4K3 levels, for both untreated MAP4K3-GFP 293T-REx (Figure 21 B) as well as the 'Empty' 293T-REx (Figure 22 B), were kept to the same levels.

MAP4K3-GFP expression found to enhance the heavier polysomes and to lose in peak intensity at the 40S and 60S compared to its untreated control, an observation that would support the hypothesis of a translational upregulating event. Doxycycline seemed to have very little effect on the resulting profiles, with but the mildest inhibitory effect on the heavier polysomes with some compensation onto the 60S peak.

Analysis of the variations in the areas under the curves reveals that the polysome area is about twice the size of the sub-polysome area (Figure 23). Overall, this ratio is kept higher in the induced cells compared to uninduced (Figure 23A) but this is not an effect due to doxycycline (Figure 23B and 23C).

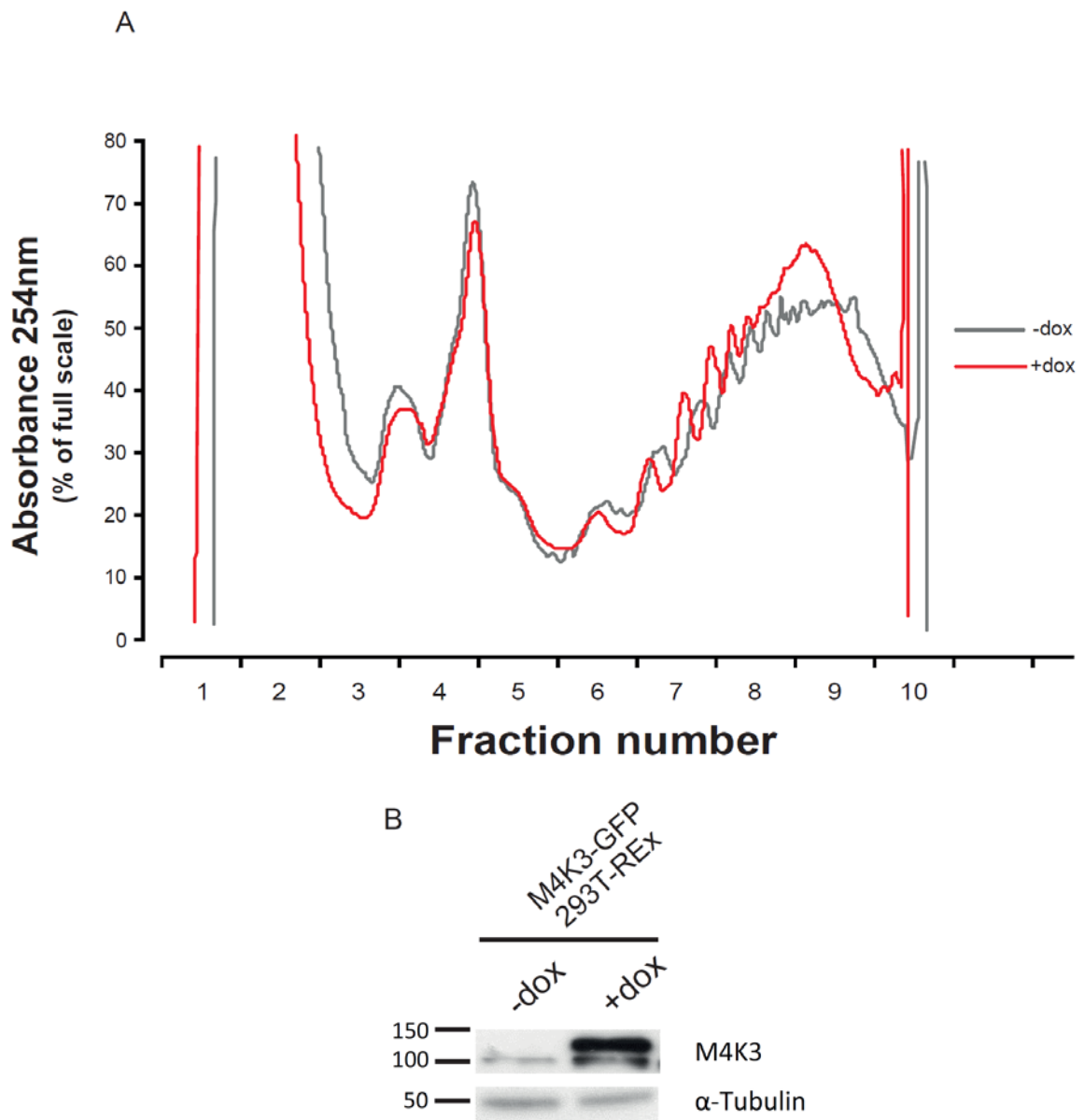


Figure 21: MAP4K3 may be driving translation from monosomes to polysomes. (A) Polysome profiles of induced and uninduced M4K3-GFP 293T-REx line reveal some increase in the denser polysome area. M4K3-GFP 293T-REx were harvested using the trypsin method for polysome profiling and a fraction kept for (B) western blotting to confirm successful induction of expression. Cell lysates were spun and run through the gradient machine as described in the methods section. Results are representative of triplicate biological repeats.

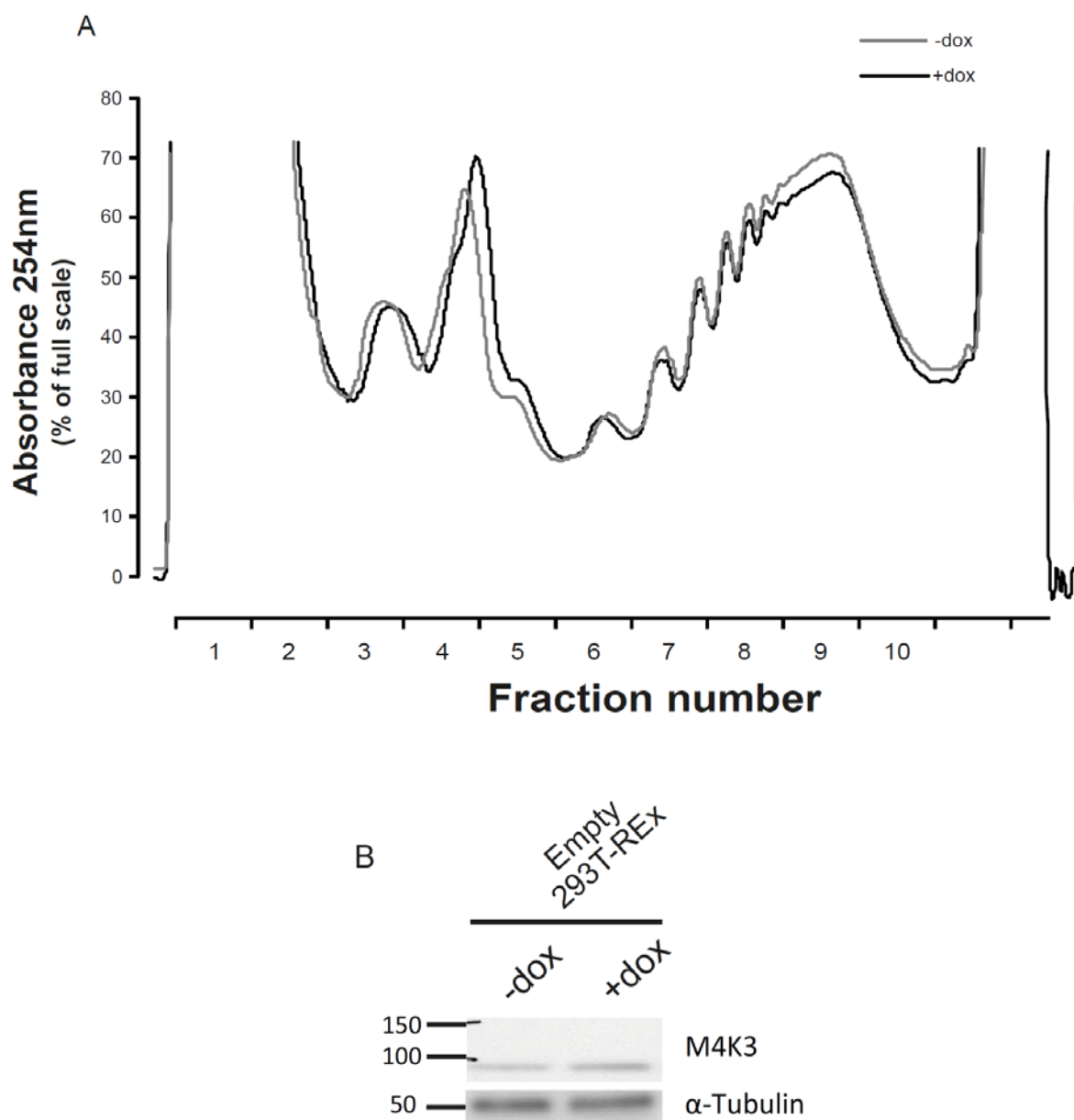


Figure 22: Polysome profiles from doxycycline treated and untreated cells are similar. (A) Polysome profiles of treated and untreated Empty 293T-REx line do not show massive differences in polysome distribution at 0.1 μ g/mL. M4K3-GFP 293T-REx were harvested using the trypsin method for polysome profiling and a fraction kept for (B) western blotting to confirm endogenous levels of MAP4K3 were being kept constant. Cell lysates were spun and run through the gradient machine as described in the methods section. Results are representative of triplicate biological repeats.

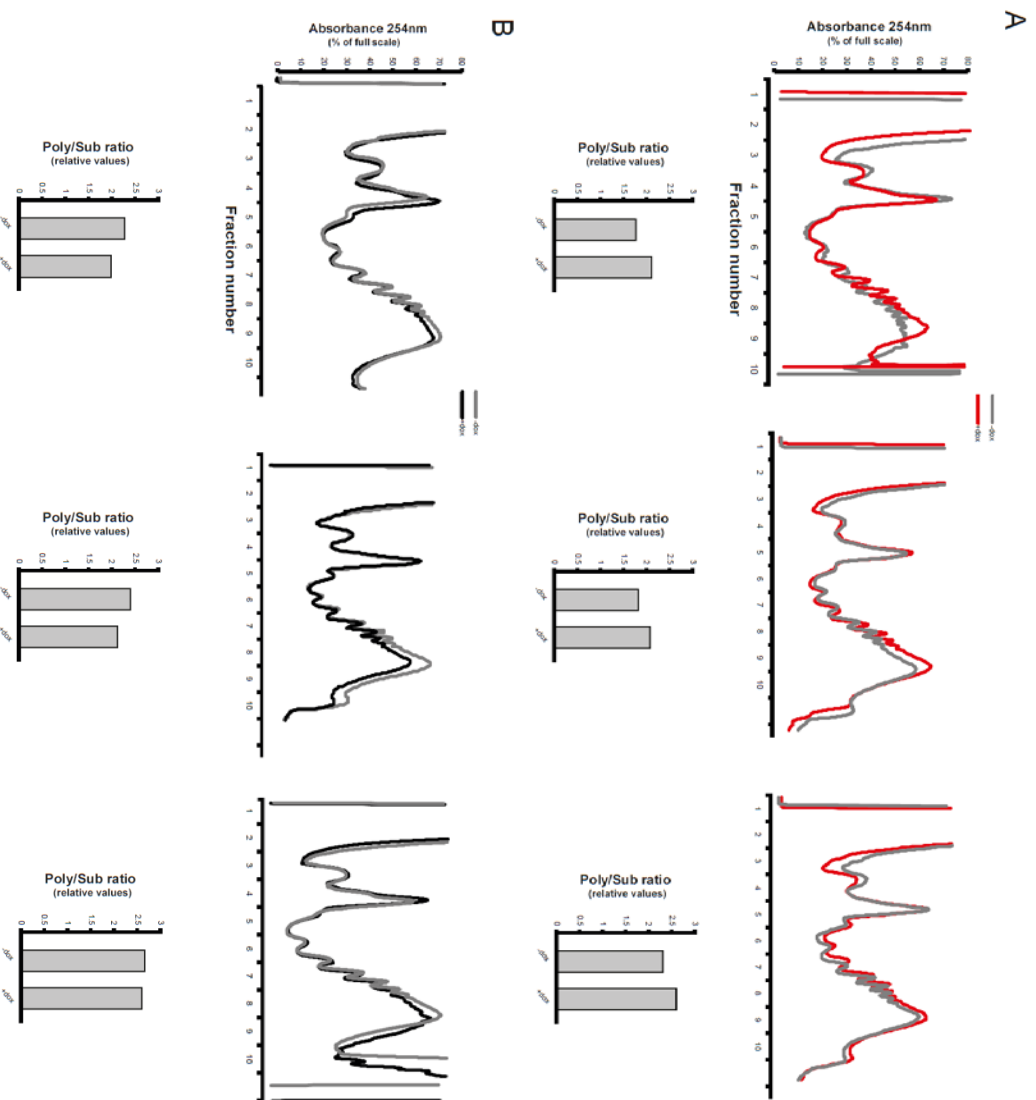


Figure 23: MAP4K3 induction increases polysome to sub-polysome ratio compared to doxycycline treatment. (A) Translation profiles of MAK3-GFP 293T-REX cells treated (red) and untreated (grey) and their associated poly to sub ratio of the calculated areas under the curve. (B) Translation profiles of Empty 293T-REX cells treated (black) and untreated (grey) and their associated poly to sub ratio of calculated areas under the curves. Translation profiles and absolute values for the areas under the curve were obtained as described in figure 20 (using Adobe Illustrator CSS Telegraphics filter), calculated and displayed in relation to one-another. (C) Mean translation ratio values and standard deviation from the means of MAK3 and Empty 293T-REX cells. Ratios (shown in A and B) were converted into relative values against their respective ratios of the untreated controls. Results are representative of triplicate biological repeats. Average values are shown with their standard deviations. Statistical analysis performed is an unpaired t-test $p = 0.0161$. * $p < 0.05$ (narrowly missing ** significance).

5.3.2 MAP4K3 and the modulation of gene expression

In order to identify genes with most robust differential expression, the Significance Analysis of Microarrays (SAM) and Rank Product Analysis (RankProd) methods were applied. RankProd is a non-parametric statistic method that describes genes that are consistently ranked high (Breitling *et al.*, 2004), whilst SAM uses t-tests to determine the reproducibility of differences between samples (Tusher *et al.*, 2001). In brief, SAM will value consistency more than high differences, whereas RankProd will highlight high differences more than variability. Following signal determination and background correction by the Genomics group analyst, signal intensities for doxycycline treated M4K3-GFP 293T-REx samples were compared to doxycycline treated 'Empty' 293T-REx samples and analysed by both SAM and RankProd.

RankProd highlights *circa* 260 genes with twofold or above upregulation and 160 genes being at least half their control expression (see appendix at the end). In the present dataset, SAM is more stringent in the way it assigns probability values, and it finds 93 downregulated *versus* 122 upregulated genes at statistical significance. I then used high-throughput comparisons of gene function, protein interactions and pathway relatedness to inquire about the nature of the gene list (Antonov, 2011).

The computational framework used by Antonov and colleagues is an interface to a number of enrichment tools. It was developed with the aim of profiling a submitted list of genes obtained from a genome-wide analysis for common patterns and relatedness with other published, and most importantly peer-reviewed, genome-wide studies. This has capabilities to provide information on gene function, pathways, protein interactions and text mining against peer-reviewed genome-wide and individual studies. The true potential of this toolkit is to provide statistically significant feedback that enables the user to characterise his dataset quickly, integrating, theoretically, all recent and validated scientific biological advances.

By using this approach, I submit statistically significant gene lists of upregulated and downregulated gene sets to identify gene groups, according to the toolkit described above. The groups identified are described in Figure 24B.

Furthermore, careful consideration of individual genes can be an indication of further relevant biological changes. Because of MAP4K3's role in the mTOR pathway, our interest in the translational control and modulation of target genes, as well as for the

previous findings of enhanced protein synthesis and translation by MAP4K3, I decided to inspect whether translation factors were being modulated. A few translation initiation factor-family members were found to be differentially expressed at, or near, statistical significance.

EIF2AK3 was found statistically ($p = 1.4 \times 10^{-3}$) downregulated (AdjExp = 0.444). The protein coded is the eIF2 α kinase-3, also known as PERK, and one of its well-known substrates is eIF2 α . eIF2 α , as described in previous sections, is involved in ternary complex formation that ultimately results in formation of a 43S. eIF2 α phosphorylation by eIF2 α kinase-3 reduces ternary complex formation (Sonenberg and Hinnenbusch, 2009) and this is a known translational inhibition mechanism (Holcik and Sonenberg, 2005). Another initiation factor found to be statistically likely to be modulated by MAP4K3 at the translational level, was *EIF1AY* which was found upregulated ($p = 1.2 \times 10^{-3}$ and AdjExp = 2.124). It codes for eIF1AY and it is functionally similar to eIF1A which is needed for binding of the 43S to the eIF4F complex as described earlier (Sonenberg and Hinnenbusch, 2009).

Interestingly, the transcriptional arrays revealed that MAP4K3 was found only about 20% upregulated and narrowly misses the statistical minimum ($p=0.0589$), whereas there is no additional shift into the highly translated fractions. The translational arrays did not show any shift in MAP4K3 expression, showing that induction likely does not function by increasing translation, but rather transcription. This is not particularly surprising given how this inducible cell line causes MAP4K3 expression, but it is indicative that this sort of transcriptional upregulation is enough to drive the increases in MAP4K3 expression described previously.

5.4 Discussion

I have submitted the different collected fractions as ‘free’ and ‘ribosome bound’ mRNAs to microarray analysis to identify the gene expression changes due to MAP4K3. I have controlled for doxycycline translational changes, as well as MAP4K3 transcriptional changes, and identified pathways that MAP4K3 may be involved in.

Doxycycline is not expected to have any transcriptional effect on eukaryotic systems (Wishart *et al.*, 2005), and it does not have massive effects on the polysome profiles of these cells at the concentrations used. There was, however, no control for GFP presence, and although there are no reports on either translational or transcriptional consequences due to GFP, there are bound to be some effects. Because it is so widely used as a reporter of gene expression, however, it is likely to affect the present study as it is to affect all other studies looking at gene expression of particular proteins of interest. We lack, however, wider knowledge of the genome-wide changes caused by GFP.

In our study of translational expression changes brought about in our system, our experiment was designed to yield data on the comparison between ‘free’ and polysome fractions, as the type I experiment illustrates. The theoretical nature of this method inherently makes us lose resolution of changes in the low and high polysomal changes. Furthermore, the 80S complex, which is mRNA bound and likely actively translating, is included into the subpolysomal ‘free’ fraction for purposes of simplicity. The mRNAs bound to those complexes may well be actively translated, as they may also be untranslated (with the ribosome being stalled onto the mRNA). This may seem to make the argument for using the indirect comparison more valid. There are, however, other limitations of the indirect comparison, that in the end make it worthwhile to perform the type I comparison despite relatively lower resolution. Our used comparison method is more efficient in the detection of wider changes in gene expression. This method gives more statistical power to data obtained, thus increasing the chances of obtaining biologically relevant leads.

The previous point brings us to the nature of the data analysis itself. The dataset obtained, from translational, transcriptional and pure translational (translational minus transcriptional) gene sets is a fold change relative to other genes, and not an absolute

account of the gene expression changes. This is important when reading the next, future directions, section. In this section, I describe potential avenues in the investigation of MAP4K3's biological influence. Overall, I use the statistical significant gene sets and apply them to worldwide datasets with the goal of identifying the most promising routes for understanding MAP4K3's wider impact. The ones that stood out the most ($p \ll 0.01$) were synaptic transmission and cell adhesion. Synaptic transmission genes had a hint towards receptors and their associated coupled signalling, whereas cell adhesion seems to involve neuronal as well as more generic cell to cell and cell to surface adhesion.

Our use of a HEK line in the study of the effect of MAP4K3 on translation initiation is justified by a good number of studies on polysome profiles in 293s. MAP4K3 itself has also been studied in HEK lines for its signal transduction contribution. For the purposes of research into its apoptotic involvement and for identifying new targets posttranscriptionally modulated, this cell line is appropriate. The group that initially transformed this cell line reported it to be, however, more closely related to neuronal cells than kidney cells (Shaw *et al.*, 2002). They demonstrate that it is likely that the initially transformed line was derived from a neuronal population as transformation happens more readily on neuronal cells in the mixed kidney population. They also find that they share many molecular characteristics with neuronal cell lines. The implications of this for this study, is that MAP4K3's role in translational regulation may be more related to neuronal cells, and this seems very likely given the results of the Gene Ontology analyses. Nonetheless, this may yield more results about the wider role of targeted translation by MAP4K3.

Moreover, this dataset may reveal hints as to how MAP4K3 positively regulates protein synthesis in the long term. Modulation of target translation initiation factors may be an avenue for sustained translation supporting our previous results, and *EIF2AK3* and *EIF1AY* come up with statistically significant changes. There are, however, no particular genes that stand out for their apoptotic contribution.

What is crucial to keep in mind is the nature of the results itself. Because they are relative gene expression changes, they will gain in significance when validated, giving more absolute biological relevance. By relating the comparisons obtained to known studies about MAP4K3, it can be possible to pinpoint the group of genes most likely to be modulated by MAP4K3 at the translational level, and so give us relevant targets for validation. In the next section, I attempt to consolidate those groups of targets with the

studies carried out on MAP4K3, and propose interesting new paths to follow in the understanding of MAP4K3 involvement in targeted control of gene expression and ailments that this may ultimately involve.

Chapter 6

6. Discussion – MAP4K3 and the proposed mechanism of control over translational regulation

In the above study I set out to evaluate MAP4K3's control over the mTOR pathway. I tested the models from both Martins and colleagues and Lamb and colleagues to investigate the type of control that MAP4K3 exerts over the translational initiation pathway. I used transient expression and an inducible cell line to evaluate mTORC1 signalling and physiological changes in the cells. The phosphorylation states of mTORC1 targets p70S6K and 4E-BP1 did not seem to be altered following transient or induced expression of MAP4K3, either in a normal nor in amino acid restimulation conditions. Interestingly, controlled MAP4K3 induction caused consistent increases in the protein translation rates and in cell size. Analysis of the profiles of expression revealed a clear increase in the translation rates following induction. In particular, genes found modulated at the translation initiation level were linked to other functions of MAP4K3, and targeted expression of factors involved in translation initiation.

MAP4K3 transient expression showed no increase in expression of BH3-only proteins Puma nor Bad (Figure 12). Regardless of the transfection state of the cells, there was no variation in the levels of the protein. A positive control for the increase in Puma expression was used to confirm specificity of the antibody, and to confirm the feasibility of detecting such variations by western blot. In effect transient transfection with a *PUMA* expressing vector caused considerable increases in the expression of the Puma protein, detectable by western, with all three different antibodies used. It is therefore unlikely that such variations were missed from a technical standpoint, and it is far more likely that such result does in fact not exist. As for the model, the same expression archetype was used as the one used in previous published experiments. Furthermore, the same aliquot of the CellSignaling antibody used in 2009 (Lam *et al.*) was tried, with no variation detected caused by MAP4K3, yet a substantial increase was detected for *PUMA* overexpressed samples. No control was used to illustrate a Puma expression decrease, which could have been done using interference RNA, but this was deemed unnecessary given that basal

expression of Puma, relative to the overexpression, was so low and constant between conditions.

Similarly Bad did not vary upon overexpression of wild-type MAP4K3. No expression control was used like with Puma, mainly because previously published results seemed to be more conclusive for Puma rather than Bad. Bid levels were not tested altogether (Lam and Martins, 2010), given the failure to see any variation in the other BH3-only proteins.

There was no change in the phosphorylation of 4E-BP1 nor in that of p70S6K in transient MAP4K3 expression experiments (Figure 12). Although a variety of conditions were used to control for transfection, dephosphorylation and expression levels of MAP4K3, no statistically significant variations were found dependent on the kinase activity of MAP4K3. In effect, MAP4K3 kinase-active overexpression caused massive phosphorylation of JNK compared to transfection and untreated controls, whereas kinase-inactive overexpression did not. This supports the idea that if there were to be an effect on the phosphorylation statuses of mTORC1 targets 4E-BP1 and p70S6K they would have been detected. In fact, dephosphorylation of 4E-BP1, p70S6K, and its downstream target S6 was detectable following rapamycin treatments. From those results, it seemed clear that any kinase-mediated action on these targets would have been revealed in the performed experiments, but it is not clear from these results whether there is any potential effect from amino acid control. To test this, I submitted the inducible cell line to amino acid starvation, and amino acid restimulation.

Although amino acid starvation caused extremely significant dephosphorylation of mTORC1 targets 4E-BP1, p70S6K and S6, MAP4K3 expression did not rescue the dephosphorylation 30min after starvation as shown by others, and amino acid restimulation failed to show statistically significant increases in the phosphorylation statuses of these proteins following induction of MAP4K3 (Figure 19). Amino acid restimulation did however cause an increase in phosphorylation compared to normal culturing conditions and amino acid starvation clearly caused a decrease in the phosphorylation of these proteins, with great statistical significance. Findlay *et al.* (2010) used phosphorylation reporters to evaluate phosphorylation of the above targets, which may be the reason why these results were not reproduced with endogenous expression of the targets. I did not run a timecourse of restimulation as Findlay *et al.* (2010) because this was beyond the scope of the study, it was however found that induction of MAP4K3

caused an increase in protein synthesis, which was further increased upon amino acid restimulation (Figure 19). This seemed to be in line with the observed increase in p70S6K, S6 and 4E-BP1 phosphorylation under the same conditions, although statistically independent of MAP4K3 induction. To further understand and characterise the rise in protein synthesis caused by MAP4K3, I decided to look at translation initiation rates.

Interestingly, translation initiation rates, as identified by translation profiling experiments, showed a consistent increase in the polysome and heavy polysome area following induction (Figure 23). This could likely account for at least part of the 30% increase in protein synthesis caused by MAP4K3 induction.

In trying to understand MAP4K3 and its control over translation initiation, I decided to identify the RNAs being driven into the polysome fractions. MAP4K3 itself was found increased in transcriptional arrays, but fell just short of the list of highly modulated genes obtained (Figure 24B). Overall, there were more genes upregulated to a higher extent than those downregulated, which were of varying degrees of downregulation (Gene list appendix). Among the most interesting considerations, were the gene groups identified from the gene list submissions to enrichment databases. In particular, the ones likely related to the observed morphological changes shown in the previous transient expression experiments, but also those related to other recently published works. Those may provide evidence to support a role in morphology, cell to cell adhesion, the neuronal response to alcohol consumption and a new mechanism for the regulation of translation initiation through initiation factor translation.

Among the most statistically significant modulated genes relevant to previous results, are the eukaryotic initiation factors. A number of these were picked up as likely being upregulated consistently between the biological triplicates, at considerable fold-increase levels. This may well give indication as to how MAP4K3 is causing the increase in protein synthesis (Figure 19), which is also in line with the observed rise in the polysome area (Figure 23). The rationale for this observed effect would be that MAP4K3 would push the genes of these initiation factors into the highly translated fractions which in turn would cause an increase in protein synthesis rates through an increase in translation initiation rates. At present, there is no further evidence to neither refute nor sustain this hypothesis. Furthermore, the levels observed may be a remnant of a stronger modulation prior to the 24h mark chosen to undertake the microarray screens. It may be of particular interest to study the effect throughout time to identify the initial effects, and

the primary and secondary genes modulated. A timecourse for protein synthesis would be a much needed first step in recognising the time of appearance of the first statistically relevant increase in synthesis following MAP4K3 induction. The times chosen, that is 24h induction of MAP4K3, followed by 30min amino acid starvation and restimulation, are the same ones used by Findlay *et al.* (2010) and I follow their reasoning in their present study. It is quite apparent that 30min are sufficient to completely lose phosphorylation of proteins involved in translation initiation, and so this is a reasonable way to observe that there is an effect in protein synthesis (Figure 19) by MAP4K3, and the 24h induction time is necessary for maintained and consistent expression both at the mRNA as well as at the protein level (Figure 17). Nonetheless it may be of particular interest to study the initial effects obtained from early induction. These may be unlikely to be translated as a detectable increase in protein synthesis but may yield initial translation initiation changes and modulation of genes of particular significance in explaining the increase seen at 24h in Figure 19.

It is needless to say that, although quite interesting in assessing MAP4K3's role in translation initiation and its other cellular functions, these results remain quite preliminary and need validations that go beyond confirming modulation of the genes identified in the screen.

In the next section I review with more detail the groups of genes picked up by the arrays and propose more interesting avenues to pursue in relation to recently published data and discuss their relevance to MAP4K3's role in posttranscriptional control of gene expression.

Future directions

MAP4K3 and translational regulation of the neuronal response to alcohol consumption. In previous sections, I described the study by Coln *et al.* that implicated the *Drosophila* ortholog of MAP4K3 – *hppy* – in ethanol hypersensitivity and describe it as a possible target for treatment of AUDs (2009). More recently, a GWAS finds that there is a high statistical correlation between alcoholism and glutamate signalling (Joslyn *et al.*, 2010). In the present study, there is statistical likelihood that MAP4K3 promotes translation of a number of target genes reported, upregulating them to at least double normal expression. One such group of genes whose translation is likely to be enhanced at least twofold is the gene set encoding glutaminergic receptors and other genes that correlate highly with the study from White and colleagues. Now, I propose an interesting new investigation route where increased MAP4K3 levels may have a positive regulatory impact on development of AUDs through enhancement of translation of glutamate receptors.

Heberlein and colleagues use the *Drosophila* system to screen for flies that were hyposensitive to ethanol sedation and expanded a fly line that has an inactivating mutation on the *hppy* gene (2009). They find that these flies have an increased time tolerance to ethanol sedation on a number of ethanol concentrations, and that this is not related to ethanol absorption mechanisms. The overexpression of a wild-type form of *hppy* in neurons of transgenic flies with the inactivating mutation of *hppy* rescued this difference in ethanol sedation. Interestingly, they found that overexpressing *hppy* in neurons hypersensitised the flies to ethanol exposure, demonstrating a negative regulation on resistance to alcohol effects. They then link this to a negative regulatory effect on the EGFR-Erk pathway, but not JNK or p38 MAPK pathways, and establish a possible mammalian link.

White and colleagues conduct a study to investigate the relationship between genetic inheritance and the etiology of AUD development. For this, they use alcohol level of response to identify patients with actual alcohol dependency. Because AUD diagnosis is based in part on the symptoms that are consequent to the disease, it is centred upon fulfilling 3 of 7 symptom criteria, making it possible for AUD to be diagnosed upon entirely different conditions. To increase the probability of the study to detect relevant

genetic factors involved in AUDs, they use the alcohol level of response, a widely used and highly advanced stage of the disease, to assess genetic variations attributable to increased risk of developing the disease. In their resulting gene list, they identify glutamate receptor signalling and metabolism genes sets at its top with highest likelihood of a genetic link ($p < 9 \times 10^{-6}$). They then submit the entire dataset to a gene set enrichment technique and ingenuity pathway analysis and propose a biological explanation for their dataset that involves glutamate metabolism in presynaptic neurons and glutamate receptor and their downstream signalling responses in the postsynaptic neurons.

In our study, I identify genes whose expression is likely to be enhanced at the translational level by MAP4K3. I selected the most stringent candidates that are most likely ($p < 0.01$) and most differentially expressed (6-fold to 2-fold increase) and find that there is high likelihood ($p < 0.05$; as calculated by the *bioprofiling.de* portal) of relatedness with the gene list from Joslyn *et al.* (2010). The same glutamate receptor gene family members seem to be statistically significant in both our as well as their 'leading-edge' lists. One interesting new path to follow would be to investigate this upregulation of synaptic transmission related genes in an appropriate model. There is no particular model for AUDs, but a neuronal cell line may be appropriate to investigate whether there is detectable upregulation of glutamate receptors, such as the SH-SY5Y neuroblastoma line, which is known to rely on glutamate signalling. Since MAP4K3 involvement has already been established in *D.melanogaster*, it would be an excellent *in vivo* system to verify reproducibility in neuronal driven *hppy* expressing flies. With enough evidence of MAP4K3/*hppy* driven expression of glutamate receptors, a new pathway may be established by which ethanol-induced behaviours are regulated.

MAP4K3 and the positive regulation of translation. As discussed earlier, MAP4K3 was found to have control over the mTORC1 pathway and was proposed to be responsible for targeted translation. Many eukaryotic-translation initiation factors (eIFs) come together to promote translation initiation, the main regulatory step in the regulation of protein synthesis. The dataset obtained from microarray of polysome profiling experiments reveals marked downregulation of *EIF2AK3* and upregulation of *EIF1AY*, both of which are involved in ternary complex formation and 43S joining. It may be of interest to validate the downregulation of *EIF2AK3* as it is known to inhibit GTP loading on eIF2 by eIF2B. Phosphorylation of eIF2 by eIF2 α kinase-3 (PERK) inhibits ternary complex formation by preventing the charged tRNA to bind to eIF2 and this cannot proceed to

form the 43S. Loss of PERK is thought to lead to diabetes through loss of translational regulation as shown in transgenic mice (Hardling *et al.*, 2001) and to an early-onset diabetic disease in humans (Delepine *et al.*, 2000).

EIF1AY was also found to be significantly upregulated by MAP4K3, and it would be interesting to see eIF1A protein increases. It is known to promote the generation of a usable pool of 40S and to stabilise binding of the ternary complex to the 40S, forming the 43S. It is also thought to be essential for scanning of the initiation codon, for its selection and to promote eIF5B interactions that allow for subunit joining and formation of a working 80S (Sonenberg and Hinnenbusch, 2009). Although there has not been extensive work on its *in vivo* role, it is needed for growth, as loss-of-function abolishes yeast replication, translation initiation and protein synthesis (Olsen *et al.*, 2003) and it is found upregulated by JAK/STAT in hyper-proliferative signalling in *Drosophila* (Myrick and Dearolf, 2000).

MAP4K3 and the regulation of cell morphology. The wider implications of studying the effects of MAP4K3 induced changes in morphology are unknown. Like many other MAP kinases, it is very likely that MAP4K3 has an effect on morphological changes through the JNK pathway. Yet, it seems that MAP4K3 is causing modulation of genes that are related to cell-cell adhesion, neuron cell adhesion and extracellular matrix formation at the translational level, too. The gene list comprising both up- and down-regulated MAP4K3 genes obtained was found to bear significant similarity ($p < 0.02$) to alternatively spliced and/or differentially expressed genes at the transcriptional level in motoneurons from sporadic ALS patients (Rabin *et al.*, 2010). However, the wider implications of this and how MAP4K3's translational control may fit in are still unclear.

It is clear that the role that MAP4K3 plays in translation initiation and targeted gene expression is worth pursuing. Its pro-growth characteristics seem to show more promise than its pro-apoptotic role in the context of amino acid-dependent mTORC1 regulation.

Upregulated gene list

| Gene | Gene Description | Pval | Adjusted expression |
|-----------------|---|-------------|---------------------|
| OR9G1 | ref Homo sapiens olfactory receptor, family 9, subfamily G, member 1 (OR9G1), mRNA [NM_001005213] | 4.47E-06 | 3.063178369 |
| XLOC_012622 | linc BROAD Institute lincRNA (XLOC_012622), lincRNA [TCONS_00026274] | 8.65E-06 | 6.275505235 |
| LOC100652962 | ref PREDICTED: Homo sapiens myelin gene regulatory factor-like (LOC100652962), mRNA [XM_003403525] | 1.67E-05 | 3.543138949 |
| XLOC_004739 | linc BROAD Institute lincRNA (XLOC_004739), lincRNA [TCONS_00009608] | 2.86E-05 | 3.044857871 |
| ENST00000455991 | Unknown | 6.02E-05 | 2.921000196 |
| C20orf203 | ref Homo sapiens chromosome 20 open reading frame 203 (C20orf203), mRNA [NM_182584] | 6.92E-05 | 2.70793591 |
| LYPD4 | ref Homo sapiens LY6/PLAUR domain containing 4 (LYPD4), mRNA [NM_173506] | 0.000118955 | 2.750466445 |
| XLOC_003070 | linc BROAD Institute lincRNA (XLOC_003070), lincRNA [TCONS_00005751] | 0.000126409 | 2.748229538 |
| THC249007 | Unknown | 0.000147278 | 2.601826121 |
| XLOC_002825 | linc BROAD Institute lincRNA (XLOC_002825), lincRNA [TCONS_00006981] | 0.000148172 | 2.60144976 |
| B3GALT5 | ref Homo sapiens UDP-Gal:betaGlcNAc beta 1,3-galactosyltransferase, polypeptide 5 (B3GALT5), transcript variant 5, mRNA [NM_033173] | 0.000173514 | 2.522346767 |
| XLOC_008439 | gb BX114033 NCI_CGAP_GCB1 Homo sapiens cDNA clone IMAGp998C012036, mRNA sequence [BX114033] | 0.000185439 | 3.360798408 |
| Q952V6 | tc Q952V6_95MEG (Q952V6) Cytochrome b (Fragment), partial (5%) [THC2780555] | 0.00018842 | 2.612777002 |
| FL4399 | ref Homo sapiens uncharacterized LOC646113 (FL4399), non-coding RNA [NR_015358] | 0.000192892 | 2.683196043 |
| IL14orf105 | ref Homo sapiens chromosome 14 open reading frame 105 (IL14orf105), mRNA [NM_018168] | 0.000206001 | 2.620264821 |
| GRIN2 | ref Homo sapiens glutamate receptor, ionotropic, kainate 2 (GRIN2), transcript variant 3, mRNA [NM_001166247] | 0.000215551 | 2.627955444 |
| XLOC_007590 | linc BROAD Institute lincRNA (XLOC_007590), lincRNA [TCONS_00015582] | 0.000219128 | 2.676952826 |
| ENST00000474213 | tc HS92319 unnamed HERV-H protein (Homo sapiens) [exp=1, wgp=0, cg=0], partial (20%) [THC2608401] | 0.000234035 | 2.490519836 |
| LOC100128979 | ref PREDICTED: Homo sapiens hypothetical LOC100128979 (LOC100128979), miscRNA [NR_109205] | 0.000245662 | 2.609921269 |
| THC2601316 | tc Q96PM8_HUMAN (Q96PM8) B lymphocyte activation-related protein BC-1514, complete [THC2601316] | 0.000259078 | 2.502473515 |
| XLOC_001093 | gb AV658777 GLC.Homo sapiens cDNA clone GLCFOA09_3', mRNA sequence [AV658777] | 0.000300519 | 2.425611274 |
| XLOC_008346 | linc BROAD Institute lincRNA (XLOC_008346), lincRNA [TCONS_00017765] | 0.000300519 | 2.369910171 |
| LOC400655 | gb Homo sapiens cDNA clone IMAGE:4825594, [BC047643] | 0.000328245 | 2.421234323 |
| XLOC_008089 | linc BROAD Institute lincRNA (XLOC_008089), lincRNA [TCONS_00017027] | 0.000329438 | 2.525996169 |
| XLOC_003142 | linc BROAD Institute lincRNA (XLOC_003142), lincRNA [TCONS_00006518] | 0.000331227 | 2.447365266 |
| KCNH1 | ref Homo sapiens potassium voltage-gated channel, subfamily H (eag-related), member 1 (KCNH1), transcript variant 1, mRNA [NM_172362] | 0.000333313 | 2.635522883 |
| LOC286186 | ref Homo sapiens uncharacterized LOC286186 (LOC286186), non-coding RNA [NR_033893] | 0.000344344 | 2.463267028 |
| FAM9C | ens family with sequence similarity 9, member C [Source:HGNC Symbol;Acc:18405] [ENST00000339955] | 0.000355972 | 2.400427262 |
| SPAG16 | ref Homo sapiens sperm associated antigen 16 (SPAG16), transcript variant 1, mRNA [NM_024532] | 0.000376245 | 2.418365441 |
| XLOC_006082 | gb CR737490 Soares_testis_NHT.Homo sapiens cDNA clone IMAGp971C1779, IMAGE:1839330_5', mRNA sequence [CR737490] | 0.00038012 | 2.37874875 |
| LOC100506172 | ref Homo sapiens uncharacterized LOC100506172 (LOC100506172), non-coding RNA [NR_038234] | 0.000392994 | 2.295751546 |
| C2orf83 | ref Homo sapiens chromosome 2 open reading frame 83 (C2orf83), transcript variant 1, mRNA [NM_020161] | 0.000400394 | 2.409592582 |
| XLOC_010668 | linc BROAD Institute lincRNA (XLOC_010668), lincRNA [TCONS_00021673] | 0.000411101 | 2.02723777 |
| AFAPI1-AS1 | ref Homo sapiens AFAPI1 antisense RNA 1 (non-protein coding) (AFAPI1-AS1), antisense RNA [NR_026892] | 0.00044094 | 2.292392577 |
| XLOC_004885 | linc BROAD Institute lincRNA (XLOC_004885), lincRNA [TCONS_00010377] | 0.000445412 | 2.385089706 |
| LOC1159 | ens chromosome 1 open reading frame 159 [Source:HGNC Symbol;Acc:26062] [ENST00000379319] | 0.00044571 | 2.431461893 |
| PPP1R3A | ref Homo sapiens protein phosphatase 1, regulatory subunit 3A (PPP1R3A), mRNA [NM_002711] | 0.000455846 | 2.439665417 |
| NKIL2 | ens MKL1/myocardin-like 2 [Source:HGNC Symbol;Acc:29819] [ENST00000389126] | 0.000478505 | 2.461150704 |
| C7orf60 | ref Homo sapiens chromosome 7 open reading frame 60 (C7orf60), mRNA [NM_152556] | 0.000583149 | 3.566858888 |
| XLOC_013765 | tc Q6RG03_XENLA (Q6RG03) Smad7 (Fragment), partial (8%) [THC2621363] | 0.00058792 | 2.373814245 |
| SLC26A3 | ref Homo sapiens solute carrier family 26, member 3 (SLC26A3), mRNA [NM_000111] | 0.000589708 | 2.404524642 |
| ENST00000502675 | ens zinc finger protein 826, pseudogene [Source:HGNC Symbol;Acc:33875] [ENST00000502675] | 0.000633236 | 2.164614501 |
| XLOC_010838 | linc BROAD Institute lincRNA (XLOC_010838), lincRNA [TCONS_00022514] | 0.000666031 | 2.30131985 |
| RBMY18 | ref Homo sapiens RNA binding motif protein, Y-linked, family 1, member B (RBMY18), mRNA [NM_001006121] | 0.000669931 | 2.378751717 |
| FL40288 | ref PREDICTED: Homo sapiens hypothetical FL40288 (FL40288), miscRNA [XR_132534] | 0.000687794 | 2.361344416 |
| ZFYF | ref Homo sapiens zinc finger protein, Y-linked (ZFY), transcript variant 1, mRNA [NM_003411] | 0.000690179 | 2.258232336 |
| XLOC_008133 | gb 601273442F1 NIH_MGC_20.Homo sapiens cDNA clone IMAGE:3614530_5', mRNA sequence [BE386236] | 0.000702105 | 2.353046908 |
| XLOC_012875 | linc BROAD Institute lincRNA (XLOC_012875), lincRNA [TCONS_00026550] | 0.000716117 | 2.394265008 |
| XLOC_004799 | gb BX098598 Soares_NFL_T_GBC_S1.Homo sapiens cDNA clone IMAGp998F243903, mRNA sequence [BX098598] | 0.000741116 | 2.430511902 |
| XLOC_014196 | gb 3777224H1 BRSTN072.Homo sapiens cDNA clone 3777224_5', mRNA sequence [BU584377] | 0.000825532 | 2.316520502 |
| XLOC_000149 | linc BROAD Institute lincRNA (XLOC_000149), lincRNA [TCONS_00000896] | 0.000829706 | 2.321406106 |
| XLOC_009639 | linc BROAD Institute lincRNA (XLOC_009639), lincRNA [TCONS_00020294] | 0.000887246 | 2.196546847 |
| LOC100508939 | ref PREDICTED: Homo sapiens hypothetical LOC100508939 (LOC100508939), miscRNA [XR_113072] | 0.000889299 | 2.930536025 |
| XLOC_004727 | linc BROAD Institute lincRNA (XLOC_004727), lincRNA [TCONS_00010263] | 0.000922127 | 2.329416269 |
| XLOC_004394 | linc BROAD Institute lincRNA (XLOC_004394), lincRNA [TCONS_00009404] | 0.000929879 | 1.911722238 |
| XLOC_009456 | linc BROAD Institute lincRNA (XLOC_009456), lincRNA [TCONS_00019651] | 0.000933755 | 2.23777445 |
| PIGC | ens phosphatidylinositol glycan anchor biosynthesis, class C [Source:HGNC Symbol;Acc:8960] [ENST00000465374] | 0.000999344 | 2.25507319 |
| PTPRO | ref Homo sapiens protein tyrosine phosphatase, receptor type, O (PTPRO), transcript variant 1, mRNA [NM_030667] | 0.001012164 | 2.313390933 |
| XLOC_013947 | linc BROAD Institute lincRNA (XLOC_013947), lincRNA [TCONS_00029024] | 0.001029157 | 2.192050283 |
| LOC100287558 | ref PREDICTED: Homo sapiens hypothetical LOC100287558 (LOC100287558), miscRNA [XR_110220] | 0.001040785 | 2.257964288 |
| LOC100652797 | ref PREDICTED: Homo sapiens hypothetical protein LOC100652797 (LOC100652797), mRNA [NM_003404376] | 0.001058971 | 3.180375507 |
| SLC6A1 | ref Homo sapiens solute carrier family 6 (neurotransmitter transporter, GABA), member 1 (SLC6A1), mRNA [NM_003042] | 0.001068213 | 2.178081676 |
| C9orf128 | ref Homo sapiens chromosome 9 open reading frame 128 (C9orf128), mRNA [NM_001012446] | 0.001072387 | 2.275835956 |
| XLOC_007531 | linc BROAD Institute lincRNA (XLOC_007531), lincRNA [TCONS_00016139] | 0.001083716 | 2.16610148 |
| XLOC_013685 | linc BROAD Institute lincRNA (XLOC_013685), lincRNA [TCONS_00028338] | 0.001084014 | 2.328383261 |
| LOC129178 | tc AB003177 proteasome subunit 27 (Homo sapiens) [exp=1, wgp=0, cg=0], partial (9%) [THC612751] | 0.001090275 | 2.30751809 |
| FOXC2 | ref Homo sapiens forkhead box C2 (MEF-1, mesenchyme forkhead 1) (FOXC2), mRNA [NM_005251] | 0.001096526 | 2.312029585 |
| ENST00000446589 | gb BX281297 Soares_NFL_T_GBC_S1.Homo sapiens cDNA clone IMAGp998G075145, IMAGE:2087454, mRNA sequence [BX281297] | 0.001098815 | 2.20492579 |
| XLOC_006117 | linc BROAD Institute lincRNA (XLOC_006117), lincRNA [TCONS_00013465] | 0.0011022 | 2.258765789 |
| A_33_P3345304 | Unknown | 0.00110846 | 1.911055896 |
| XLOC_004260 | linc BROAD Institute lincRNA (XLOC_004260), lincRNA [TCONS_00009848] | 0.001138274 | 2.296965742 |
| EHF | ref Homo sapiens ets homologous factor (EHF), transcript variant 2, mRNA [NM_012153] | 0.001145131 | 2.589426247 |
| C16orf46 | ref Homo sapiens chromosome 16 open reading frame 46 (C16orf46), transcript variant 2, mRNA [NM_152337] | 0.001153181 | 2.049285612 |
| XLOC_I2_009764 | linc BROAD Institute lincRNA (XLOC_I2_009764), lincRNA [TCONS_I2_00007421] | 0.001160038 | 2.289998953 |
| OR6F1 | ref Homo sapiens olfactory receptor, family 6, subfamily F, member 1 (OR6F1), mRNA [NM_001005286] | 0.001179715 | 2.097201534 |
| XLOC_I2_011095 | linc BROAD Institute lincRNA (XLOC_I2_011095), lincRNA [TCONS_I2_00021099] | 0.001206845 | 2.224371207 |
| XLOC_I2_007452 | linc BROAD Institute lincRNA (XLOC_I2_007452), lincRNA [TCONS_I2_00015413] | 0.001213106 | 2.250666055 |
| XLOC_I2_000253 | gb BX117229 Soares_NFL_T_GBC_S1.Homo sapiens cDNA clone IMAGp998I184005, mRNA sequence [BX117229] | 0.001233677 | 2.068290251 |
| XLOC_I2_013434 | linc BROAD Institute lincRNA (XLOC_I2_013434), lincRNA [TCONS_I2_00025918] | 0.001245901 | 2.283393683 |
| EIF1A1 | ref Homo sapiens eukaryotic translation initiation factor 1A, Y-linked (EIF1A1), mRNA [NM_004681] | 0.001245901 | 2.124593092 |
| CPYF21 | ref Homo sapiens cytochrome P450, family 4, subfamily 2, polypeptide 1 (CPYF21), mRNA [NM_178134] | 0.001262 | 2.172414259 |
| CHRM3 | ref Homo sapiens cholinergic receptor, muscarinic 3 (CHRM3), mRNA [NM_000740] | 0.001368857 | 2.634969771 |
| XLOC_005523 | tc C23605_ARATH (C23605) Sperm protein homolog, partial (5%) [THC2689312] | 0.001387341 | 2.657696563 |
| XLOC_006730 | linc BROAD Institute lincRNA (XLOC_006730), lincRNA [TCONS_00014637] | 0.001396583 | 2.084840131 |
| LOC100169752 | ref Homo sapiens uncharacterized LOC100169752 (LOC100169752), non-coding RNA [NR_023362] | 0.001347444 | 2.250997085 |
| XLOC_011610 | linc BROAD Institute lincRNA (XLOC_011610), lincRNA [TCONS_00023836] | 0.001352334 | 2.189166003 |
| LOC100652782 | ref PREDICTED: Homo sapiens hypothetical LOC100652782 (LOC100652782), miscRNA [XR_132724] | 0.001363365 | 2.203529426 |
| TSPYL6 | ref Homo sapiens TSPYL-like 6 (TSPYL6), mRNA [NM_001003937] | 0.001375291 | 2.266182326 |
| EGF6 | ref Homo sapiens fibroblast growth factor 6 (EGF6), mRNA [NM_020996] | 0.001395564 | 2.02082779 |
| XLOC_008342 | linc BROAD Institute lincRNA (XLOC_008342), lincRNA [TCONS_00017761] | 0.001408682 | 2.080051816 |
| UTY | ens Ubiquitously transcribed tetratricopeptide repeat gene, Y-linked [Source:HGNC Symbol;Acc:12638] [ENST00003828923] | 0.001428955 | 2.26636588 |
| LOC100507632 | ref Homo sapiens uncharacterized LOC100507632 (LOC100507632), non-coding RNA [NR_038236] | 0.001465923 | 2.24008382 |
| XLOC_004765 | linc BROAD Institute lincRNA (XLOC_004765), lincRNA [TCONS_00009626] | 0.001521078 | 2.243176666 |
| TNFSF11 | ref Homo sapiens tumor necrosis factor (ligand) superfamily, member 11 (TNFSF11), transcript variant 2, mRNA [NM_033012] | 0.001551786 | 2.102524905 |
| LINC00281 | ref Homo sapiens long intergenic non-protein coding RNA 281 (LINC00281), non-coding RNA [NR_027278] | 0.00164611 | 2.197378265 |
| GRIN1 | ref Homo sapiens glutamate receptor, ionotropic, N-methyl D-aspartate 1 (GRIN1), transcript variant 5, mRNA [NM_001185091] | 0.001658518 | 2.159036753 |
| XLOC_I2_013029 | tc U92819 unnamed HERV-H protein (Homo sapiens) [exp=1, wgp=0, cg=0], partial (20%) [THC2608401] | 0.001692207 | 2.637704215 |
| SULT1B1 | ref Homo sapiens sulfotransferase family, cytosolic, 1B, member 1 (SULT1B1), mRNA [NM_014465] | 0.001692207 | 2.220769627 |
| XLOC_000269 | linc BROAD Institute lincRNA (XLOC_000269), lincRNA [TCONS_00000243] | 0.001703536 | 1.956432009 |
| XLOC_002852 | tc Q8SP5_95MEG (Q8SP5) Cytochrome b (Fragment), partial (6%) [THC2677314] | 0.001707412 | 1.12918838 |
| TMPRSS11B | ref Homo sapiens transmembrane protease, serine 11B (TMPRSS11B), mRNA [NM_182502] | 0.001738418 | 2.086366494 |
| LOC100124692 | ref Homo sapiens maltase-glucoamylase (alpha-glucosidase) pseudogene (LOC100124692), non-coding RNA [NR_003717] | 0.001835907 | 2.099982613 |
| DEFA10P | ref Homo sapiens defensin, alpha 10 pseudogene (DEFA10P), non-coding RNA [NR_029386] | 0.001838292 | 2.155324929 |
| PRLR | ref Homo sapiens prolactin receptor (PRLR), transcript variant 1, mRNA [NM_000949] | 0.001860652 | 2.065986272 |
| P39194 | tc ALU7_HUMAN (P39194) Alu subfamily SQ sequence contamination warning entry, partial (10%) [THC2521457] | 0.001920577 | 2.167060974 |
| LOC647589 | ref Homo sapiens uncharacterized protein LOC647589 (LOC647589), mRNA [NM_001191054] | 0.001934888 | 1.933242528 |
| SPZ1 | ref Homo sapiens spermatogenic leucine zipper 1 (SPZ1), mRNA [NM_032567] | 0.00196649 | 2.151137049 |
| XLOC_001517 | Unknown | 0.001990937 | 2.138888481 |
| KLK11 | ref Homo sapiens kallikrein-related peptidase 11 (KLK11), transcript variant 2, mRNA [NM_144947] | 0.002023675 | 2.133150349 |
| FL43903 | gb Homo sapiens cDNA FL43903 fs, clone TEST4010211, [AKI125891] | 0.002036253 | 2.127862643 |
| ENST0000044635 | gb Homo sapiens cDNA FLJ33594 fs, clone BRAMY2012776, [AKO90913] | 0.002036551 | 2.132948843 |
| XLOC_I2_013484 | linc BROAD Institute lincRNA (XLOC_I2_013484), lincRNA [TCONS_I2_00026028] | 0.002075905 | 2.006464204 |
| XLOC_012889 | tc HSU93049 SLP-76 associated protein (Homo sapiens) [exp=1, wgp=0, cg=0], partial (3%) [THC2615169] | 0.002093389 | 1.989203337 |
| A_33_P3391542 | Unknown | 0.002179983 | 2.015707728 |
| HBZ | ref Homo sapiens hemoglobin, zeta (HBZ), mRNA [NM_005322] | 0.002201121 | 2.109829266 |
| XLOC_011940 | linc BROAD Institute lincRNA (XLOC_011940), lincRNA [TCONS_00025003] | 0.002210065 | 2.104808894 |
| LOC100288077 | ref Homo sapiens Wilms tumor 1 associated protein pseudogene (LOC100288077), non-coding RNA [NR_038390] | 0.002213344 | 1.940437731 |
| ENST00000400831 | gb Homo sapiens cDNA FLJ32038 fs, clone NTONG2000583, [AKO56600] | 0.002222587 | 2.039813513 |
| C6orf208 | ref Homo sapiens chromosome 6 open reading frame 208 (C6orf208), non-coding RNA [NR_026780] | 0.002229444 | 2.10081449 |
| XLOC_008615 | linc BROAD Institute lincRNA (XLOC_008615), lincRNA [TCONS_00018335] | 0.00223004 | 2.059121654 |
| XLOC_011723 | linc BROAD Institute lincRNA (XLOC_011723), lincRNA [TCONS_00024408] | 0.002286387 | 1.958109734 |
| XLOC_004787 | linc BROAD Institute lincRNA (XLOC_004787), lincRNA [TCONS_00010304] | 0.002316791 | 2.087827871 |
| XLOC_004935 | gb BX094454 Soares_NFL_T_GBC_S1.Homo sapiens cDNA clone IMAGp998F134012, mRNA sequence [BX094454] | 0.002324548 | 2.061412403 |
| XLOC_003194 | gb DKFZp790522.1.779 (synonym: hnc1) Homo sapiens cDNA clone DKFZp790522.5, mRNA sequence [BX956887] | 0.00235615 | 2.002247074 |
| DMBT1 | ref Homo sapiens deleted in malignant brain tumors 1 (DMBT1), transcript variant 2, mRNA [NM_007329] | 0.002362411 | 2.06717261 |
| LOC100505776 | ref Homo sapiens uncharacterized LOC100505776 (LOC100505776), transcript variant 1, non-coding RNA [NR_038325] | 0.002380896 | 2.070394881 |

| | | | |
|-----------------|--|-------------|-------------|
| XLOC_002795 | linc1[BROAD Institute lincRNA (XLOC_002795), lincRNA [TCONS_0006199] | 0.002523403 | 2.057051205 |
| XLOC_007946 | linc1[BROAD Institute lincRNA (XLOC_007946), lincRNA [TCONS_00017149] | 0.002548745 | 1.989055339 |
| LOC732275 | ref Homo sapiens uncharacterized LOC732275 (LOC732275), non-coding RNA [NR_024406] | 0.002563955 | 1.943388131 |
| LSAMP | ref Homo sapiens limbic system-associated membrane protein (LSAMP), mRNA [NM_002338] | 0.002573192 | 2.006742891 |
| XLOC_010679 | linc1[BROAD Institute lincRNA (XLOC_010679), lincRNA [TCONS_0002302] | 0.002580943 | 2.070979469 |
| PLD5 | ref Homo sapiens phospholipase D family, member 5 (PLD5), transcript variant 1, mRNA [NM_152666] | 0.002610459 | 2.112679555 |
| ENST00000390452 | ens T cell receptor delta variable 1 [Source:HGNC Symbol;Acc:12262] [ENST00000390452] | 0.002619403 | 1.960379576 |
| LOC284950 | ref Homo sapiens uncharacterized LOC284950 (LOC284950), non-coding RNA [NR_038888] | 0.00262626 | 2.121064459 |
| LINC00111 | ref Homo sapiens long intergenic non-protein coding RNA 111 (LINC00111), non-coding RNA [NR_024367] | 0.002647129 | 1.983642019 |
| XLOC_I2_011579 | linc1[BROAD Institute lincRNA (XLOC_I2_011579), lincRNA [TCONS_I2_0002305] | 0.002659949 | 2.109381408 |
| WFDC6 | ref Homo sapiens WAP four-disulfide core domain 6 (WFDC6), mRNA [NM_008027] | 0.002682309 | 2.015725163 |
| XLOC_002830 | tc Q7N146_GLOVI (Q7N146) Cytochrome c550, partial (8%) [THC2717131] | 0.002699042 | 2.10343072 |
| SLC6A3 | ref Homo sapiens solute carrier family 6 (neurotransmitter transporter, dopamine), member 3 (SLC6A3), mRNA [NM_001044] | 0.002783376 | 2.099433245 |
| XLOC_004627 | linc1[BROAD Institute lincRNA (XLOC_004627), lincRNA [TCONS_00010164] | 0.002815275 | 2.098863656 |
| CERS3 | ref Homo sapiens ceramide synthase 3 (CERS3), mRNA [NM_178842] | 0.002848181 | 2.062071631 |
| XLOC_013696 | linc1[BROAD Institute lincRNA (XLOC_013696), lincRNA [TCONS_00028347] | 0.002866853 | 1.99934894 |
| OR5AP2 | ref Homo sapiens olfactory receptor, family 5, subfamily AP, member 2 (OR5AP2), mRNA [NM_00102925] | 0.002920816 | 1.979305664 |
| XLOC_002993 | linc1[BROAD Institute lincRNA (XLOC_002993), lincRNA [TCONS_00005711] | 0.002932443 | 2.076287112 |
| XLOC340515 | ref Homo sapiens uncharacterized LOC340515 (LOC340515), non-coding RNA [NR_034157] | 0.002933635 | 2.039455975 |
| BOLL | ref Homo sapiens bol, boule-like (Drosophila) (BOLL), transcript variant 2, mRNA [NM_033030] | 0.002954505 | 1.982096929 |
| DK6 | ref Homo sapiens docking protein 6 (DK6), mRNA [NM_152721] | 0.002954803 | 2.066841983 |
| MGP | ref Homo sapiens matrix Gla protein (MGP), transcript variant 2, mRNA [NM_000900] | 0.002956889 | 2.062668427 |
| FHL1 | ens four and a half LIM domains 1 [Source:HGNC Symbol;Acc:3702] [ENST00000370674] | 0.003023076 | 1.963796517 |
| AK093006 | ab Homo sapiens cDNA FLJ35687 fs, clone SPLE2019349, [AK093006] | 0.003027846 | 2.292854464 |
| XLOC_003020 | ab BX101095 NIC1 CGAP Kid5 Homo sapiens cDNA clone IMAGE9598094073, mRNA sequence [BX101095] | 0.003049908 | 2.069273966 |
| SIRP3 | ab Homo sapiens cDNA FLJ3233 fs, clone THNU3000036, AK124242 | 0.003091268 | 2.142458253 |
| ENST00000446592 | ab Homo sapiens coiled-coil domain containing 26, mRNA (cDNA clone IMAGE:4305364), [BC070152] | 0.003075249 | 1.931261096 |
| XLOC_003444 | tc Q9C614_9CL0T (Q9C614) Helix-turn-helix protein Bp1: Sugar isomerase (SIS), partial (5%) [THC2615290] | 0.003098957 | 2.086797245 |
| KRTAP26-1 | ref Homo sapiens keratin associated protein 26-1 (KRTAP26-1), mRNA [NM_203405] | 0.003117584 | 1.898527398 |
| XLOC_011252 | linc1[BROAD Institute lincRNA (XLOC_011252), lincRNA [TCONS_00023404] | 0.003141733 | 1.974471754 |
| XLOC_010688 | linc1[BROAD Institute lincRNA (XLOC_010688), lincRNA [TCONS_00022082] | 0.003255918 | 2.062955783 |
| XLOC_I2_011612 | linc1[BROAD Institute lincRNA (XLOC_I2_011612), lincRNA [TCONS_I2_00023403] | 0.003264266 | 2.336430308 |
| XLOC_010903 | linc1[BROAD Institute lincRNA (XLOC_010903), lincRNA [TCONS_00022597] | 0.003280961 | 1.993655259 |
| AR | ref Homo sapiens androgen receptor (AR), transcript variant 1, mRNA [NM_000044] | 0.003282452 | 2.077010793 |
| LOC340090 | gb Homo sapiens hypothetical protein LOC340090, mRNA (cDNA clone IMAGE:5187356), partial cds. [BC043557] | 0.003286328 | 2.018555219 |
| PRO1768 | ref Homo sapiens PRO1768 (PRO1768), non-coding RNA [NR_024620] | 0.003310775 | 1.951013271 |
| XLOC390660 | ref PREDICTED: Homo sapiens FL00317 protein (LOC390660), miscRNA [XR_109177] | 0.003318824 | 2.029506609 |
| XLOC_004631 | linc1[BROAD Institute lincRNA (XLOC_004631), lincRNA [TCONS_00010168] | 0.003385308 | 2.02337634 |
| XLOC10055827 | ref PREDICTED: Homo sapiens hypothetical LOC10055827 (LOC10055827), miscRNA [XR_109685] | 0.003423469 | 2.06422829 |
| NOX1 | ref Homo sapiens NADPH oxidase 4 (NOX1), transcript variant NOH-1LV, mRNA [NM_013955] | 0.003433009 | 2.195974564 |
| XLOC_005277 | linc1[BROAD Institute lincRNA (XLOC_005277), lincRNA [TCONS_00011801] | 0.003491444 | 1.987732698 |
| XLOC_003243 | linc1[BROAD Institute lincRNA (XLOC_003243), lincRNA [TCONS_00006522] | 0.003516487 | 1.989895357 |
| GRK4 | ref Homo sapiens glutamate receptor, ionotropic, kainate 4 (GRK4), mRNA [NM_014619] | 0.003524835 | 2.066418525 |
| XLOC_I2_015703 | linc1[BROAD Institute lincRNA (XLOC_I2_015703), lincRNA [TCONS_I2_00030467] | 0.003562101 | 1.980975948 |
| XLOC_004881 | linc1[BROAD Institute lincRNA (XLOC_004881), lincRNA [TCONS_00010962] | 0.003562399 | 2.00920095 |
| A_33_P3221059 | Unknown | 0.003585952 | 1.984400058 |
| CTNND2 | ref Homo sapiens catenin (cadherin-associated protein), delta 2 (neural plakophilin-related arm-repeat protein) (CTNND2), mRNA [NM_001332] | 0.003587144 | 1.966893934 |
| LOC100507059 | ref PREDICTED: Homo sapiens hypothetical LOC100507059 (LOC100507059), miscRNA [XR_109002] | 0.003608312 | 2.050915481 |
| CCL11 | ref Homo sapiens chemokine (C-C motif) ligand 11 (CCL11), mRNA [NM_002986] | 0.003632461 | 1.927990352 |
| XLOC_004765 | linc1[BROAD Institute lincRNA (XLOC_004765), lincRNA [TCONS_00009627] | 0.003681057 | 2.128299063 |
| XLOC_006124 | linc1[BROAD Institute lincRNA (XLOC_006124), lincRNA [TCONS_00014152] | 0.003716534 | 1.928608798 |
| XLOC_I2_014217 | tc Q9K756_BACHD (Q9K756) BH3517 protein, partial (8%) [THC2737635] | 0.003724584 | 1.946771677 |
| FAM99A | ref Homo sapiens family with sequence similarity 99, member A (non-protein coding) (FAM99A), non-coding RNA [NR_026643] | 0.003726075 | 1.909660568 |
| RFX8 | ref Homo sapiens regulatory factor X, 8 (RFX8), mRNA [NM_001145664] | 0.003733528 | 2.054499841 |
| A_33_P3264524 | Unknown | 0.003736509 | 2.006927655 |
| XLOC_I2_005246 | linc1[BROAD Institute lincRNA (XLOC_I2_005246), lincRNA [TCONS_I2_00009776] | 0.003802695 | 1.966675828 |
| LRRC7 | ens leucine rich repeat containing 7 [Source:HGNC Symbol;Acc:185311] [ENST00000370958] | 0.003883787 | 1.986262471 |
| FAM74A3 | ref Homo sapiens family with sequence similarity 74, member A3 (FAM74A3), non-coding RNA [NR_026801] | 0.003944805 | 2.040673895 |
| XLOC_010897 | Unknown | 0.003964008 | 2.000308419 |
| XLOC_000329 | linc1[BROAD Institute lincRNA (XLOC_000329), lincRNA [TCONS_00002109] | 0.003966371 | 1.916467976 |
| XLOC_009599 | linc1[BROAD Institute lincRNA (XLOC_009599), lincRNA [TCONS_00019800] | 0.004004233 | 1.987308709 |
| XLOC_001307 | linc1[BROAD Institute lincRNA (XLOC_001307), lincRNA [TCONS_00002791] | 0.004005128 | 2.04627713 |
| XLOC_001508 | linc1[BROAD Institute lincRNA (XLOC_001508), lincRNA [TCONS_00003719] | 0.004033749 | 1.938730066 |
| LOC100505734 | ref PREDICTED: Homo sapiens hypothetical LOC100505734 (LOC100505734), miscRNA [XR_110588] | 0.004066842 | 2.030739764 |
| SIRPB1 | ref Homo sapiens signal-regulatory protein beta 1 (SIRPB1), transcript variant 1, mRNA [NM_006065] | 0.004087413 | 2.037304711 |
| LCE4A | ref Homo sapiens late cornified envelope 4A (LCE4A), mRNA [NM_178356] | 0.004097847 | 1.980422667 |
| LOC100505964 | ref Homo sapiens uncharacterized LOC100505964 (LOC100505964), non-coding RNA [NR_037881] | 0.004133325 | 1.951964306 |
| MMP20 | ref Homo sapiens matrix metalloproteinase 20 (MMP20), mRNA [NM_004771] | 0.00413422 | 2.025535164 |
| LOC100506502 | ref PREDICTED: Homo sapiens hypothetical LOC100506502 (LOC100506502), miscRNA [XR_110926] | 0.00414376 | 1.92251735 |
| CA6 | ref Homo sapiens carbonic anhydrase VI (CA6), mRNA [NM_001215] | 0.004152108 | 2.032386606 |
| ERMN | ref Homo sapiens ermin, ERM-like protein (ERMN), transcript variant 2, mRNA [NM_020711] | 0.004203983 | 1.906699716 |
| ENST00000457402 | ab Homo sapiens hypothetical gene supported by BC042100, mRNA (cDNA clone IMAGE:5787371), [BC042100] | 0.0042332 | 1.995898863 |
| DEFB109P18 | ref Homo sapiens defensin, beta 109, pseudogene 18 (DEFB109P18), non-coding RNA [NR_030688] | 0.00426033 | 1.935308955 |
| ENST00000367561 | ens regulator of G-protein signaling 1 like 1 [Source:HGNC Symbol;Acc:181636] [ENST00000367561] | 0.004264504 | 1.970439840 |
| XLOC_I2_003803 | linc1[BROAD Institute lincRNA (XLOC_I2_003803), lincRNA [TCONS_I2_00006951] | 0.004328603 | 1.96554002 |
| XLOC_008950 | linc1[BROAD Institute lincRNA (XLOC_008950), lincRNA [TCONS_00018049] | 0.00436587 | 1.924099636 |
| XLOC_I2_007541 | linc1[BROAD Institute lincRNA (XLOC_I2_007541), lincRNA [TCONS_I2_00015473] | 0.004393894 | 1.926379209 |
| XLOC_001744 | linc1[BROAD Institute lincRNA (XLOC_001744), lincRNA [TCONS_00003045] | 0.004418043 | 1.921820222 |
| AK126601 | gb Homo sapiens cDNA FLJ44638 fs, clone BRACE2027312, [AK126601] | 0.004419832 | 1.917697294 |
| C4orf11 | ref Homo sapiens chromosome 4 open reading frame 11 (C4orf11), transcript variant 1, non-coding RNA [NR_024087] | 0.004429968 | 1.938585626 |
| XLOC_I2_009899 | tc Q4H3P1_CIOIN (Q4H3P1) Transcription factor protein, partial (9%) [THC2610693] | 0.004489595 | 1.902323061 |
| XLOC_002096 | linc1[BROAD Institute lincRNA (XLOC_002096), lincRNA [TCONS_00004253] | 0.004504204 | 1.99880584 |
| ENST00000369474 | ens Uncharacterized protein cDNA FLJ27030 fs, clone SLV07741 [Source:UniProtKB/TREMBL;Acc:Q6ZWN3] [ENST00000369474] | 0.004521794 | 2.097549775 |
| Csorf64 | ref Homo sapiens chromosome 5 open reading frame 64 (Cсорf64), mRNA [NM_173667] | 0.004542663 | 1.971207723 |
| GRIN2A | ref Homo sapiens glutamate receptor, ionotropic, N-methyl D-aspartate 2A (GRIN2A), transcript variant 2, mRNA [NM_000833] | 0.004557868 | 2.011895767 |
| XLOC_000471 | tc Q7N1K1_GLOVI (Q7N1K1) Gli2182 protein, partial (3%) [THC2753106] | 0.004558762 | 1.95449884 |
| CASC4 | ens cancer susceptibility candidate 4 [Source:HGNC Symbol;Acc:24892] [ENST00000429162] | 0.004558762 | 1.931860148 |
| ENST00000431698 | Unknown | 0.00469322 | 1.992158407 |
| XLOC_004635 | tc Q330J9_HUMAN (Q330J9) Cyclin M1 (Fragment), partial (29%) [THC2723318] | 0.004735555 | 1.942775017 |
| LOC100506853 | ref PREDICTED: Homo sapiens hypothetical LOC100506853 (LOC100506853), miscRNA [XR_110548] | 0.004743207 | 1.984750239 |
| XLOC_I2_000979 | linc1[BROAD Institute lincRNA (XLOC_I2_000979), lincRNA [TCONS_I2_00018977] | 0.004747183 | 1.954652849 |
| XLOC_I2_005692 | linc1[BROAD Institute lincRNA (XLOC_I2_005692), lincRNA [TCONS_I2_00010604] | 0.004767754 | 1.923277779 |
| B3GALT1 | ref Homo sapiens UDP-Gal-4-epitGalNAc beta 1,3-galactosyltransferase, polypeptide 1 (B3GALT1), mRNA [NM_020981] | 0.004810685 | 1.889212012 |
| LOC423366 | ref PREDICTED: Homo sapiens hypothetical LOC423366 (LOC423366), miscRNA [XR_108597] | 0.004846461 | 1.899051333 |
| XLOC_001134 | linc1[BROAD Institute lincRNA (XLOC_001134), lincRNA [TCONS_00001763] | 0.004889094 | 1.994239812 |
| XLOC12586 | ens Glycosyltransferase 54 domain-containing protein (Source:UniProtKB/Swiss-Prot;Acc:A6GN13) [ENST00000513106] | 0.004958858 | 1.991519752 |
| SERPINC1 | ref Homo sapiens serpin peptidase inhibitor, clade C (antithrombin), member 1 (SERPINC1), mRNA [NM_000488] | 0.004977044 | 1.93282157 |
| A_33_P3288434 | Unknown | 0.005034882 | 1.902369348 |
| XLOC_004325 | linc1[BROAD Institute lincRNA (XLOC_004325), lincRNA [TCONS_00009913] | 0.005053068 | 1.917350098 |
| ORAQ3 | ref Homo sapiens olfactory receptor, family 4, subfamily Q, member 3 (ORAQ3), mRNA [NM_172194] | 0.00506708 | 1.98816866 |
| XLOC_003980 | gb DB036142 TEST12 Homo sapiens cDNA clone TEST12021722 5', mRNA sequence [DB036142] | 0.005117125 | 1.985197695 |
| ANKRD30BP2 | ref Homo sapiens ankryrin repeat domain 30B pseudogene 2 (ANKRD30BP2), non-coding RNA [NR_026916] | 0.005267724 | 1.901922245 |
| XLOC_003965 | gb RST15642 Athersys RAGE Library Homo sapiens cDNA, mRNA sequence [BG196424] | 0.005403077 | 1.954637447 |
| LOC41493 | ref PREDICTED: Homo sapiens hypothetical LOC41493 (LOC41493), miscRNA [XR_113304] | 0.005410828 | 1.912804745 |
| CD40L6 | ref Homo sapiens CD40 ligand (CD40L6), mRNA [NM_000074] | 0.005445232 | 1.928292849 |
| LOC100128657 | ref PREDICTED: Homo sapiens mitochondrial intermembrane space import and assembly protein 40-like (LOC100128657), miscRNA [XR_132562] | 0.005461213 | 1.88926326 |
| XLOC_004577 | linc1[BROAD Institute lincRNA (XLOC_004577), lincRNA [TCONS_00010109] | 0.00552561 | 1.906491814 |
| LOC728767 | tc OST2A2_HUMAN (OST2A2) Cilary rootlet coiled-coil, rootletin, partial (3%) [THC263898] | 0.005565858 | 1.956208631 |
| HPGD5 | ref Homo sapiens hematoopoietic prostaglandin D synthase (HPGD5), mRNA [NM_014485] | 0.005690478 | 1.887807543 |
| XLOC_I2_000866 | linc1[BROAD Institute lincRNA (XLOC_I2_000866), lincRNA [TCONS_I2_00001147] | 0.005703595 | 1.911270756 |
| XLOC_I2_007693 | Unknown | 0.005779918 | 1.911364441 |
| XLOC_007120 | linc1[BROAD Institute lincRNA (XLOC_007120), lincRNA [TCONS_00015039] | 0.005868463 | 1.90918265 |
| TAAR3 | ref Homo sapiens trace amine associated receptor 3 (gene/pseudogene) (TAAR3), non-coding RNA [NR_028511] | 0.005989904 | 1.916551336 |
| LALBA | ref Homo sapiens lactalbumin, alpha- (LALBA), mRNA [NM_002289] | 0.005996959 | 1.95618505 |
| XLOC_I2_012168 | linc1[BROAD Institute lincRNA (XLOC_I2_012168), lincRNA [TCONS_I2_00023043] | 0.006091766 | 1.945595648 |
| XLOC_002369 | linc1[BROAD Institute lincRNA (XLOC_002369), lincRNA [TCONS_00004479] | 0.006123007 | 1.925207079 |
| PW1L1 | ref Homo sapiens piwi-like 1 (Drosophila) (PW1L1), transcript variant 1, mRNA [NM_004764] | 0.006158684 | 1.930272899 |
| XLOC_014356 | linc1[BROAD Institute lincRNA (XLOC_014356), lincRNA [TCONS_00029688] | 0.006266727 | 1.932374268 |
| SCN4A | ref Homo sapiens sodium channel, voltage-gated, type IV, alpha subunit (SCN4A), mRNA [NM_000334] | 0.006275416 | 1.889464007 |
| XLOC_I2_013436 | ab 603253725F1 NIH_MGC_97 Homo sapiens cDNA clone IMAGE:5296015 5', mRNA sequence [B1561188] | 0.006437076 | 1.907840998 |
| XLOC_000576 | linc1[BROAD Institute lincRNA (XLOC_000576), lincRNA [TCONS_00010548] | 0.00653032 | 1.950842122 |
| LOC286184 | ref Homo sapiens uncharacterized LOC286184 (LOC286184), non-coding RNA [NR_038875] | 0.006592328 | 1.904893263 |
| LIGL1 | ref Homo sapiens lethal giant larvae homolog 1 (Drosophila) (LIGL1), mRNA [NM_004140] | 0.006675809 | 1.931551835 |
| SELP | ref Homo sapiens selectin P (granule membrane protein 140kDa, antigen CD62) (SELP), mRNA [NM_003005] | 0.006806267 | 1.895047005 |
| TG1BL1 | ref Homo sapiens integrin, beta-like 1 (with EGF-like repeat domains) (TG1BL1), mRNA [NM_004791] | 0.007285791 | 1.924309558 |
| OR4F4 | ref Homo sapiens olfactory receptor, family 4, subfamily F, member 4 (OR4F4), mRNA [NM_001004195] | 0.007414883 | 1.888542488 |
| DARC | ref Homo sapiens Duffy blood group, chemokine receptor (DARC), transcript variant 2, mRNA [NM_002036] | 0.007570807 | 1.892859571 |
| SPARCL1 | ref Homo sapiens SPARC-like 1 (hevin) (SPARCL1), transcript variant 2, mRNA [NM_004684] | 0.007646235 | 1.914364586 |
| GYPB | ref Homo sapiens glycoporphin B (MNS blood group) (GYPB), mRNA [NM_002100] | 0.007790531 | 1.888140626 |

| | | | |
|-------------|--|-------------|-------------|
| CST11 | ref Homo sapiens cystatin 11 (CST11), transcript variant 1, mRNA [NM_130794] | 0.00788176 | 1.907604029 |
| XLOC_002619 | linc BROAD Institute lincRNA (XLOC_002619), lincRNA [TCONS_00005994] | 0.00812354 | 1.887228547 |
| NRG3 | ref Homo sapiens neuregulin 3 (NRG3), transcript variant 1, mRNA [NM_001010848] | 0.008178403 | 1.897791965 |
| SLAMF6 | ref Homo sapiens SLAM family member 6 (SLAMF6), transcript variant 2, mRNA [NM_052931] | 0.008286029 | 1.893516306 |
| WDR49 | ens WDR repeat domain 49 [Source:HGNC Symbol;Acc:26587] [ENST00000453925] | 0.008527816 | 1.88965544 |

Downregulated gene list

| Gene | Gene Description | Pval | Adjusted expression |
|-----------------|--|-------------|---------------------|
| SPARC | ref Homo sapiens secreted protein, acidic, cysteine-rich (osteonectin) (SPARC), mRNA [NM_003118] | 0 | 0.167981259 |
| LCPI1 | ref Homo sapiens lymphocyte cytosolic protein 1 (L-plastin) (LCPI1), mRNA [NM_002298] | 0 | 0.176713785 |
| MAGEH1 | ref Homo sapiens melanoma antigen family H, 1 (MAGEH1), mRNA [NM_014061] | 2.98134E-07 | 0.254923536 |
| RAB17 | ref Homo sapiens RAB17, member RAS oncogene family (RAB17), transcript variant 1, mRNA [NM_022449] | 5.96267E-07 | 0.287024041 |
| ODZ1 | ref Homo sapiens odz, odd Oz/ten-m homolog 1 (Drosophila) (ODZ1), transcript variant 1, mRNA [NM_001163278] | 7.15521E-06 | 0.317977098 |
| LCK | ref Homo sapiens lymphocyte-specific protein tyrosine kinase (LCK), transcript variant 2, mRNA [NM_005356] | 1.04347E-05 | 0.309936226 |
| ENST00000399093 | ens Uncharacterized protein ENST00000399093 [Source:UniProtKB/Swiss-Prot;Acc:ABMWPF] [ENST00000399093] | 4.05462E-05 | 0.328214686 |
| DKO7 | ref Homo sapiens docking protein 7 (DKO7), transcript variant 1, mRNA [NM_173660] | 4.65809E-05 | 0.353937309 |
| ENST00000434150 | Unknown | 4.88939E-05 | 0.355744807 |
| CL3orf77 | ref Homo sapiens chromosome 19 open reading frame 77 (Cl3orf77), mRNA [NM_001136503] | 0.00011895 | 0.379327351 |
| NAV3 | ref Homo sapiens neuron navigator 3 (NAV3), mRNA [NM_014903] | 0.000124028 | 0.362321616 |
| LOC283710 | ref Homo sapiens uncharacterized LOC283710 (LOC283710), mRNA [NM_001243538] | 0.000133862 | 0.377151206 |
| OR6K1 | ref Homo sapiens olfactory receptor, family 6, subfamily X, member 1 (OR6K1), mRNA [NM_001005188] | 0.000135055 | 0.128278852 |
| XLOC_02_000773 | linc BROAD Institute lincRNA (XLOC_02_000773), lincRNA [TCONS_I2_0002430] | 0.000157173 | 0.388746707 |
| DSCR6 | ref Homo sapiens Down syndrome critical region gene 6 (DSCR6), mRNA [NM_018962] | 0.000163079 | 0.390102492 |
| C2CD2 | ref Homo sapiens C2 calcium-dependent domain containing 2 (C2CD2), transcript variant 1, mRNA [NM_015500] | 0.000170831 | 0.380850157 |
| CDC164 | ref Homo sapiens coiled-coil domain containing 164 (CDC164), mRNA [NM_145038] | 0.000182458 | 0.408111944 |
| SNAI3 | ref Homo sapiens snail homolog 3 (Drosophila) (SNAI3), mRNA [NM_178310] | 0.000227774 | 0.393267531 |
| MAGEA6 | ref Homo sapiens melanoma antigen family A, 6 (MAGEA6), transcript variant 2, mRNA [NM_175868] | 0.000270109 | 0.39612856 |
| XLOC_011183 | Unknown | 0.000299028 | 0.385087072 |
| KIAA1671 | ref Homo sapiens KIAA1671 (KIAA1671), mRNA [NM_001145206] | 0.000302009 | 0.403730322 |
| CDH1 | ref Homo sapiens cadherin 1, type 1, E-cadherin (epithelial) (CDH1), mRNA [NM_004360] | 0.000303798 | 0.399525706 |
| KDM3A | ref Homo sapiens lysine (K)-specific demethylase 3A (KDM3A), transcript variant 1, mRNA [NM_018433] | 0.000316022 | 0.402971491 |
| XLOC_009434 | linc BROAD Institute lincRNA (XLOC_009434), lincRNA [TCONS_00019633] | 0.000320792 | 0.406141676 |
| CDH1 | ref Homo sapiens cadherin 1, type 1, E-cadherin (epithelial) (CDH1), mRNA [NM_004360] | 0.000343152 | 0.405992643 |
| LOC100528278 | ref Homo sapiens hypothetical LOC100528278 (LOC100528278), mRNA [NR_132588] | 0.000344344 | 0.394658689 |
| LOC339822 | ref Homo sapiens uncharacterized LOC339822 (LOC339822), non-coding RNA [NR_033880] | 0.000352096 | 0.123494043 |
| A_33_P335590 | Unknown | 0.000376841 | 0.446637517 |
| OVOL2 | ref Homo sapiens ovo-like 2 (Drosophila) (OVOL2), mRNA [NM_021220] | 0.00042812 | 0.406068374 |
| LOC285501 | ref Homo sapiens uncharacterized LOC285501 (LOC285501), non-coding RNA [NR_028342] | 0.00044243 | 0.454376411 |
| XLOC_02_001288 | linc BROAD Institute lincRNA (XLOC_02_001288), lincRNA [TCONS_I2_00001738] | 0.000442423 | 0.434834202 |
| CXCL12 | ref Homo sapiens chemokine (C-X-C motif) ligand 12 (CXCL12), transcript variant 1, mRNA [NM_199168] | 0.000444219 | 0.411806258 |
| PAX7 | ref Homo sapiens paired box 7 (PAX7), transcript variant 3, mRNA [NM_001135254] | 0.000448393 | 0.407026336 |
| CD1A | ref Homo sapiens CD1a molecule (CD1A), mRNA [NM_001763] | 0.000482678 | 0.4142576 |
| ZCHC6 | ref Homo sapiens zinc finger, CCHC domain containing 6 (ZCHC6), transcript variant 1, mRNA [NM_024617] | 0.000489237 | 0.291066133 |
| ABCC11 | ref Homo sapiens ATP-binding cassette, sub-family C (CFTR/MRP), member 11 (ABCC11), transcript variant 2, mRNA [NM_033151] | 0.000507424 | 0.413483339 |
| MYO10 | ref Homo sapiens myosin X (MYO10), mRNA [NM_012334] | 0.000511001 | 0.194682009 |
| CDH1 | ref Homo sapiens cadherin 1, type 1, E-cadherin (epithelial) (CDH1), mRNA [NM_004360] | 0.000526206 | 0.421139936 |
| SLPI | ref Homo sapiens secretory leukocyte peptidase inhibitor (SLPI), mRNA [NM_003064] | 0.000536771 | 0.414048031 |
| FAM98B | ref Homo sapiens family with sequence similarity 98, member B (FAM98B), transcript variant 2, mRNA [NM_001042429] | 0.000600143 | 0.256615649 |
| SLC16A8 | ref Homo sapiens solute carrier family 16, member 8 (monocarboxylic acid transporter 3) (SLC16A8), mRNA [NM_013356] | 0.000642776 | 0.432116493 |
| PODNL1 | ref Homo sapiens podocan-like 1 (PODNL1), transcript variant 1, mRNA [NM_024825] | 0.000655298 | 0.420117823 |
| ABC81 | ref Homo sapiens ATP-binding cassette, sub-family B (MDR/TAP), member 8 (ABC81), mRNA [NM_000927] | 0.000672291 | 0.443203845 |
| HSPA1A | ref Homo sapiens heat shock 70kDa protein 1A (HSPA1A), mRNA [NM_005345] | 0.000720887 | 0.423177928 |
| S1PR5 | ref Homo sapiens sphingosine 1-phosphate receptor 5 (S1PR5), transcript variant 1, mRNA [NM_003060] | 0.000736986 | 0.435932886 |
| RAB17 | ref Homo sapiens RAB17, member RAS oncogene family (RAB17), transcript variant 1, mRNA [NM_022449] | 0.00075875 | 0.423807854 |
| CDH1 | ref Homo sapiens cadherin 1, type 1, E-cadherin (epithelial) (CDH1), mRNA [NM_004360] | 0.000776694 | 0.42443476 |
| XLOC_008644 | linc BROAD Institute lincRNA (XLOC_008644), lincRNA [TCONS_00018839] | 0.000782899 | 0.46348118 |
| HSPA1A | ref Homo sapiens heat shock 70kDa protein 1A (HSPA1A), mRNA [NM_005345] | 0.000788862 | 0.424567511 |
| ENST00000382320 | ens tetrapeptide repeat domain 6 [Source:HGNC Symbol;Acc:19739] [ENST00000382320] | 0.000796017 | 0.432016195 |
| FAM150A | ref Homo sapiens family with sequence similarity 150, member A (FAM150A), mRNA [NM_020413] | 0.00080960 | 0.432367481 |
| DCLK1 | ref Homo sapiens doublecortin-like kinase 1 (DCLK1), transcript variant 1, mRNA [NM_004734] | 0.000899469 | 0.427951977 |
| NMI | ref Homo sapiens N-myc (and STAT) interactor (NMI), mRNA [NM_004688] | 0.000925705 | 0.43151194 |
| CDCP1 | ref Homo sapiens CUB domain containing protein 1 (CDCP1), transcript variant 1, mRNA [NM_022842] | 0.001058375 | 0.442571304 |
| MGC15885 | ref Homo sapiens uncharacterized protein MGC15885 (MGC15885), non-coding RNA [NR_026897] | 0.001066722 | 0.433013225 |
| HSPA1A | ref Homo sapiens heat shock 70kDa protein 1A (HSPA1A), mRNA [NM_005345] | 0.001094151 | 0.43362626 |
| ACO2 | ref Homo sapiens acyl-CoA oxidase 2, branched chain (ACO2), mRNA [NM_003500] | 0.001106672 | 0.440309959 |
| A_33_P339477 | Unknown | 0.001126945 | 0.441289542 |
| HSPA1A | ref Homo sapiens heat shock 70kDa protein 1A (HSPA1A), mRNA [NM_005345] | 0.001140361 | 0.443020366 |
| XLOC_006598 | gb 6028912211 NIH_MGC_97 Homo sapiens cDNA clone IMAGE-482325 5', mRNA sequence [BG719813] | 0.001171367 | 0.485844256 |
| XLOC_004182 | linc BROAD Institute lincRNA (XLOC_004182), lincRNA [TCONS_00091176] | 0.001171665 | 0.456166327 |
| TAL1 | ref Homo sapiens T-cell acute lymphocytic leukemia 1 (TAL1), mRNA [NM_003189] | 0.00122682 | 0.43875764 |
| C13orf15 | ref Homo sapiens chromosome 13 open reading frame 15 (C13orf15), mRNA [NM_014059] | 0.001243814 | 0.44355352 |
| CDH1 | ref Homo sapiens cadherin 1, type 1, E-cadherin (epithelial) (CDH1), mRNA [NM_004360] | 0.00124441 | 0.438228171 |
| PF4 | ref Homo sapiens platelet factor 4 (PF4), mRNA [NM_002619] | 0.00125723 | 0.436068574 |
| CD40 | ref Homo sapiens CD40 molecule, TNF receptor superfamily member 5 (CD40), transcript variant 1, mRNA [NM_001250] | 0.001261404 | 0.440238711 |
| OR51F2 | ref Homo sapiens olfactory receptor, family 51, subfamily F, member 2 (OR51F2), mRNA [NM_001004753] | 0.001269453 | 0.17787974 |
| XLOC_004309 | gb DA675095 NTRP2 Homo sapiens cDNA clone NTRP2005971 5', mRNA sequence [DA675095] | 0.001327291 | 0.455640423 |
| PDZRN3 | ref Homo sapiens PDZ domain containing ring finger 3 (PDZRN3), mRNA [NM_015009] | 0.001377974 | 0.452126599 |
| WFDC2 | ref Homo sapiens WAP four-disulfide core domain 2 (WFDC2), mRNA [NM_006103] | 0.001400334 | 0.455630494 |
| ATM | ref Homo sapiens ataxia telangiectasia mutated (ATM), mRNA [NM_000051] | 0.001406893 | 0.455879238 |
| XLOC_02_009899 | linc BROAD Institute lincRNA (XLOC_02_009899), lincRNA [TCONS_I2_00018877] | 0.00141852 | 0.475359015 |
| CXCL12 | ref Homo sapiens chemokine (C-X-C motif) ligand 12 (CXCL12), transcript variant 1, mRNA [NM_199168] | 0.001432434 | 0.467080951 |
| E1F2AK3 | ref Homo sapiens eukaryotic translation initiation factor 2-alpha kinase 3 (E1F2AK3), mRNA [NM_004836] | 0.001434619 | 0.444274849 |
| CHP2 | ref Homo sapiens calcineurin B homologous protein 2 (CHP2), mRNA [NM_022097] | 0.001449238 | 0.450263893 |
| OR2M2 | ref Homo sapiens olfactory receptor, family 2, subfamily M, member 2 (OR2M2), mRNA [NM_001004688] | 0.00147936 | 0.492463716 |
| OLFML2A | ref Homo sapiens olfactomedin-like 2A (OLFML2A), mRNA [NM_182487] | 0.001585475 | 0.44681141 |
| XLOC_02_008352 | linc BROAD Institute lincRNA (XLOC_02_008352), lincRNA [TCONS_I2_00014990] | 0.001595015 | 0.455887389 |
| XLOC_011068 | linc BROAD Institute lincRNA (XLOC_011068), lincRNA [TCONS_00027911] | 0.001618568 | 0.462075375 |
| LACTB | ref Homo sapiens lactamase, beta (LACTB), nuclear gene encoding mitochondrial protein, transcript variant 2, mRNA [NM_171846] | 0.00162781 | 0.45493278 |
| XLOC_004099 | linc BROAD Institute lincRNA (XLOC_004099), lincRNA [TCONS_00008592] | 0.001693996 | 0.462628612 |
| PAR-SN | ref Homo sapiens paternally expressed transcript PAR-SN (PAR-SN), non-coding RNA [NR_022011] | 0.001741399 | 0.485340766 |
| APOBEC3B | ref Homo sapiens apolipoprotein B mRNA editing enzyme, catalytic polypeptide-like 3B (APOBEC3B), mRNA [NM_004900] | 0.001774492 | 0.448990725 |
| CDCP1 | ref Homo sapiens CUB domain containing protein 1 (CDCP1), transcript variant 1, mRNA [NM_022842] | 0.00179387 | 0.463007819 |
| XLOC_008144 | linc BROAD Institute lincRNA (XLOC_008144), lincRNA [TCONS_00017054] | 0.001968875 | 0.191404016 |
| ANKRD36BP2 | tc Q15694 HUMAN (Q15694) Protein immuno-reactive with anti-PTH polyclonal antibodies (Fragment), partial (42%) [THC249590] | 0.001978117 | 0.450484771 |
| A_33_P3345821 | Unknown | 0.002041321 | 0.492067354 |
| RBKS | ref Homo sapiens ribokinase (RBKS), mRNA [NM_022128] | 0.002108401 | 0.470886655 |
| XLOC_02_005179 | linc BROAD Institute lincRNA (XLOC_02_005179), lincRNA [TCONS_I2_00009678] | 0.002139407 | 0.488782457 |
| XLOC_011407 | linc BROAD Institute lincRNA (XLOC_011407), lincRNA [TCONS_00023594] | 0.002197543 | 0.477232345 |
| ZNF469 | ref Homo sapiens zinc finger protein 469 (ZNF469), mRNA [NM_001127464] | 0.002204997 | 0.471980187 |
| CXCL12 | ref Homo sapiens chemokine (C-X-C motif) ligand 12 (CXCL12), transcript variant 1, mRNA [NM_199168] | 0.002278338 | 0.474471133 |
| BCAN | ref Homo sapiens brevican (BCAN), transcript variant 2, mRNA [NM_198427] | 0.00230666 | 0.476017067 |
| NP11779 | tc GB MR0470.1 AAAG6955.1 MHC class I HLA-J antigen [NP11779] | 0.002323163 | 0.471206191 |
| ITLN1 | ref Homo sapiens intelectin 1 (galactofuranose binding) (ITLN1), mRNA [NM_017625] | 0.002351082 | 0.466089793 |
| XLOC_004300 | tc Q91YV8_MOUSE (Q91YV8) Pprc1 protein, partial (3%) [THC2691515] | 0.002404448 | 0.470758228 |
| GBP1P1 | ref Homo sapiens gamma-interferon binding protein 1, interferon-inducible pseudogene 1 (GBP1P1), non-coding RNA [NR_003133] | 0.002433069 | 0.475386178 |
| CDH1 | ref Homo sapiens cadherin 1, type 1, E-cadherin (epithelial) (CDH1), mRNA [NM_004360] | 0.00246346 | 0.46345956 |
| LCK | ref Homo sapiens lymphocyte-specific protein tyrosine kinase (LCK), transcript variant 2, mRNA [NM_005356] | 0.002492398 | 0.47020613 |
| A_33_P3363680 | Unknown | 0.00249836 | 0.49608888 |
| CACNA1B | ref Homo sapiens calcium channel, voltage-dependent, N type, alpha 1B subunit (CACNA1B), transcript variant 1, mRNA [NM_000718] | 0.002505814 | 0.482009283 |
| LRP1 | ref Homo sapiens low density lipoprotein receptor-related protein 1 (LRP1), mRNA [NM_002332] | 0.002533242 | 0.469399366 |
| TSHR | ref Homo sapiens thyrotrophic stimulating hormone receptor (TSHR), transcript variant 2, mRNA [NM_001018036] | 0.002556198 | 0.474730959 |
| SLC7A9 | ref Homo sapiens solute carrier family 7 (glycoprotein-associated amino acid transporter light chain, bo+ system), member 9 (SLC7A9), transcript variant 1, mRNA [NM_014270] | 0.00257826 | 0.460915701 |
| HVCN1 | ref Homo sapiens hydrogen voltage-gated channel 1 (HVCN1), transcript variant 1, mRNA [NM_001040107] | 0.002662036 | 0.480707341 |
| XLOC_02_005921 | linc BROAD Institute lincRNA (XLOC_02_005921), lincRNA [TCONS_I2_00011008] | 0.00273961 | 0.465583848 |
| HSPA1A | ref Homo sapiens heat shock 70kDa protein 1A (HSPA1A), mRNA [NM_005345] | 0.002800071 | 0.481175009 |
| XLOC_013293 | linc BROAD Institute lincRNA (XLOC_013293), lincRNA [TCONS_00027800] | 0.002805754 | 0.470380021 |
| ST6GALNAC1 | ref Homo sapiens ST6 (alpha-N-acetylneuraminyl-2,3-beta-galactosyl-1,3)-N-acetylglucosaminide alpha 2,6-sialyltransferase 1 (ST6GALNAC1), mRNA [NM_018144] | 0.002873711 | 0.47528137 |
| BHCE | ref Homo sapiens Rh blood group, CcEe antigens (BHCE), transcript variant 1, mRNA [NM_020485] | 0.00297925 | 0.472085738 |
| CTS2 | ref Homo sapiens cathepsin Z (CTS2), mRNA [NM_001336] | 0.002994753 | 0.47150415 |
| DPEP2 | ref Homo sapiens dipeptidase 2 (DPEP2), mRNA [NM_022355] | 0.002997138 | 0.473656251 |
| XLOC_008244 | linc BROAD Institute lincRNA (XLOC_008244), lincRNA [TCONS_00017379] | 0.003004293 | 0.471962543 |
| XLOC_02_011309 | linc BROAD Institute lincRNA (XLOC_02_011309), lincRNA [TCONS_I2_00021350] | 0.00301592 | 0.49323377 |
| XLOC_014066 | linc BROAD Institute lincRNA (XLOC_014066), lincRNA [TCONS_00029116] | 0.00305111 | 0.491342517 |
| SLC24A2 | ref Homo sapiens solute carrier family 24 (sodium/potassium/calcium exchanger), member 2 (SLC24A2), transcript variant 1, mRNA [NM_020344] | 0.003072268 | 0.473578654 |
| HPR | ref Homo sapiens haptoglobin-related protein (HPR), mRNA [NM_020995] | 0.003075845 | 0.469254368 |
| FEZ2 | ref Homo sapiens fasciculation and elongation protein zeta 2 (zyprin II) (FEZ2), transcript variant 2, mRNA [NM_001042548] | 0.003085684 | 0.47693478 |
| PAOX | ref Homo sapiens polyamine oxidase (exo-N4-amino) (PAOX), transcript variant 5, mRNA [NM_207128] | 0.003092243 | 0.47560909 |

| | | | |
|----------------|--|-------------|-------------|
| PPP1R21 | ref Homo sapiens protein phosphatase 1, regulatory subunit 21 (PPP1R21), transcript variant 2, mRNA [NM_152994] | 0.003098503 | 0.466301348 |
| XLOC_12_015892 | tc 1718340A KALIG-1 gene. [Homo sapiens] [exp=-1; wgp=0; cg=0], partial [11%] [THC2783530] | 0.003113112 | 0.481622052 |
| PIGU | ref Homo sapiens phosphatidylinositol glycan anchor biosynthesis, class U (PIGU), mRNA [NM_080476] | 0.003137261 | 0.48979318 |
| LOC100129048 | gb Homo sapiens cDNA FLJ46195 fs, clone TEST14006539. [AK128074] | 0.003171844 | 0.283220365 |
| IL2 | ref Homo sapiens interleukin 2 (IL2), mRNA [NM_000586] | 0.003259197 | 0.491990718 |
| ZNF671 | ref Homo sapiens zinc finger protein 671 (ZNF671), mRNA [NM_024833] | 0.003261881 | 0.47509523 |
| INHBA | ref Homo sapiens inhibin, beta A (INHBA), mRNA [NM_002192] | 0.003279471 | 0.483183572 |
| LOC100506667 | ref PREDICTED: Homo sapiens hypothetical protein LOC100506667 (LOC100506667), mRNA [XM_003118611] | 0.00331793 | 0.498803562 |
| AMN1 | ref Homo sapiens antagonist of mitotic exit network 1 homolog (S. cerevisiae) [AMN1], transcript variant 1, mRNA [NM_001113402] | 0.003385308 | 0.484812998 |
| XLOC_002193 | tc GB BC021164.2 BC021164.2 Homo sapiens cDNA clone IMAGE 3689998, partial cds [NP_1135451] | 0.003433606 | 0.47975023 |
| LOC100505834 | ref PREDICTED: Homo sapiens hypothetical LOC100505834 (LOC100505834), miscRNA [XR_110888] | 0.003441953 | 0.481946177 |
| KISS1R | ref Homo sapiens KISS1 receptor (KISS1R), mRNA [NM_032551] | 0.003557927 | 0.494719782 |
| USH1G | ref Homo sapiens Usher syndrome 1G (autosomal recessive) [USH1G], mRNA [NM_173477] | 0.003616958 | 0.484657843 |
| NR2E1 | ref Homo sapiens nuclear receptor subfamily 2, group E, member 1 (NR2E1), mRNA [NM_003269] | 0.003630374 | 0.484271981 |
| NMI | ref Homo sapiens N-myc (and STAT) interactor (NMI), mRNA [NM_004688] | 0.003635442 | 0.488201152 |
| HSPA1A | ref Homo sapiens heat shock 70kDa protein 1A (HSPA1A), mRNA [NM_005345] | 0.003637827 | 0.484497832 |
| KIRREL2 | ref Homo sapiens kin of IRRE like 2 (Drosophila) (KIRREL2), transcript variant 3, mRNA [NM_199180] | 0.003661082 | 0.482620256 |
| LNX1 | ref Homo sapiens ligand of numb-protein X 1 (LNK1), transcript variant 2, mRNA [NM_032622] | 0.003668833 | 0.473908963 |
| AMPD3 | ref Homo sapiens adenosine monophosphate deaminase 3 (AMPD3), transcript variant 3, mRNA [NM_001025390] | 0.003712659 | 0.476713233 |
| LOC100507513 | ref PREDICTED: Homo sapiens hypothetical LOC100507513 (LOC100507513), miscRNA [XR_110261] | 0.003782422 | 0.486285 |
| LCK | ref Homo sapiens lymphocyte-specific protein tyrosine kinase (LCK), transcript variant 2, mRNA [NM_005356] | 0.003921352 | 0.481580019 |
| XLOC_12_013300 | gb DB053965 TEST12 Homo sapiens cDNA clone TEST12044682 5', mRNA sequence [DB053965] | 0.003960408 | 0.496288734 |
| XLOC_014243 | linc BROAD Institute lincRNA (XLOC_014243), lincRNA [TCONS_00029424] | 0.003981277 | 0.47769457 |
| RAPGEF6 | ref Homo sapiens Rap guanine nucleotide exchange factor (GEF) 6 (RAPGEF6), transcript variant 2, mRNA [NM_016340] | 0.003989923 | 0.495232157 |
| LOC100506869 | ref PREDICTED: Homo sapiens hypothetical LOC100506869, transcript variant 2 (LOC100506869), miscRNA [XR_110368] | 0.004009004 | 0.482133967 |
| SLC35D2 | ref Homo sapiens solute carrier family 35, member D2 (SLC35D2), mRNA [NM_007001] | 0.004033451 | 0.485713864 |
| EMIL5 | linc BROAD Institute lincRNA (XLOC_001478), lincRNA [TCONS_00003684] | 0.004056705 | 0.497262229 |
| LOC338653 | gb Homo sapiens partial mRNA for KCNQ1OT2 protein. [AJ251642] | 0.004059477 | 0.476603493 |
| ATP2B4 | ref Homo sapiens ATPase, Ca+ transporting, plasma membrane 4 (ATP2B4), transcript variant 2, mRNA [NM_001684] | 0.004094866 | 0.481084476 |
| NTM | ref Homo sapiens neurotrophin (NTM), transcript variant 4, mRNA [NM_001144059] | 0.004118419 | 0.493850082 |
| TLR8-AS1 | ref Homo sapiens TLR8 antisense RNA 1 (non-protein coding) (TLR8-AS1), non-coding RNA [NR_030727] | 0.004166418 | 0.493786539 |
| XLOC_004104 | linc BROAD Institute lincRNA (XLOC_004104), lincRNA [TCONS_00008600] | 0.004221871 | 0.481553786 |
| CDCP1 | ref Homo sapiens CUB domain containing protein 1 (CDCP1), transcript variant 1, mRNA [NM_022842] | 0.004400751 | 0.487709843 |
| XLOC_006237 | linc BROAD Institute lincRNA (XLOC_006237), lincRNA [TCONS_00013076] | 0.004497347 | 0.491375694 |
| APOBEC3H | ref Homo sapiens apolipoprotein B mRNA editing enzyme, catalytic polypeptide-like 3H (APOBEC3H), transcript variant 4, mRNA [NM_001166004] | 0.004545644 | 0.495685934 |
| ARL13B | ref Homo sapiens ADP-ribosylation factor-like 13B (ARL13B), transcript variant 1, mRNA [NM_182896] | 0.004613022 | 0.492105345 |
| THC2662725 | tc [AF396935 seven-span membrane protein FIRE (Mus musculus)] [exp=-1; wgp=0; cg=0], partial [5%] [THC2662725] | 0.004655954 | 0.494870241 |
| XLOC_006819 | linc BROAD Institute lincRNA (XLOC_006819), lincRNA [TCONS_00014734] | 0.004659009 | 0.388036146 |
| ZNF730 | ens zinc finger protein 730 [Source:HGNC Symbol;Acc:32470] [ENST00000327867] | 0.00497764 | 0.484132832 |
| A_33_P3224050 | Unknown | 0.005177986 | 0.497501738 |
| ASB5 | ref Homo sapiens ankyrin repeat and SOCS box containing 5 (ASB5), mRNA [NM_080874] | 0.005256693 | 0.494463606 |
| GPRIN2 | ref Homo sapiens G protein regulated inducer of neurite outgrowth 2 (GPRIN2), mRNA [NM_014696] | 0.005427226 | 0.491711594 |
| IRAK3 | ref Homo sapiens interleukin-1 receptor-associated kinase 3 (IRAK3), transcript variant 1, mRNA [NM_007199] | 0.005497882 | 0.492017166 |
| ZNF610 | ref Homo sapiens zinc finger protein 610 (ZNF610), transcript variant 3, mRNA [NM_173530] | 0.00568213 | 0.489079035 |
| MYOF | ens myoferlin [Source:HGNC Symbol;Acc:3656] [ENST00000371488] | 0.005862203 | 0.493672081 |
| CRYM-AS1 | ref Homo sapiens CRYM antisense RNA 1 (non-protein coding) (CRYM-AS1), non-coding RNA [NR_026675] | 0.005943295 | 0.495460847 |
| PRRX2 | ref Homo sapiens paired related homeobox 2 (PRRX2), mRNA [NM_016307] | 0.006280838 | 0.495591707 |

Appendix: Gene lists of up- and down-regulated genes following MAP4K3 induction at the translational level. This stringest list was generated using RankProd and is capped at very high statistical significance with at least 2-fold increase/decrease in expression. Gene names are listed as found in UniProt.

References

- Antonov A., 2011. Bioprofiling.de: analytical web portal for high-throughput cell biology. *Nucleic Acids Res.* **39**, 323-327.
- Breitling R., Armengaud P., Amtmann A., Herzyk P., 2004. Rank products: a simple, yet powerful, new method to detect differentially regulated genes in replicated microarray experiments. *FEBS Letters* **573**, 83-92.
- Bryk B., Hahn K., Cohen M. S., Teleman A. A., 2010. MAP4K3 regulates body size and metabolism in *Drosophila*. *Developmental biology* **344**, 150-157.
- Chuang C. Huai-Chia; Lan L. Joung-Liang; Chen Y. Der-Yuan, Yang Y. Chia-Yu, Chen M. Yi-Ming, Li P. Ju-Pi, Huang Y. Ching-Yu, Liu E. Pao-En, Wang Xiaohong, Tan H. Tse-Hua. The kinase GLK controls autoimmunity and NF- κ B signaling by activating the kinase PKC- θ in T cells. *Nature Immunology* **12**, 1113-1118.
- Chen D.Y., Chuang H.C., Lan J.L., Chen Y.M., Hung W.T., Lai K.L., Tan T.H., 2012. Germinal center kinase-like kinase (GLK/MAP4K3) expression is increased in adult-onset Still's disease and may act as an activity marker. *BMC Medicine* **10**:84.
- Corl A.B., Berger K.H., Ophir-Shohat G., Gesch J., Simms J.A., Bartlett S.E., Heberlein U., 2009. Happyhour, a Ste20 family kinase, implicates EGFR signaling in ethanol-induced behaviors. *Cell* **137**, 949-960.
- Dan I., Watanabe N.M., Kusumi A., 2001. The Ste20 group kinases as regulators of MAP kinase cascades. *Trends in cell biology* **11**, 220-230.
- Davis J.R., 2000. Signal Transduction by the JNK Group of MAP Kinases. *Cell*, 103, 239-252.
- Delepine M., Nicolino M., Barrett T., Golamaully M., Lathrop G., Julier C., 2000. *EIF2AK3*, encoding translation initiation factor 2 α kinase 3, is mutated in patients with Wolcott-Rallison syndrome. *Nat. Genet.* **25**, 406-409.
- Diener K., Yao Z., Wang X.S., Zukowski M., Matsumoto G., Zhou G., Mo R., Sasaki T., Nishina H., Hui C.C., Tan T.H., Woodgett J.P., Penninger J.M., 1997. Activation of stress-activated protein kinases/c-Jun N-terminal protein kinases (SAPKs/JNKs) by a novel mitogen-activated protein kinase kinase. *J. Biol. Chem.* **272**, 32378-32383.
- Green D.R., 2005. Apoptotic pathways: Ten minutes to dead. *Cell Volume* **121**, 671-674.
- Duran A., Amanchy R., Linares R., Joshi, J., Abu-Baker S., Porollo A., Hansen M., Moscat J., Diaz-Meco T., 2011. p62 is a key regulator of nutrient sensing in the mTORC1 pathway. *Mol. Cell* **44**, 134-146.
- Elion E.A., 2000. Pheromone response, mating and cell biology. *Current opinion in microbiology* **3**, 573-81.

- Findlay M.G., Yan L., Procter J., Mieulet V., Lamb F.R., 2007. A MAP4 kinase related to Ste20 is a nutrient-sensitive regulator of mTOR signalling. *The Biochemical journal* **403**, 13-20.
- Fingar, D.C., Salama S., Tsou C., Harlow E., Blenis J., 2002. Mammalian cell size is controlled by mTOR and its downstream targets S6K1 and 4EBP1/eIF4E. *Genes Dev.* **16**, 1472–1487
- Gotoh I., Fukuda M., Adachi M., Nishida E., 1999. Control of the Cell Morphology and the S Phase Entry by Mitogen-activated Protein Kinase Kinase. *The Journal of Biological Chemistry* **274**, 11874-11880.
- Hanahan D., Weinberg R., 2011. Hallmarks of cancer: the next generation. *Cell* **144**, pages 646-674.
- Hara K., Yozenawa K., Weng Q.P., Kozlowski M.T., Belham C., Avruch J., 1998. Amino acid sufficiency and mTOR regulate p70 S6 kinase and eIF-4E BP1 through a common effector mechanism. *Journal of Biol. Chem.* **273**, 14484-14494.
- Harding P., Zeng H., Zhang Y., Jungries R., Chung P., Plesken H., Sabatini D., Ron D., 2001. Diabetes mellitus and exocrine pancreatic dysfunction in Perk^{-/-} mice reveals a role for translational control in secretory cell survival. *Mol. Cell* **7**, 1153–1163.
- Holcik M., Sonenberg N., 2005. Translational control in stress and apoptosis. *Nature Reviews* **6**, 318-327.
- Holz M.K., Ballif B.A., Gygi S.P., Blenis J., 2005. mTOR and S6K1 mediate assembly of the translation preinitiation complex through dynamic protein interchange and ordered phosphorylation events. *Cell* **123**, 569–580.
- Huang C., Rajfur Z., Borchers C., Schaller M.D., Jacobson K., 2003. JNK phosphorylates paxillin and regulates cell migration. *Nature* **424**, 219-223.
- Jacobson A., Peltz W., 1996. Interrelationships of the pathways of mRNA decay and translation in eukaryotic cells. *Annu. Rev. Biochem* **65**, 693-773.
- Jones S, et al., 2008. Core signaling pathways in human pancreatic cancers revealed by global genomic analyses. *Science* **321**,1801–1806.
- Joslyn G., Ravindranathan A., Brush G., Schuckit M., White R., 2010. Human Variation in Alcohol Response Is Influenced by Variation in Neuronal Signaling Genes. *Alcoholism: Clinical and Experimental Research* **34**, 800-813.
- Kim D., Sarbassov D., Ali S., King E.J., Latek R., Erdjument-Bromage H., Tempst P., Sabatini M.D., 2006. mTOR Interacts with Raptor to Form a Nutrient-Sensitive Complex that Signals to the Cell Growth Machinery. *Cell* **110**, 163-175.
- Kurokawa M. and Kornbluth S., 2009. Caspases and kinases in a death grip. *Cell* **138**, 838-854.
- Lam D., Dickens D., Reid B. Elizabeth B Loh H. Samantha, Moiso Nicoleta, Martins L. Miguel, 2009. MAP4K3 modulates cell death via the post-transcriptional regulation of BH3-only proteins. *Proc. of the National Acad. of Sciences* **106**, 11978-11983.

- Lam D., Martins L.M., 2009. MAP4K3 enhances the expression of the BH3-only protein BID. *Cell cycle* **8**, 3248-3249.
- Lee Meng-H., Koria P., Qu J., Andreadis S., 2009. JNK phosphorylates β -catenin and regulates adherens junctions. *FASEB J.* **23**, 3874-3883.
- Lee Meng-H., Padmashali R., Koria P., Andreadis S., 2011. JNK regulates binding of α -catenin to adherens junctions and cell-cell adhesion. *FASEB J.* **25**, 613-623.
- Leeuw T., Wu C., Joseph D. Schrag, Whiteway M., David T., Ekkehard L., 1998. Interaction of a G-protein beta-subunit with a conserved sequence in Ste20/PAK family protein kinases. *Nature* **391**, 191-195.
- Ma X., and Blenis J., 2009. Molecular mechanisms of mTOR-mediated translational control. *Nature Reviews Molecular Cell Biology* **10**, 307-318.
- McKee E., Ferguson M., Bentley A. T. and Marks T., 2006. Inhibition of Mammalian Mitochondrial Protein Synthesis by Oxazolidinones. *Antimicrob. Agents Chemother* **50**, 2042-2049.
- Melamev D., Arava Y., 2007. Genome-Wide Analysis of mRNA Polysomal Profiles with Spotted DNA Microarrays. *Methods in Enzymology* **431**, 177-201.
- Myrick K., Dearolf C., 2000. Hyperactivation of the *Drosophila* Hop Jak kinase causes preferential overexpression of eIF1A transcripts in larval blood cells. *Gene* **244**, 119-125.
- Olsen D., Savner M., Mathew A., Zhang F., Krishnamoorthy T., Phan L., Hinnenbusch G., 2003. Domains of eIF1A that mediate binding to eIF2, eIF3 and eIF5B and promote ternary complex recruitment in vivo. *EMBO Journal* **22**, 193-204.
- Pel H., Grivell L., 1994. Protein synthesis in mitochondria. *Molecular Biology Reports* **19**, 183-194.
- Pirooznia M., Nagarajan V., Deng Y., 2007. GeneVenn – A web application for comparing gene lists using Venn diagrams. *Bioinformatics* **1**, 420-422. Portal accessible at <http://genevenn.sourceforge.net/index.htm>
- Rabin S., Kim J., Baughn M., Libby R., Fan Y., Libby R., La Spada A., Stone B., Ravits J., 2010. Sporadic ALS has compartment-specific aberrant exon splicing and altered cell-matrix adhesion biology. *Human Molecular Genetics* **19**, 313-328.
- Ramet M., Lanot R., Zachary D., Manfruelli P., 2002. JNK signalling pathway is required for efficient wound healing in *Drosophila*. *Developmental Biology* **241**, 145-156.
- Ramirez V. Carmen, Vilela Cristina, Berthelot Karine, and McCarthy E. G. John, 2002. Modulation of Eukaryotic mRNA Stability via the Cap-binding Translation Complex eIF4F. *Journal of Molecular Biology* **318**, 951-962.
- Ramjaun R. A., Angers A., Legendre-Guillemain V., Tong X.K., McPherson S. Peter, 2001. Endophilin Regulates JNK Activation through Its Interaction with the Germinal Center Kinase-like Kinase. *The Journal of Biol. Chem.* **276**, 28913-28919.

- Resnik-Docampo M., de Celis F.J., 2011. MAP4K3 is a component of the TORC1 signalling complex that modulates cell growth and viability in *Drosophila melanogaster*. *PLoS ONE* **6**, 1-14.
- Riesgo-Escovar J.R., Jenni M., Fritz A., Hafen E., 1996. The *Drosophila* Jun-N-terminal kinase is required for cell morphogenesis but not for DJun-dependent cell fate specification in the eye. *Genes Dev.* **10**, 2759-2768.
- Sancak Y., Peterson T.R., Shaul Y.D., Lindquist R.A., Thoreen C.C., Bar-Peled L., Sabatini D.M., 2008. The Rag GTPases bind raptor and mediate amino acid signaling to mTORC1. *Science* **320**, 1496–1501.
- Sancak Y., Bar-Peled L., Zoncu R., Markhard A.L., Nada S., Sabatini D.M., 2010. Regulator-Rag complex targets mTORC1 to the lysosomal surface and is necessary for its activation by amino acids. *Cell* **141**, 290–303.
- Selvaraj A., Thomas G., 2010. Phosphatase 2A Puts the Brakes on mTORC1 Nutrient Signaling. *Cell Metabolism* **11**, 245-247.
- Shaulian E., Karin M., 2001. AP-1 in cell proliferation and survival. *Oncogene* **20**, 2390–2400.
- Shaw G., Morse S., Ararat M., Graham F., 2002. Preferential transformation of human neuronal cells by human adenoviruses and the origin of HEK 293 cells. *FASEB Journal* **16**, 869-871.
- Sonenberg N., Hinnebusch A. G., 2009. Regulation of translation initiation in eukaryotes: mechanisms and biological targets. *Cell* **136**, 731-745.
- Tusher V. G., Tibshirani R., Chu G., 2001. Significance analysis of microarrays applied to the ionizing radiation response. *Proc. of the National Acad. of Sciences* **98**, 5116-5121.
- Yan L., Mieulet V., Burgess D., Findlay M.G., Sully K., Procter J., Goris J., Janssens V., Morrice A.N., Lamb F.R., 2010. PP2A T61 epsilon is an inhibitor of MAP4K3 in nutrient signaling to mTOR. *Molecular Cell* **37**, 633-642.
- Youle J.R., Strasser A., 2008. The BCL-2 protein family: opposing activities that mediate cell death. *Nature reviews* **9**, 47-59.
- Wang Y., Dolhman G. H., 2004. Pheromone signaling mechanisms in yeast: a prototypical sex machine. *Science* **306**, 1508-1509.
- Wishart A. J., Hayes A., Wardleworth L., Zhang N., Oliver S. G., 2005. Doxycycline, the drug used to control the tet-regulatable promoter system, has no effect on global gene expression in *Saccharomyces cerevisiae*. *Yeast* **22**, 565-569.
- Zhang S., Readinger J., DuBois W., Janka-Junttila M., Robinson R., Pruitt M., Bliskovsky V., Wu J., Sakakibara K., Patel J., Parent C., Tessarollo L., Schwartzberg P., Mock B., 2010. Constitutive reductions in mTOR alter cell size, immune cell development, and antibody production. *Blood* **117**, 1228-1238.

Zid B.M, Rogers A.N., Katewa S.D., Vargas M.A., Kolipinski M.C., Lu T.A., Benzer S., Kapahi P., 2009. 4E-BP extends lifespan upon dietary restriction by enhancing mitochondrial activity in *Drosophila*. *Cell* **139**, 149-160.